From Research Center Borstel

Leibniz Lung Center

Director: Prof. Dr. Stefan Ehlers

“Novel mouse models to delineate the pathogenesis of systemic sclerosis ”

Dissertation for fulfillment of requirement for

the Doctoral Degree

of the university of Lübeck

from the department of natural sciences

submitted by

Xiaoyang Yue

From Henan, China

Lübeck, 2019

First referee: Pd. Dr. Xinhua Yu

Second referee: Prof. Dr. Peter König

Third referee: Prof. Dr. Norbert Tautz

Date of oral examination: 27. June. 2019

Approved for printing on 01. July. 2019

Table of Contents

Zusammenfassung

Die Systemische Sklerose (SSc) ist eine komplexe Autoimmunerkrankung, welche durch Autoimmunität, Vaskulopathie und Fibrose gekennzeichnet ist. In zahlreiche Studien wurde eine Fehlregulierung des Immunsystems in der SSc nachgewiesen, was auf eine zentrale Rolle von Immunzellen und Autoantigenen bei der Pathogenese der Erkrankung hinweist. So zeigen bisherige Befunde, dass sowohl autoreaktive T- als auch B-Zellen an der Entwicklung der SSc beteiligt sind. Die der pathogenen Wirkung dieser Zellen zugrunde liegenden Mechanismen sind jedoch nur unzureichend verstanden. Obwohl die mit der SSc in Verbindung gebrachten Autoantigene noch nicht klar definiert sind, konnten in neueren Studien beispielsweise mit Angiotensin II Typ 1 Rezeptor (AT1R) einige vielversprechende Kandidaten hierfür identifiziert werden. Eine Validierung der tatsächlichen Rolle in der Pathogenese dieser SSc-assoziierten Autoantigene steht jedoch noch aus. Hierfür haben sich bisher vor allem Tiermodelle als vielseitige und leistungsfähige Werkzeuge zur Untersuchung menschlicher Autoimmunerkrankungen bewährt. Bisherige Tiermodelle für die SSc bilden die Erkrankung des Menschen jedoch nur unvollständig ab. Ziel meiner Arbeit war es daher, neuartige Tiermodelle für die SSc zu etablieren, die eine besseres Verständnis für die Pathogenese der Krankheit, insbesondere mit Hinblick auf die Rolle der Immunzellen und potentieller Autoantigene, ermöglichen.

Um die pathogene Rolle von aus Patienten stammenden Immunzellen untersuchen zu können, habe ich im ersten Teil dieser Studie ein neues humanisiertes Modell für SSc etabliert. Dafür wurden periphere mononukleäre Blutzellen (PBMC) dem SSc-Patienten entnommen und in immundefiziente $Rag2^{-/-}/IL2rg^{-/-}$ Mäuse übertragen. Zwölf Wochen nach dem Transfer bildeten die Empfängermäuse menschliche Autoantikörper gegen AT1R sowie Endothelinrezeptor Typ A (ETAR) aus und entwickelten schwere, von B-Zellen dominierte, Entzündungsinfiltrate in zahlreichen Organen wie Lunge, Niere und Muskelgewebe. Im Gegensatz dazu produzierten Mäuse, die PBMC von gesunden Spendern erhielten, keine oder nur geringe Mengen an anti-AT1R- und anti-ETAR-Autoantikörpern und entwickelten keine sichtbaren Entzündungssyptome. Interessanterweise entwickelten Empfängertiere, welche Zellen aus SSc-Patienten nach B-Zelltherapie mit Retuximab erhalten hatten, keine Pathologien. Diese Ergebnisse zeigen, dass wesentliche immunologische und histologische Merkmale der SSc durch der Transfer von PBMC

aus SSc-Patienten übertragbar sind. Weiterhin weisen die Befunde auf eine zentrale Rolle von B-Zellen im Krankheitsgeschehen hin.

Im zweiten Teil dieser Studie sollte geklärt werden, ob und in welcher Weise Autoantikörper gegen AT1R, ein in bereits mehreren epidemiologischen Studien identifiziertes Autoantigen der SSc, an der Pathogenese der Erkrankung beteiligt sind. Da vermutet wird, dass die pathogene Wirkung von ant-AT1R Autoantikörpern über deren Kapazität zur Aktivierung des Zielrezeptors verläuft, wurden von mir Mäuse mit humanem AT1R in nativer Konformation immunisiert. Die mit AT1R immunisierten Mäuse produzierten Autoantikörper gegen AT1R und Seren aus AT1R-immunsierten Tieren aktivierten Angiotensinrezeptoren *in vitro*. AT1R-immunisierte Mäuse entwickelten eine komplexe Entzündung in der Lunge, welche durch Vaskulopathie, interstitielle Entzündung des Lungengewebes sowie perivaskuläre Infiltrationen gekennzeichnet war. Diese Symptome wurden begleitet durch Infiltration von Entzündungszellen und Fibrosen in der Haut, wie sie für die SSc typisch sind. Interessanterweise ließ sich durch Übertragung von aus AT1R-immunisierten Mäusen stammendes IgG induzierte in gesunde Mäuse eine lokale Entzündung im Empfänger induzieren. In ihrer Zusammenfassung zeigen diese Ergebnisse, dass die Autoimmunantwort gegen AT1R pathogen ist und die Erkrankung durch Transfer von Autoantikörpern übertragbar ist. Die Immunisierung von Mäusen mit hAT1R stellt damit ein neues Mausmodell für die SSc dar, in welchem weitergehende Mechanismen der Pathogenese der Erkrankung untersucht werden können.

In dieser Studie konnte erstmals *in vivo* nachgewiesen werden, dass die SSc durch Transfer sowohl von Immunzellen als auch von pathogenen Antikörpern übertragen werden kann und damit zwei wichtige Kriterien für Autoimmunerkrankungen erfüllt. Weiterhin konnten B-Zellen und Autoantikörper gegen AT1R als wesentliche Treiber in der experimentellen SSc identifiziert werden. In Verbindung mit den in dieser Arbeit etablierten neuen Mausmodellen können diese Erkenntnisse eine Grundlage für weitere Untersuchungen zur Pathogenese der Erkrankung und für die Entwicklung zukünftiger Therapien zu deren Behandlung darstellen.

Abstract

Systemic sclerosis (SSc) is a complex autoimmune disease, which is characterized by autoimmunity, vasculopathy and fibrosis. Numerous studies have revealed prominent dysregulation of immune system in SSc which further suggests the important roles of immune cells and autoantigens in the pathogenesis of SSc. For example, it is believed that both autoreactive T- and B cells are involved in the development of SSc, but the mechanisms behind the pathogenicity of these cells are not completely understood. Regarding SSc-associated autoantigens, recent studies have identified some novel candidates of pathogenic autoantigens, e.g. angiotensin II type 1 receptor (AT1R). However, the pathogenicity of SSc-associated autoantigens needs to be validated. Animal models are powerful tools for investigating the pathogenesis of human autoimmune diseases. In this study, my first aim was to use the mouse model organism to investigate the role of immune cells as well as putative candidate autoantigen in the pathogenesis of SSc. In a second aim, I tried to establish novel mouse models for SSc.

In the first part of this study, in order to investigate the pathogenic role of patient immune cells, I established a novel humanized model for SSc by transferring peripheral blood mononuclear cell (PBMC) from patients with SSc into $Rag2^{-/-}/IL2rg^{-/-}$ immunodeficient mice. Twelve weeks after the transfer of PBMC from SSc patients, the recipient mice generated human autoantibodies against AT1R as well as endothelin receptor type A (ETAR), and showed severe B cells dominated inflammatory infiltrates in multiple organs such as lung, kidney, and muscle. By contrast, mice which received PBMC from healthy donors produced significantly lower levels of anti-AT1R and anti-ETAR autoantibodies than those having received PBMS from SSc patients, although both groups of mice generated comparable levels of total human IgG. I also found that consistant transfer of PBMC from healthy donors did not induce obvious inflammation in any organs of recipient mice. Furthermore, neither autoantibodies nor tissue inflammation was detected in mice which received PBMC from SSc patients treated with rituximab, a common anti-B cells medication used for SSc treatment. These results indicate that transfer of PBMC from SSc patients can induce immunological and histological features resembling human SSc, and show that B cells are indispensable for the disease manifestation. By my novel humanized SSc model, I could demonstrate the pathogenic role of human immune cells, in particular B cells, in the development of SSc.

In the second part of this study, I aimed to investigate the pathogenicity of autoimmunity against AT1R *in vivo*. Previous studies have demonstrated that anti-AT1R autoantibodies with stimulatory function are present in SSc patients and associated with the development and prognosis of the disease, suggesting the involvement of autoimmunity against AT1R in the pathogenesis of SSc. However, this hypothesis has not been validated *in vivo* so far, e.g. by animal models. Here I investigated the pathogenicity of autoimmunity against AT1R *in vivo*, by immunizing mice with membrane extracts prepared from CHO cells overexpressing hAT1R. The AT1R-immunized mice produced autoantibodies against AT1R. Notably, these autoantibodies showed agonistic effects on AT1R as indicated by stimulatory effects on human monocytes which could be ameliorated by AT1R blockade. Moreover, the AT1R-immunized mice developed vasculopathy and interstitial inflammation in lung, as well as perivascular infiltrations and fibrosis in the skin, partially resembling clinical manifestations of SSc. I also found that the immunological and clinical features were not observed in mice immunized with control membrane extract (ME). In addition, transfer of IgG from AT1R-immunized mice could induce local inflammation in healthy recipient mice, which was not observed in the control ME-immunized mice. In summary, these findings clearly show that autoimmunity against AT1R is pathogenic *in vivo* and immunization with AT1R presents a novel mouse model for SSc.

Taken together, this study provides first *in vivo* evidence that immune cells, in particular B cells, and autoantibodies to AT1R are pathogenic drivers in SSc, Therefore, my results suggest that B cells and AT1R could be potential therapeutic targets for the disease. Furthermore, the two novel mouse models established here will be useful research tools to investigate SSc pathomechanisms and to develop new therapeutic strategies.

1. Appendix

1.1 List of abbreviation

ACA: anti-centromere antibodies

ACE: angiotensin converting enzyme

ANA: autoantibodies against nucleus autoantigen

Ang II: angiotensin II

ARA: anti-RNA polymerase antibodies

AT1R: angiotensin II type 1 receptor

AT2R: angiotensin II type 2 receptor

ATA: anti-topoisomerase I antibodies

BALF: Bronchoalveolar lavage fluid

CCL2: CC-chemokine ligand 2

CCL8: CC-chemokine ligand 8

CHO cells: Chinese hamster ovary (CHO) cells

CTDs: connective tissue diseases

CTGF：connective tissue growth factor

CXCR4: C-X-C chemokine receptor type 4

DCs: dendritic cells

dcSSc: diffused cutaneous systemic sclerosis

ECM: extra-cellular matrix

ETAR: Endothelin receptor type A

Fli-1: Friend leukemia virus integration 1

Fra-2: Fos-related antigen 2

GD: Grave's disease

GVHD: graft versus host disease

HEp-2 cells: human epithelioma-2 cells

ICAM-1: inter-cellular adhesion molecules-1

i.d.: intradermal injection

i.p.: intraperitoneal injection

IL13: Interlukin-13

IL4: Interlukin-4

IL6: Interlukin-6

IL8: Interlukin-8

ILD: interstitial lung disease

Klf5： Krüppel-like factor 5

lcSSc: limited cutaneous systemic sclerosis

MCP-1: monocytes chemoattractant protein 1

MIP-2: macrophage inflammatory protein 2

PAH: pulmonary arterial hypertension

PBMC: peripheral blood mononuclear cells

PCR: Polymerase chain reaction

PDGFR: platelet derived growth factor receptor

ROS: reactive oxygen species

SRC: scleroderma renal crisis

SSc: systemic sclerosis

TGF-β: Transforming growth factor- β

Th1 cells: type 1 T helper cells

Th2 cells: type 2 T helper cells

TSH-R: thyrotropin receptor

Tsk1：tight skin-1 mice

Tsk2：tight skin-2 mice

T β RI mice : transgenic mice overexpressing TGF-β receptor I on fibroblasts

T β RII△k mice: transgenic mice overexpressing kinase-deficient human type II TGF- β receptor on fibroblasts

TUNEL: Terminal deoxynucleotidyl transferase dUTP nick end labeling

U1-RNP： U1 small nuclear ribonucleoprotein

VCAM-1: vascular cell adhesion molecules-1

VEGF: vascular endothelial growth factor

1.2 List of tables

1.3 List of figures

2. Introduction

2.1 Systemic sclerosis

2.1.1 Epidemiology

Systemic sclerosis (SSc) is an autoimmune connective tissue disease characterized by three key pathophysiologic features: autoimmunity, vasculopathy and fibrosis [1]. Depending on geographic location and time period of observation, the prevalence of SSc varies considerably, ranging from 31 to 658 cases per million [2]. Due to the involvement of inner organs, the risk of mortality in patients with SSc is rather high, with a 10-year survival rate of 60%-70% [3]. The leading causes for the death in SSc patients are pulmonary fibrosis and pulmonary arterial hypertension (PAH) which account for approximately 60% of SSc-related death [4]. Like many autoimmune diseases, SSc has a female predominance, with a female to male ratio of 3:1 or higher [5]. Besides sex, many other factors have been suggested to be associated with the disease risk, including age, family history, infection and genetic factors [5]. However, the etiology and pathology of the disease are still largely unknown.

2.1.2 Classification of SSc

Based on the extent of skin manifestation, involvement of internal organs and laboratory parameters, SSc can be classified into two distinct subsets: limited cutaneous form (lcSSc) and diffused cutaneous form (dcSSc) (Table 1). Among all patients with SSc, approximately 60% are affected by lcSSc, while 35% develop dcSSc [6]. Patients with lcSSc have cutaneous thickening limited to the distal extremities, but in some cases affected areas may also involve the face and neck. In contrast, dcSSc is characterized by more extensive skin involvement, extending from proximity to the elbows, knees or trunk. Patientes suffering from dsSSc also devlope SSc more rapidly and exhibit pathology in internal organ earlier than patiens with lcSSc [7], [8]. Among serious complications in inner organs, pulmonary arterial hypertension (PAH) is more common

in lcSSc, while interstitial lung disease (ILD) and rental crisis are typical for dcSSc [8]. There are several SSc-specific autoantibodies, such as anti-centromere antibodies (ACA), anti-topoisomerase I antibodies (ATA) and anti-RNA polymerase antibodies (ARA). Although these antibodies can be detected in both subsets of the disease, ACA is highly prevalent in lcSSc patients and ATA and ARA are common in patients with dcSSc [9]. Collectively, dcSSC is generally considered to be the more severe than lsSSc, and these patients generally have a worse prognosis (Table 1).

Table 1. Classification of SSc

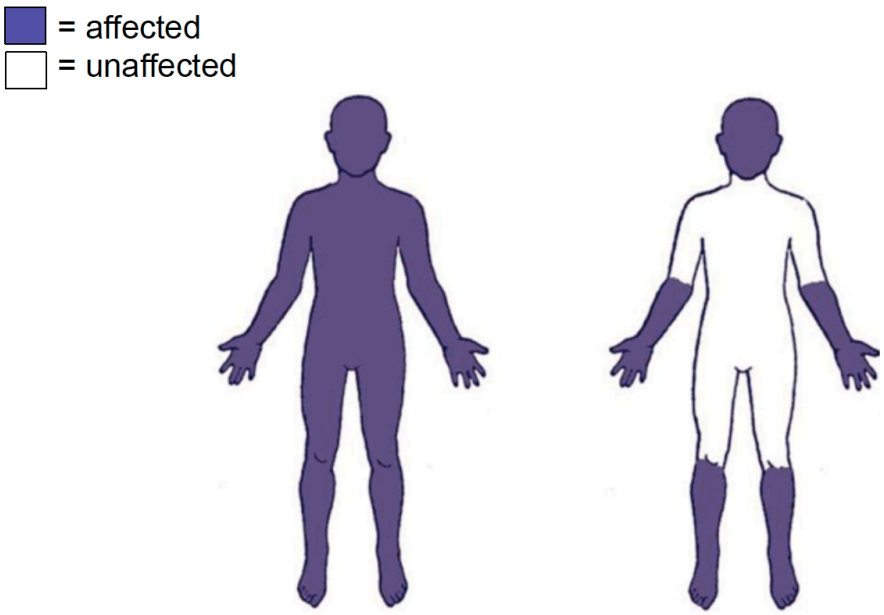

	lcSSc	dcSSc
Skin involvement	Extremities, area below elbows and knees, face	Extremities, area above and below elbows and knees, face and trunk
Disease progress	Slow, rarely softens	Rapid, may soften late in course
Internal organ involvement	late	Early
Most frequent serious complications	pulmonary arterial hypertension	interstitial lung disease, renal crisis
ANA	ACA	ATA, ARA
Prognosis (10-year survival rate)	> 70%	40-60%

2.1.3 Disease manifestations

SSc is a systemic autoimmune disease, multiple organs are involved in the disease process [6], [10] (Table 2). At the early onset of SSc or even at the presymptomatic phase, a panel of SSc-specific autoantibodies are detectable in SSc patients, including ACA, ATA and ARA [11]. Since those SSc-specific autoantibodies are associated with clinical features and prognosis of the disease, it is conceivable that they are involved in the clinical manifestations [10]. Following autoantibodies production, vasculopathy develops in the microvasculature of the skin, which usually starts with injury and apoptosis of endothelial cells and then proceeds to loss of capillaries, proliferative vasculopathy of small arteries, and perivascular infiltrates [12]. Clinically, the vasculopathy is manifested in the skin as Raynaud's phenomenon and digital ulcers [13]. In addition to cutaneous vascular changes, skin fibrosis frequently develops. The fibrotic skin is characterized by dense accumulation of compact collagen bundles and infiltrates of inflammatory cells, which progressively invade the adjacent adipose layer [14]. Besides skin, inner organs are often affected in SSc, among of which the lung is the main target organ. Both vasculopathy and fibrosis are able to affect lung, resulting in pulmonary arterial hypertension (PAH) and interstitial lung disease (ILD) which are leading causes for SSc-related death [15]. PAH is more common in lcSSc than in dcSSc and usually observed in the late phase of the disease. The histopathological changes of PAH include intimal proliferation, luminal obstruction with perivascular infiltration of immune cells and the narrowing of the small-to-medium sized arteries, which consequently increases blood resistance to the right ventricle and causes heart failure [16], [17].

In contrast to PAH, ILD is more common in patients with dcSSc than in patients with lcSSc. After the diagnosis of SSc, 25% of patients develop clinically significant lung disease within 3 years [8], [18]. Majority of patients with SSc-ILD patients have a histological feature of pulmonary fibrosis, whereas some of these patients show more inflammatory characteristics [19]. At the early phase of SSc-ILD, the lungs of patients are characterized by patchy infiltration of lymphocytes as well as endothelial and epithelial injury [20], which are believed to initiate and promote the fibrotic process [21]. With progression of disease, fibrosis dominates ILD, causing overt distortion of lung structure and severe damage to lung function [22]. In addition to skin and lung damage, the esophagus is also frequently affected in SSc, with pathological changes such as

vasculopathy, fibrosis and atrophy, all of which contribute to esophageal motor disturbance [23]. Although not lethal, dysfunction of esophagus movement in SSc patients often leads to gastroesophageal reflux, which causes progressive damage to the lungs and thus promote the development of ILD [24], [25], [26]. Moreover, renal manifestations are often observed in patients with SSc. For exapmle, some patients with SSc develop scleroderma renal crisis (SRC) that is characterized by intimal thickening of arterioles with thrombi, glomerular ischemia and glomerulosclerosis [27]. Although the incidence of SRC is relatively low, ranging from 5% to 10% of total SSc patients, it is a lethal complication resulting in malignant hypertension and renal failure [28], [29]. Previously, the 5 years cumulative survival rate of SSc patient with SRC was below 10%, since the invention and application of angiotensin converting enzyme (ACE) inhibitor the survival rate has increased to about 65% [30]. Furthermore, several other organs such as heart, intestine, muscle and joint are also affected in SSc, with clinical manifestation of myocarditis, malabsorption, myositis and inflammatory polyarthritis, respectively [6].

Collectively, the involvement of multiple organs increases the complexity of SSc, which greatly hinders the exploration of the pathogenesis and development of effective treatment for the disease. Moreover, since the abovementioned manifestations can present in individual patients in different combinations, SSc shows a highly heterogeneous nature that further complicates the disease [10].

Table 2. Disease manifestations of systemic sclerosis

Disease manifestations	Incidence in SSc patients (%)
Skin fibrosis	>90
Raynaud phenomenon	90
Digital ulcers	25
Interstitial lung disease	40
PAH	15
Myocardial disorders	20-25
Renal crisis	5-10
Gastrointestinal involvement	90
Musculoskeletal problems	65

2.1.4 Immunological abnormalities

2.1.4.1 SSc-specific autoantibodies

Autoimmunity is a hallmark of SSc, which is characterized by production of autoantibodies. As summarized in table 3, a panel of SSc related autoantibodies have been reported, including ACA, ATA and ARA, as well as some other autoantibodies such as anti-fibrillarin, anti-PM-Scl, anti-U1RNP and anti-Th/To [31], [32]. These antibodies are rarely found in healthy people or patients with other connective tissue diseases (CTDs), and thus are useful for diagnosis of SSc. Beside their value in disease diagnostics, these autoantibodies are also associated with disease features and prognosis of SSc [11].

In 1979, Douvas et al. first identified ATA in SSc patients [33]. ATA are found in 40% patients with dcSSc and 10% patients with lcSSc patients, while they are present in 2% patients with other connective tissue diseases, and in less than 1% healthy controls [9], [34]. The presence of ATA is associated with the development, clinical features, and prognosis of SSc. ATA not only can be utilized as a good predictive marker for development of SSc [35], but also is associated with increased risks for development of myocardial disease, SRC and ILD in SSc patients, and the SSc-related mortality [36], [37], [38], [39], [40].

ACA were first identified by Tan and colleagues in patients with SSc in 1980 [41]. Like ATA, ACA are common in patients with SSc and rarely detectable in healthy people or patients with other connective tissue diseases [42], [43]. In contrast to ATA, ACA are more frequently observed in patients with lcSSc than those with dcSSc [44]. The presence of ACA is associated with development of digital ischemic loss and PAH [44], [45]. Unlike patients positive for ATA, SSc patients positive for ACA show a higher survival rate [46], [47], since they do not develop severe ILD, cardiomyopathy, or SRC [48], [49].

In addition to ACA and ATA, ARA are another type of highly SSc-specific autoantibodies used as a diagnostic marker for disease [31]. Almost all SSc patients positive for ARA suffer from rapidly progressive skin thickening, and are more likely to develop diffuse cutaneous SSc than ATA-positive patients with SSc [50]. ARA are also correlated to high risk for the development of severe renal crisis (SRC), which often develops at the early stage of disease when skin thickness

progresses rapidly [51]. Apart from the abovementioned three autoantibodies, several other autoantibodies have been detected in patients with SSc, including anti-fibrillarin antibodies, anti-PM-Scl antibodies and anti-Th/To antibodies. These antibodies are also associated with certain clinical feature of the disease as described in Table 2.

Although the abovementioned autoantibodies show significant values in diagnosis and prognosis of SSc, their roles in pathogenesis of the disease are still largely unknown.

Table 3. Autoantibodies and their association with organ involvement in SSc

Autoantibodies	Prevalence (%)	Clinical association
Anti-topoisomerase 1	15-20	dcSSc, Lung fibrosis
Anti-centremere	20-30	lcSSc, Pulmonary hypertension, esophageal disease, CREST syndrome
Anti-RNA polymerase	20	dcSSc, pulmonary hypertension, renal involvement
Anti-fibrillarin	4	dcSSc, Pulmonary hypertension, renal disease, myositis
Anti-PM-Scl	2-3	Myositis
Anti-U1RNP, anti-Ku, anti-Sm	Rare	Myositis, joint involvement
Anti-Th/To	2-5	lcSSc, Pulmonary hypertension and fibrosis, small bowel

2.1.4.2 Immune cells

Autoimmunity is a key feature of SSc, thus it is conceivable that immune cells play an essential role in the pathogenesis of SSc. Indeed, many immune cells have been suggested to be involved in the development of SSc by initiating autoimmune and inflammatory events which further contributes to the development of vasculopathy and fibrosis [52], [53]. Figure 1 summarizes the role of immune cells in the pathogenesis of SSc.

In the early phase of SSc, infiltration of activated immune cells into the skin or lung is detectable before any sign of fibrosis [12]. These infiltrates are composed predominantly of T cells, and macrophages, but also mast cells and occasionally B cells are detected [12], [54], [55]. Along with the progression of fibrosis and vasculopathy, inflammatory infiltrates contribute to the pathological processes. For example, T cells generate a strong pro-fibrotic effect via cytokine production and direct cellular stimulation. In patients with SSc, Th2 and Th17 cells produce a panel of cytokines such as IL-4, IL-6, IL-13, and IL-17 which are capable to enhance collagen production by myofibroblasts [56], [57], [58], [59], [60], [61]. Besides releasing pro-fibrotic cytokines, T cells are also able to stimulate and to activate fibroblast through direct intercellular contact via CD40-CD154 system [62]. Although present in the fibrotic skin only at low frequency, B cells play an important role in fibrosis of SSc by producing pro-fibrotic autoantibodies and cytokines [63], [64]. Before and during disease development of SSc, various autoantibodies are generated by B cells, some of which stimulate the production of collagen. For example, anti-platelet derived growth factor receptor (PDGFR) autoantibodies are able to recognize and activate native PDGFR on fibroblasts and consequently promote their differentiation to collagen-producing myofibroblasts [63]. In addition, autoantibodies targeting endothelial cells are able to mediate apoptosis of endothelial cells which release pro-inflammatory and pro-fibrotic molecules [65], [64].

Besides T and B cells, macrophages have been shown to take part in the development of SSc. In consistence with the Th2 biased immune response in SSc, macrophages in patients with SSc display alternative activation phenotypes (M2), which is driven by Th-2 related cytokines and characterized by strong pro-fibrotic effects [66]. Upon activation, macrophages promote inflammation and fibrosis by producing cytokines such as pro-fibrotic factor PDGF and chemoattractant CCL2 [67], [68].

Taken together, accumulating evidences suggest a critical role of immune cells in pathogenesis of SSc. However, these data are primarily obtained from clinical observations or *in vitro* experiments with human cells, while the functions of individual immune cell types and interactions among theses cells or between immune cells and target organs have not been investigated *in vivo* due to lack of proper animal models. Therefore, animal models and especially humanized models for SSc are required to address these crucial issues.

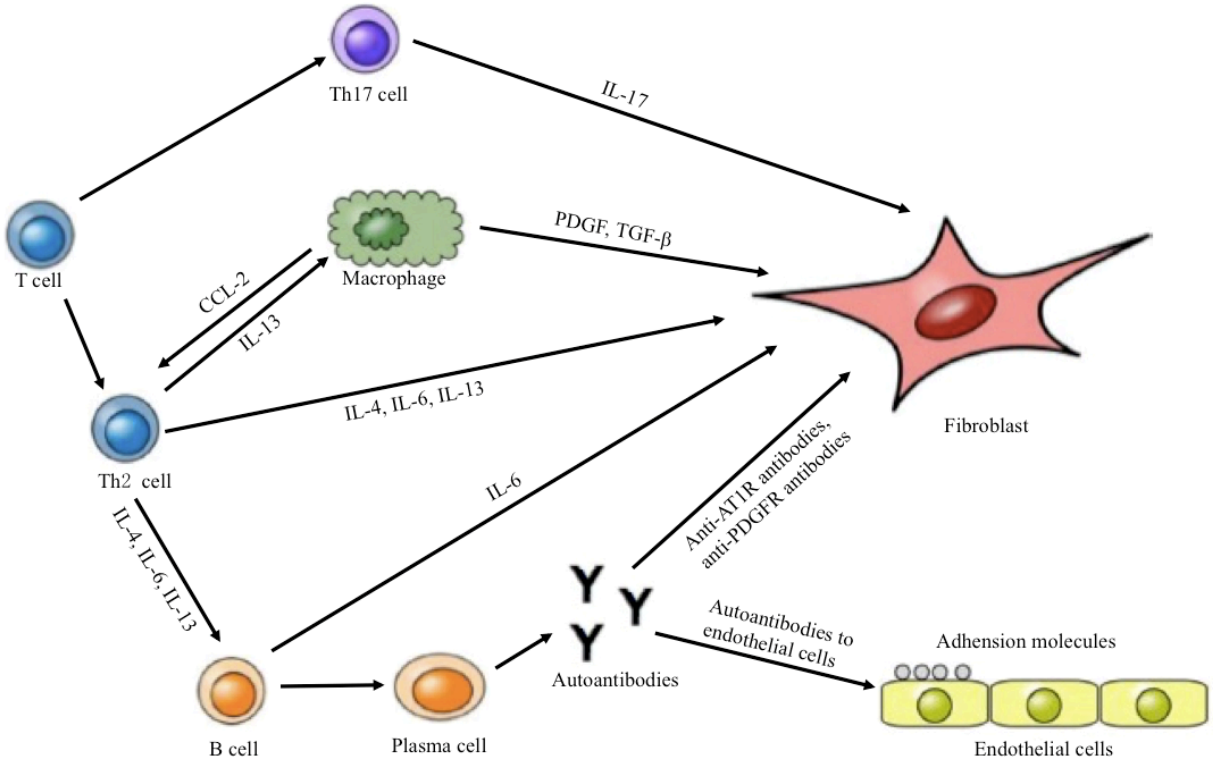

Figure 1. Pathogenic roles of immune cells in SSc.
In SSc patients, multiple immune cells interact with each other and contribute to the progression of fibrosis and vascular dysregulation.

2.2 Angiotensin II type 1 receptor (AT1R) in SSc

2.2.1 Angiotensin and angiotensin receptors

Angiotensin II (Ang II) is the active peptide of the renin angiotensin system that plays a crucial role in controlling blood pressure [69]. In humans, Ang II receptors contain two subtypes, type 1 (AT1R) and type 2 (AT2R), both of which are G protein coupled receptors (GPCR) with typical structure of 7 transmembrane domains. Although both types of receptors interact with Ang II, the classical biological actions of Ang II are mediated by AT1R [70], [71]. Under physiological conditions, activation of AT1R can elevates blood pressure by increasing vasoconstriction, enhancing cardiac contractility, as-well-as augmenting renal tubular sodium reabsorption [72]. In

addition to homeostatic functions, AT1R has been reported to be involved in several pathological processes, such as inflammatory responses, fibrosis and oxidative stress [73], [74], [75] (figure 2).

There is accumulating evidence indicating that AT1R signaling is involved in several pivotal events in inflammatory processes. First, activation of AT1R can promote inflammation by dysregulating vessel endothelium. Under inflammatory conditions, activation of AT1R by excessive local Ang II increases the permeability of the vessel wall by augmenting the expression of vascular endothelial growth factor (VEGF) and prostaglandins. This facilitates the migration of inflammatory cells into target areas [76], [73]. The activation of AT1R on endothelial cells and smooth muscle cells also elevates the expression of adhesion molecules, such as P and L selectin, vascular cell adhesion molecules-1 (VCAM-1), and inter-cellular adhesion molecules-1 (ICAM-1), which promote the recruitment of immune cells to the site of inflammation [77], [78], [79]. Additionally, activation of AT1R on immune cells contributes to inflammation processes by increasing their activities and enhancing production of pro-inflammatory cytokines and chemokines.

Dendritic cells (DCs) are highly specialized antigen-presenting cells, which are crucial for inflammation defense and immune response [80]. The stimulation of AT1R on DCs by Ang II can enhance their maturation and migration, promote production of pro-inflammatory cytokines, and elevate their antigen presenting ability [81], [82], [83]. Besides DCs, macrophages are also regulated by AT1R. In response to Ang II, macrophages produce elevated levels of monocyte chemoattractant proteins, such as CCL-2 and CCL-8, which can recruit various immune cells into sites of inflammation [84], [85]. Moreover, under inflammatory condition, classically activated macrophages with pro-inflammatory features shift to alternatively activated macrophage with anti-inflammatory features when AT1R signaling is blocked. This suggests that AT1R activation is important for pro-inflammatory characteristics of macrophages [86], [87]. In addition, AT1R can also mediate inflammatory response of neutrophils. Activation of neutrophils by AT1R not only induces the production of IL-8 and macrophage inflammatory protein 2 (MIP-2), but also augments the neutrophil migration and stimulates interaction between leukocytes and endothelial cells [88], [89].

Beside innate immune cells, adaptive immune cells are also regulated by AT1R. Upon activation of AT1R, T cells increase expression of CD69, an early activation marker, as-well-as tissue-

homing receptor CD44 and CCR5 that contribute to the development of specialized immune responses [90]. Furthermore, it has been reported that Ang II can enhance the production of IFN-γ and TNF-α, which enhances a Th1 immune response [91], [92].

Fibrosis is a pathological process, in which the extracellular matrix (ECM) is over-produced in organs, which consequently leads to the impairment of their functions [92]. Numerous studies have demonstrated that AT1R is involved in the fibrogenesis [74], [93], [94], [95], [96], [97], [98]. Activation of AT1R by Ang II can result in renal fibrosis through increased expression and synthesis of ECM in renal mesangial cells, interstitial fibroblast, and tubular cells [74], [93], [94]. Studies *in vitro* have demonstrated further that the pro-fibrotic effect of Ang II is mediated by stimulating the production of transforming growth factor β (TGF-β) [95], [96]. Similarly, AT1R signaling is also involved in the development of cardiac fibrosis. One study using a rat model found that in response to Ang II perfusion, the expression of fibronectin and collagen I & IV were elevated in heart tissue, and fibrosis was identified in the interstitium and around vessels [97]. They also could show that treatment with losartan, a specific AT1R antagonist, can ameliorate cardiac fibrosis, further confirming the pro-fibrotic effect of AT1R signaling [97]. Finally, AT1R has also been suggested to play a role in dermal fibrosis by a study reported by Stawski and colleagues [98]. In this study continuous stimulation of AT1R by Ang II cause an elevated expression of pro-fibrotic cytokines, TGF-β and CTGF, and the over-production and accumulation of collagen in the skin [98].

Oxidative stress is a pathological condition, in which excessive reactive oxygen species (ROS) are produced and subsequently cause injuries in organs and tissues [99]. Accumulating evidence supports an association of AT1R activation with excessive ROS production. Upon stimulation of AT1R, both level and activity of NAD(P)H oxidases, a main source of ROS, are increased in several types of vessel cells which promotes the ROS production and leads to vascular inflammation and remodeling [75], [99], [100]. Another two sources of ROS, xanthine oxidase and mitochondria, are also enhanced by the activation of AT1R [101], [102]. By mediating oxidative stress, AT1R extends its role from inflammation and fibrosis to many other pathological processes, such as vascular damage, age-associated organ failures, and tissue injury [99], [103].

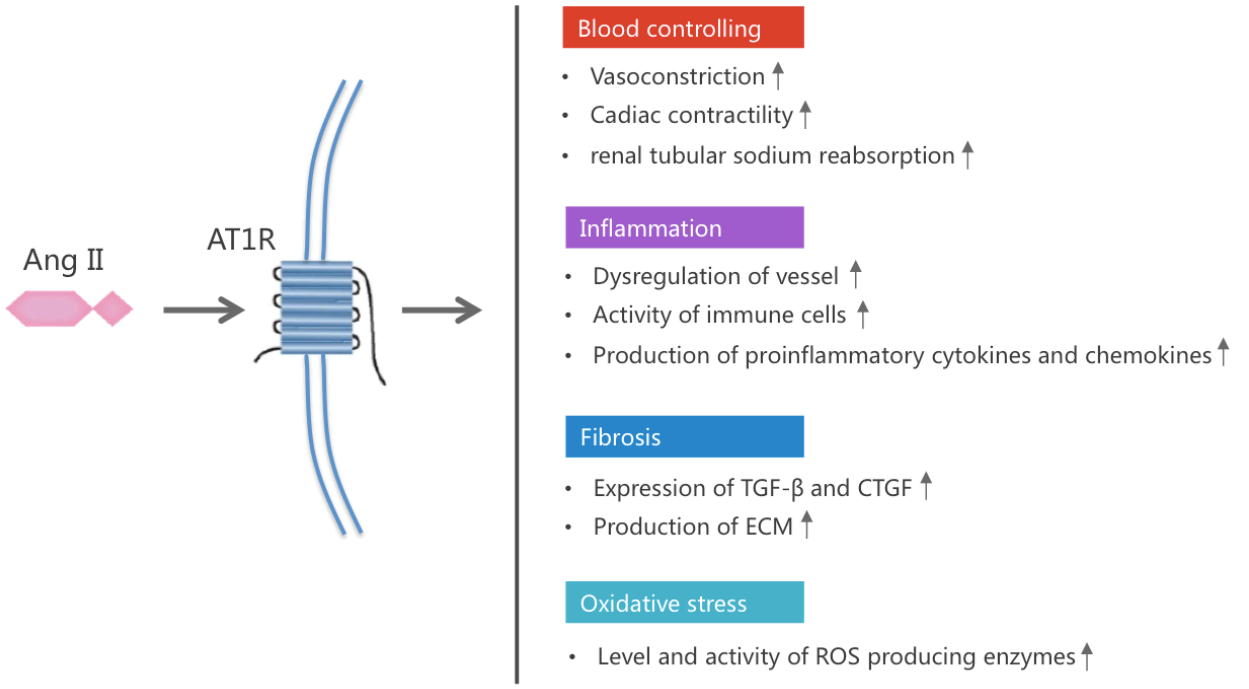

Figure 2. The physiological and pathological effects of AT1R.
Upon activation by Ang II, AT1R is able to contribute to a large spectrum of homeostatic and pathological processes, such as blood controlling, inflammation, fiborsis and oxidative stress. Ang II: Angiotensin II; AT1R: angiotensin type 1 receptor; AT2R: angiotensin type 2 receptor; ECM: Extra-cellular matrix; ROS: Reactive oxygen species.

2.2.2 Autoantibodies against AT1R in SSc

Autoantibodies, as a hallmark of SSc, are believed to contribute to the development of SSc [11]. However, among the large numbers of autoantibodies detected in SSc, it is not clear which of these promote diseass. Some clinical evidence and data derived from experiments *in vitro* suggest that autoantibodies against AT1R contributs to the pathogenesis of SSc [104], [105].

In a clinical study, Riemekasten et al. showed that autoantibodies against AT1R are more prevalent in SSc patients than in patients with other autoimmune diseases or healthy controls [106]. Furthermore, levels of anti-AT1R IgG autoantibodies are associated with severe SSc-related complications, including PAH, pulmonary fibrosis, severe renal crisis, and increased risk of mortality [106]. Interestingly, unlike other SSc-associated autoantibodies such as ATA and ACA, anti-AT1R antibodies possess an agonistic effect on its targeting antigen [104], suggesting that these autoantibodies may contribute to the development of SSc by over-activating AT1R.

Under stimulation of IgG isolated from SSc patients (SSc-IgG), arterial endothelial cells exhibit an increased Ca^{2+} influx that can be completely abolished by losartan [104], [105], indicating that anti-AT1R autoantibodies are able to bind and activate AT1R. Via AT1R activation, the anti-AT1R autoantibodies amplify the vasoconstrictive responsiveness of vessels to natural ligand and induce dysfunction of microvascular endothelial cells. This phenomenon is frequently observed in SSc patients and is regard as the pathological basis for vascular leaking and lymphocytes infiltration [107], [108]. Beside the effect on dysregulated vascular homeostasis, anti-AT1R autoantibodies are suspected to promote fibrosis, a main disease feature of SSc. When fibroblasts are challenged with SSc-IgG an increased expression of collagen is observed, which can be blocked by losartan [105]. Therefore, these autoantibodies produce a similar pro-fibrotic effect as Ang II, the nature ligand of AT1R, induces skin fibrosis in mice upon continuous administration [98]. Finally, SSc-IgG have been also demonstrated to be capable to affect inflammation via AT1R, which is another important feature of SSc and is closely associated to vasculopathy and fibrosis [105]. In addition, endothelial cells exposed to SSc-IgG express a dramatically increased level of the pro-inflammatory chemokine IL-8, which can be inhibited by AT1R antagonist [105].

Taken together, this clinical evidence and *in vitro* findings suggest an important role of functional autoantibodies against AT1R in the pathogenesis of SSc, providing a putative candidate of pathogenic autoantibodies for SSc. However, since these effects were induced by SSc patients IgG without specific purification for AT1R, the pathogenic role of anti-AT1R antibodies should to be validated *in vivo* by animal models

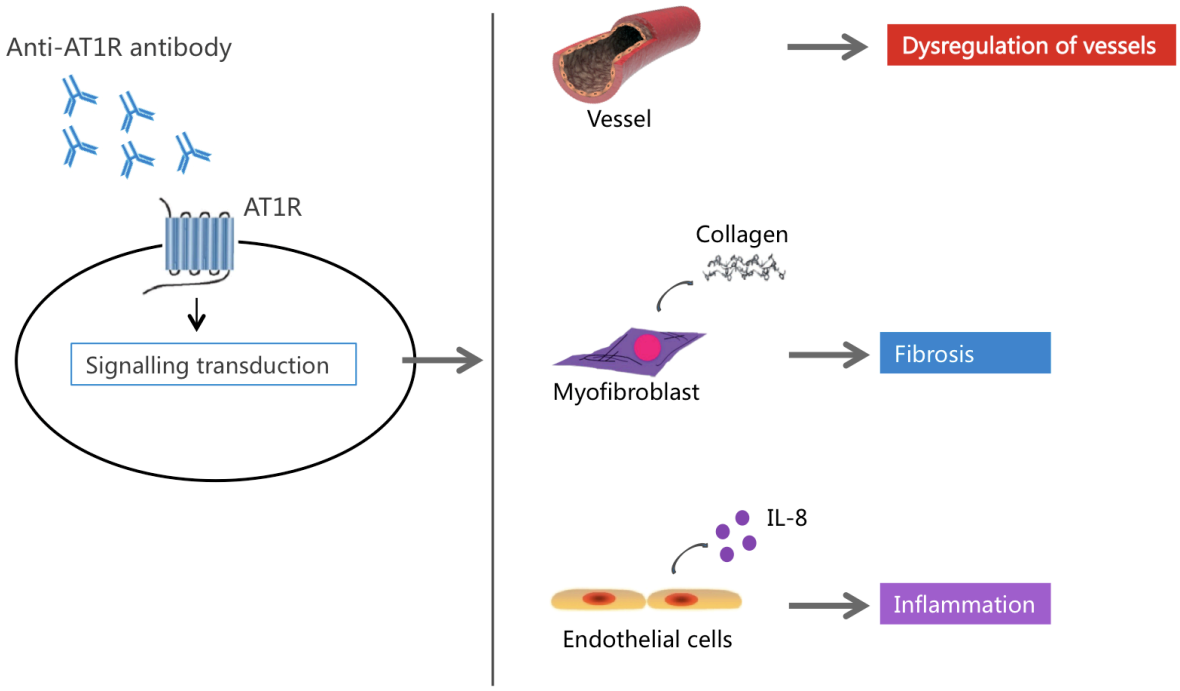

Figure 3. Potential pathological effects of autoantibodies against AT1R.
The anti-AT1R autoantibodies can activate AT1R on multiple cells *in vitro* and subsequently affect vascular homeostasis, fibrosis and inflammation which are linked to SSc pathogenesis.

2.3 SSc animal models

SSc is a complex disease, its heterogeneous nature largely hinders the exploration of the disease pathogenesis. Besides *in vitro* study, animal models are important research tools for the investigation of the pathogenesis of SSc and aide in the search of new therapeutic targets [109]. So far, more than twenty animal models for SSc have been established, each of which resembles at least one hallmark of SSc [109]. These models can be categorized into two groups, genetic models, where mice develop disease due to the genetic mutations or modifications without further experimental manipulations, and induced models, where disease is induced by immunization, transfer of autoimmune components or environmental factors (Table 4).

2.3.1 Genetic models for SSc

The first described genetic model for SSc is tight skin-1 mice (Tsk1) which carry a large in-frame duplication in the Fibrillin 1 gene [110]. Tsk1 mice spontaneously develop skin fibrosis with reduced pliability and elasticity, resembling skin abnormalities observed in SSc patients [111], [112]. This model also presents autoimmunity, a hallmark in SSc, which is characterized by production of anti-topoisomerase I autoantibodies [113], [114], [115]. Although Tsk1 mice develop autoimmunity and skin fibrosis, some SSc features are absent in the model, including (i). Inflammatory infiltrate; (ii). Typical features of SSc related vasculopathy, such as endothelial cells apoptosis, perivascular infiltrates and intimal proliferation of vessels; (iii). ILD, a main cause for SSc related death [116]. In 1995, a second tight skin mouse (Tsk2) was developed as another genetic model for SSc [117], [118]. Tsk2 mice carry a point mutation in the *Col3a1* gene which encodes pro-alpha1 chains of type III collagen, a main component of ECM [119]. Like Tsk1 mice, Tsk2 mice spontaneously develop several SSc-like features, including tight skin, extracellular matrix abnormalities, as-well-as antinuclear antibodies. As compared with Tsk1 mice, Tsk2 mice display mononuclear cell infiltrates in the lower dermis and adipose tissue [120], [121]. However, ILD and vasculopathy are missing in Tsk2 mice [109]. Collectively, the two tight skin mouse models resemble dermal fibrosis and autoimmunity of SSc, which makes them good tools for the investigation of the mechanisms underlying fibrotic processes and immune dysregulation in SSc and the determination of the efficacy of anti-fibrotic or immunomodulatory therapeutics [122].

TGF-β signaling is an essential biological process which controls tissue repair and remodeling, it is also involved in fibrogensis in numerous diseases [123]. In the skin of patients with SSc, the expression of TGF-β is increased and the downstream of the TGF-β signaling pathway is over-activated [124], [55], suggesting an important role of TGF-β in fibrotic processes of the disease. To validate the pro-fibrotic effect of TGF-β in SSc, Sonnylal et al. generated transgenic mice overexpressing TGF-β receptor I specifically on fibroblasts, which was termed as TβRI mice [125]. As compared with littermate controls, TβRI mice show pronounced and generalized fibrosis, skin fibrosis, as-well-as fibrotic thickening of small blood vessel walls in the lung and kidney, recapitulating clinical and histologic features of human SSc [125]. Similar to the TβRI

mice, TβRII△k mice overexpress kinase-deficient human type II TGF-β receptor on fibroblasts, show TGF-β over activity, and develop dermal fibrosis [126]. Additionally, the TβRII△k mice develop fibrosis in the lung [126]. These two TGF-β related genetic models suggest an essential role of TGF-β signaling in the development of tissue fibrosis in SSc.

Vasculopathy is a hallmark of SSc [127], and there are currently several mouse models which express typical vascular pathologies. Among them, Fos-related antigen 2 (Fra-2) transgenic mice are an important model because they recapitulate full pathological features of SSc-related PAH [127]. Fra-2 is a downstream mediator of the profibrotic effects of TGF-β and PDGF. Patients with SSc show a dramatically higher expression of Fra-2 in the affected skin, especially in endothelium and smooth muscle cells of skin vessels, suggesting the involvement of Fra-2 in SSc [128], [129], [130]. Therefore, transgenic mice which overexpress Fra-2 show several key features of SSc, including inflammation, fibrosis, and vasculopathy in multiple organs [131], [127], [132]. Of note, vasculopathy in Fra-2 transgenic mice is of special interest. These mice develop pulmonary vasculopathy, characterized by perivascular inflammation and intimal proliferation, which resembles the pathology of SSc-related PAH [127]. Additionally, they exhibit typical characteristics of SSc-associated skin vascular changes, such as perivascular infiltration, apoptosis of endothelial cells, and severe loss of small blood vessels [131]. Although, Fra-2 transgenic mice show inflammation, fibrosis and vasculopathy, they lack autoimmuninty [133]. Since only a few animal models for SSc show SSc-like vasculopathy, the Fra-2 transgenic mouse model is a valuable tool for the investigation of the pathogenesis of SSc-related vascular complications, especially PAH.

Although more than 20 animal models for SSc have been established, most of them only recapitulate one or two of the three hallmarks of human SSc (Table 3). Only one animal model resembles all three hallmarks of SSc, the Friend leukemia virus integration1 (Fli) and Krüppel-like factor 5 (Klf) double heterozygous ($Fli1^{+/-}$/$Klf5^{+/-}$) mouse [134]. Fli-1, a member of the family of Ets transcription factors, acts as a potent repressor of the type 1 collagen gene and mediates a non-canonical pathway of TGF-β [135]. In patients with SSc, the expression of Fli-1 is suppressed in the skin, implicating a role of Fli-1 in SSc [136]. Mice with target disruption of Fli-1 ($Fli1^{-/-}$ mice) die before the birth, but $Fli1^{+/-}$ heterozygous mice develop normally and do not show obvious phenotypic alterations [135]. Klf5 and Fli-1 synergistically repress CTGF

transcription, and similar to Fli-1, the expression of Klf5 is also suppressed in the skin of patients with SSc [134]. Like $Fli1^{+/-}$ heterozygous mice, $Klf5^{+/-}$ heterozygous mice develop normally and show no evidence of fibrosis. However, $Fli1^{+/-}/Klf5^{+/-}$ double heterozygous mice develop all three hallmarks of human SSc, including autoimmunity as indicated by the production of ANA, fibrosis in the skin and lung, vasculopathy characterized by vascular stenosis and loss of small vessel in skin, and obliterative vasculopathy in the lung [134]. Since $Fli1^{+/-}/Klf5^{+/-}$ mice spontaneously develop most pathologies of human SSc, due to the downregulation of Fli-1 and Klf5, they are an ideal animal model for SSc research and treatment development.

Apart from the above mentioned animal models for SSc, there are several other genetic models, including relaxin knockout mice [137], endothelin 1 transgene mice [138], Wnt-10b transgenic mice [139] and caveolin knock-out mice [140], etc. These SSc models also reveal the role of specific factors in the pathogenesis of SSc, and aide as a comparison with other SSc models when investigating the complex mechanistic network of this disease.

2.3.2 Inducible SSc model

Animal models for SSc can also be established by induction, e.g. immunization, exposure to chemical substance, etc. As early as 1983, graft versus host disease (GVHD) in mice was reported to resemble pathological features in patients with SSc [141]. After immune cells isolated from bone marrow and spleen of B10.D mice are transplanted to lethally irradiated MHC-matched BALB/cJ recipients, the recipients develop tissue fibrosis in numerous organs, including skin, lung, liver, and the intestinal tract, mimicking fibrotic alterations in SSc patients [142], [143]. However, autoimmunity and vasculopathy, another two hallmarks of SSc, are not observed in these BALB/cJ recipients [142], [143]. Since the GVHD model for SSc is induced by transfer of allogeneic immune cells, this model provides a valuable tool to study the activation of immune cells and the consequent development of fibrosis in SSc.

Since numerous observations have suggested a role of reactive ROS in the development of SSc [144], [145], [146], [147], injection of HOCl, one of ROS, has been used to generate another animal model for SSc [148]. Mice treated with HOCl develop skin fibrosis featured by increased thickness and elevated collagen content, display inflammatory infiltrations, and fibrotic changes

in the lung. The kidneys are also affected in HOCl-treated mice, which is characterized by accumulation of collagen in interstitial area, focal infiltration, as-well-as lumen narrowing of small renal arteries [148]. As expected, due to the oxidative property of ROS, the sera of HOCl-treated mice contain a high amount of oxidized proteins such as advanced oxidation protein products (AOPP), similar to SSc patients [148]. Additionally, HOCl-treated mice show autoimmunity, characterized by the production of ATA, one of disease-specific autoantibodies in SSc [148]. A possible mechanism behind this autoimmunity is that the oxidation of DNA topoisomerase-1 which leads to the break of immune tolerance and thus results in the production of ATA. Therefore, although some SSc-related disease manifestations are not observed in HOCl treated mice, such as vasculopathy in skin and lung, this HOCl induced model recapitulates several key features of SSc and confirms the role of ROS in the pathogenesis of SSc.

Given the evidence that some drugs for cancer treatment such as carmustine, methotrexate, bleomycin, can cause tissue fibrosis as a side effect, they can also be used to induce tissue fibrosis in animals [149]. For example, bleomycin, an antibiotic widely used in anti-cancer therapy, is repeatedly injected into the back skin of mice to induce tissue fibrosis. After 4 weeks of treatment, the bleomycin-treated mice develop SSc-like skin pathologies, including thickened skin, compact collagen bindle, inflammatory infiltration, and thickening of vascular walls [149]. Interstitial lung diseases are also observed in bleomycin-treated mice, which are characterized by lung fibrosis, intra-alveolar infiltration, and damaged lung architecture [150]. In the sera of mice treated with bleomycin, a panel of autoantibodies were detected, including ATA, anti-U1-RNP, anti-histone, and anti-ssDNA autoantibodies, all of which are observed in SSc patients [150]. Since bleomycin-induced model mimics the main feature of SSc and can be easily reproduced, it is widely used to study the pathogenesis of inflammation and fibrosis in SSc, and to evaluate the efficacy of new anti-fibrotic therapeutic approaches.

Induced animal model can also be established by immunization with autoantigens. For example, in 2011 Yoshizaki and colleagues reported a novel mouse model for SSc which is induced by immunization with topoisomerase I, a putative autoantigen for the disease [151]. These mice produce anti-topo I autoantibodies and develop SSc-like clinical features, including inflammatory infiltrates and fibrosis in skin and lung. The model is highly beneficial in the study of autoimmunity against topoisomerase I in SSc pathogenesis.

Another induced animal model for SSc of special interest is the humanized mouse model. In this model, keratinocyte and fibroblast isolated from skin biopsies of healthy subjects and SSc patients are used to generate bioengineered skin *in vitro*, which is then engrafted onto the back of SCID mice [152]. In this model, skin from SSc patients exhibited typical SSc phenotypes in the recipient mice as indicated by collagen deposition and fibroblast activation for up to 16 weeks, while skin from healthy donors developed a healthy dermal architecture [152]. Notably, the SSc phenotypes in the skin disappear 24 weeks after engraftment, suggesting that the continuous presence of additional factors is required to maintain the disease manifestation. One of such key factors inducing or stabilizing the SSc phenotype could be the presence of autoantibodies, because the SSc phenotypes could be induced in healthy skin graft by treatment of IgG from SSc patient sera [152]. This humanized mouse model provides a tool for the investigation of the skin fibrosis process, and further manipulation could enhance or extend the features which are similarly seen in patients.

In addition to the abovementioned models, animal models for SSc have been induced by some other strategies, including injection of Ang II [98] and injection of vinyl chloride [153].

Table 4. Summary of current SSc mouse models

Classification	Models name	Autoimmunity	Inflammation	Vasculopathy	Fibrosis
Spontaneous models	Tight skin mice (Tsk/+)	■			■
	Tight skin 2 mice (Tsk2/+)	■	■		■
	Fra-2 transgenic mice		■	■	■
	Relaxin ko mice				■
	MRL/lpr mice lacking IFN-γ receptor		■	■	■
	TβRI mice			■	■
	Endothelin-1 transgenic mice		■	■	■
	Wnt-10b transgenic mice				■
	Caveolin $1^{-/-}$ mice		■		■
	Fli-1 ko mice				■
	Fli1+/− Klf5+/− mice	■	■	■	■
	Endothelium specific Fli-1 ko mice			■	
	Epithelium specific Fli-1 ko mice	■	■		■
	uPAR ko		■	■	■
	SIRT 3 ko mice			■	■
	VEGF transgenic mice			■	■
	Fibroblast specific PTEN ko mice				■
Induced models	Bleomycin treated mice	■	■	■	■
	GVHD Induced systemic sclerosis	■	■		■
	HOCl-injected mice	■	■	■	■
	Vinyl chloride injected mice		■		■
	Angiotensin II induced model		■		■
	Topoisomerase-1 immunization	■	■		■
	Skin-humanized mice			■	

2.4 Hypothesis and aims of the study

Several lines of evidence derived from epidemiological studies and experiments *in vitro* suggest that systemic sclerosis is an autoimmune disease and that AT1R and ETAR are pathogenic autoantigens in the disease. However, a direct proof of these hypotheses by experiments *in vivo* demonstrating the transferability of the disease from human to animal or even between animals or by induction of autoimmunities to the receptors is lacking. In this study, I have tried to tackle both hypotheses by addressing two major goals. The first aim was to establish a novel humanized mouse model for SSc. So far, various animal models have been established and used for the investigation of the pathogenesis of SSc and the determination of the efficacy of therapeutic therapies. However, generalized failures often happen in the translation of promising therapies from laboratory bench to the clinic. Although numerous possible reasons contribute to their failure, it is apparent that mouse models do not fully recapitulate the pathological change of SSc, probably due to species differences in the immune system and microenvironment of target organs [154]. To address this issue, humanized models are favorable. In current study, peripheral blood mononuclear cells (PBMC) were transferred from SSc patients to immunodeficient mice to establish the humanized SSc mouse model, with which the pathogenicity of immune cells of the patients was determined.

The second aim of this study was to evaluate the pathogenicity of autoimmunity against AT1R *in vivo*. As aforementioned, previous studies have demonstrated that autoantibodies against AT1R in SSc patients are functional and associated with severity, progression and mortality of the disease [105], [106], suggesting that autoimmunity against AT1R is involved in the pathogenesis of SSc. However, this hypothesis has not been validated *in vivo*. Therefore, a novel active SSc mouse model was established by immunization with human AT1R. Using this model, the pathogenicity of autoimmunity to AT1R was evaluated.

3. Materials and methods

3.1 Materials

3.1.1 Equipment and consumables

Name	Manufacturer
Absorbance reader	Tecan Trading AG, Switzerland
Analytical balance	Sartorius research GmbH, Germany
Balance	Kern&Sohn GmbH, Germany
Biological safety cabinet	Thermo Fisher scientific, USA
Cannula	B. Braun melsungen AG, Germany
Cassette for paraffin embedding	VWR International GmbH, Germany
Cell culture plates	Corning Incorporated, USA
Cells counter	Schärfe system GmbH, Germany
Centrifuge	Hettich lab technology, Germany
Confocal microscope	Leica Microsystems, Germany
Cytocentrifuge	Thermo Fisher scientific, USA
Electronic pressure pot	Instant pot company, Germnay
Fluid aspiration system	Vacuubrand GmbH, Germany
Heating plate	Heidolph instrument, Germany
Heating stage	Medite GmbH, Germany
Image acquisition system	Nikon Corporation, Japan
Luer syringe	Beckton Dickinson, USA
Micro-emulsifying needle	Merck KGaA, Germany
Microscope	Olympus corporation, Japan
Microtome	Leica biosystems nussloch, Germany
Microtome blade	Feather safety razor Co., Ltd, Japan
Mini centrifuge	Carl Roth GmbH, Germany
Molds for cryo-embedding	Sakura Finetek Europe, Netherlands
Multi-channel pipettes	Sartorius research GmbH, Germany

Needles	Beckton Dickinson, USA
O.C.T. (optimum cutting temperature) compound	Sakura Finetek Europe, Netherlands
Orbital shaker	Gesellschaft für Labortechnik mbH, Germany
PAP pen	Kisker Biotech GmbH & Co. KG, Germany
Paraffin embedding workstation	Thermo Fisher scientific, USA
PH meter	Knick Elektronische Messgeräte GmbH, Germany
Pipette controller	Brand GmbH + CO KG, Germany
Protein G column (Hitrap protein G HP)	GE Healthcare， UK
RNAse free tubes	Sarstedt, AG&Co, Germany
Scissors and forceps	Karl Hammacher GmbH, Germany
SepMate-50 tube	Stemcell technologies incoporation, Germany
Serum collection tubes	Beckton Dickinson, USA
Single channel pipettes	Brand GmbH + CO KG, Germany
Slides	R. Langenbrinck GmbH, Germany
Spectrophotometer	Thermo Fisher scientific, USA
Spin tissue processor	Thermo Fisher scientific, USA
Syringe	B. Braun melsungen AG, Germany
Thermocycler	Bio-Rad Laboratories GmbH, USA
Pipette tips (10µl, 100µl, 1000µl)	Sarstedt, AG&Co, Germany
Ultra-low freezer	Thermo Fisher scientific, USA
Ultrasonicator	Branson Ultrasonics, USA
Vortex mixer	Scienfific industries, inc, USA
Water bath	Gesellschaft für Labortechnik mbH, Germany

3.1.2 Reagents and chemicals

Name	Company	Catalogue number
1 mol/L HCL	Merck KGaA, Germany	1.09057.9010
1 mol/L NaOH	Merck KGaA, Germany	1.09137.9010
30% H_2O_2 solution	Carl Roth, Germany	9681.4
4% Formalin	Carl Roth GmbH, + Co. KG, Germany	P087.1
Acetic acid	Merck KGaA, Germany	1.00063.1000
Bouin`s solution	Sigma Aldrich chemie GmbH, Germany	HT10132-1L
Bovine serum albumin	PAA laboratories GmbH, Germany	K41-001
Citric acid	Merck KGaA, Germany	1.00244.1000
EDTA	Merck KGaA, Germany	1.08418.0250
Eosin G	Carl Roth GmbH, + Co. KG, Germany	3137.2
Ethanol	Sigma Aldrich chemie GmbH, Germany	32205
Fetal bovine serum	PAN biotech, Germany	P100703
Giemsa stain solution	Sigma-aldrich international GmbH, Germany	GS1L-1L
Glycine	Carl Roth, Germany	3790.3
Hematoxylin Gill II	Carl Roth GmbH, + Co. KG, Germany	T864.2
KCl	Merck KGaA, Germany	1.04936.0500
KH_2PO_4	Merck KGaA, Germany	A434173
L-Glutamin	PAN biotech, Germany	P04-80050
May-Grünwald solution	Sigma-aldrich international GmbH, Germany	MG1L-1L
Mounting medium	Merck KGaA, Germany	1.07961.0500

Na_2HPO_4	Merck KGaA, Germany	1.06580.1000
NaCl	Merck KGaA, Germany	1.06404.5000
$NaCO_3$	Merck KGaA, Germany	1.06392.1000
NH_4Cl	Merck Chemicals, Germany	1011450500
Paraffin	Sigma-aldrich international GmbH, Germany	327204
Pepsin	Sigma Aldrich chemie GmbH, Germany	P7012
PEST (penicillin and streptomycin)	PAN biotech, Germany	P06-07100
RPMI 1640 medium	Biochrom GmbH, Germany	FG1415
TMB solution	eBioscience incorporation	00-4201-56
Tris base	Biomol, Germany	CDX-T0244

3.1.3 Buffers and Solutions

Name	Recipe
2% acitic acid	Acitic acid: 2 ml Deionized water: 98 ml
3% H_2O_2 solution	30 % H_2O_2 solution: 1 ml PBS: 9 ml
Antigen retrieval buffer Citrate acid (PH=6)	Tri-sodium citrate: 2.94 g Milli Q water: 1000 ml Mix, adjust pH to 6.0 with 1 mol/L HCl
Blocking solution	BSA: 0.5g PBS: 10 ml
Collagen extraction buffer	Absolute acetic acid: 1 ml Milli Q water: 34 ml Pepsin: 3.5 mg
Elution buffer (0.1 M glycine-HCl, pH=2.7)	Glycine: 7.5 g Milli Q water: 1000 ml Adjust pH to 2.7 with 1 mol/L HCl
Medium	Fetal bovine serum: 50 ml L-Glutamin: 5 ml PEST: 5 ml RPMI 1640: 440 ml
Neutralization buffer (1 M Tris-HCl, pH=9.0)	Tris base: 121 g Milli Q water: 1000 ml Adjust pH to 9.0 with 1 mol/L HCl
PBS	NaCl: 8 g KCl: 0.2 g Na_2HPO_4: 1.15 g KH_2PO_4: 0.2 g Milli Q water: 1 L

Red blood cells lysis buffer	NH_4Cl: 8.34 g EDTA: 0.037 g $NaCO_3$: 1.0 g Milli Q water: 1000 ml Adjust pH to 7.2--7.4
Stop solution (for stopping lysis of red blood cells)	Fetal bovine serum: 20 ml PBS: 1000 ml

3.1.4 Antibodies

Name	Company	Catalogue number
Alex546 Goat anti rat IgG	Thermo Fisher scientific, USA	A-11081
APC mouse anti human CD8	Biolegend incorporation, USA	344722
Biotin goat anti mouse IgG	Jackson immunoresearch, USA	115-066-062
Biotin goat anti-rabbit IgG	Jackson immunoresearch, USA	111-065-144
Biotin goat anti-rat IgG	Jackson immunoresearch, USA	112-066-003
BV421 mouse anti human CD3	Biolegend incorporation, USA	300434
BV650 mouse anti human CD4	Biolegend incorporation, USA	300536
Dylight 649 Goat anti mouse IgG	Biolegend incorporation, USA	405312
FITC-mouse-anti-human CD45	Biolegend incorporation, USA	368508
Mouse anti human CD20	Dako, USA	M0755
Mouse anti human IgG Fc	Southern biotech	9040-01
Percp/cy5.5 mouse anti human CD20	Biolegend incorporation, USA	302326
Rabbit anti mouse CD3	Abcam biotechnology company, HongKong	Ab5690
Rat anti mouse CD31	Biolegend incorporation, USA	102401
Rat anti mouse CD45R	eBioscience incorporation, USA	14-0452

Rat anti mouse complement 3	Cedarlane laboratories corporation, Canada	RMC11H9
Rat anti mouse Mac3	Biolegend incorporation, USA	108501
Rat anti mouse neutrophil	Cedarlane laboratories corporation, Canada	CL8993AP

3.1.5 Kits

Name	Company	Catalogue number
ABC kit	Vector laboratory, USA	PK-6100
Anti-AT1R autoantibodies detection kit	CellTrend GmbH, Germany	12000
Anti-ETAR autoantibodies detection kit	CellTrend GmbH, Germany	12100
Apoptosis detection kit	Promega biotechnology company, USA	G3250
Biotin-avidin blocking kit	Vector laboratory, USA	SP-2001
DAB kit	Vector laboratory, USA	SK-4100
Lunaris mouse 12-plex cytokines kit	AYOXXA biosystems, Germany	LHC-10121S
Masson trichrome stain kit	Sigma-aldrich international GmbH, Germany	HT15-1KT
Sircol soluble collagen kit	Biocolor, UK	S1000

3.2 Methods

Patients and healthy subjects

Seven patients with SSc were enrolled at the Department of Rheumatology, University of Lübeck, Germany. All patients were diagnosed according to standards defined by criteria of the American–European Consensus Group [155]. Four healthy controls were recruited from the Research Center Borstel. All volunteers agreed by written informed consent. Approval for these studies was obtained from the institutional ethics committee of the University of Lübeck.

Mice

Female C57BL/6J mice and female RAG2 and IL-2 receptor gamma chain double knockout mice ($Rag2^{-/-}/IL2rg^{-/-}$) were purchased from the Charles River Laboratories and Taconic Biosciences, respectively. All mice were housed under specified pathogen free conditions with 12 hour light/darkness cycles at the animal facility at Research Center Borstel. All animal studies have been reviewed and approved by the Animal Research Ethics Board of the Ministry of Environment, Kiel, Germany.

Human PBMC isolation and transfer

45 ml of peripheral blood from healthy donors or patients with SSc were collected and placed into 50 ml tubes containing heparin. To isolate human PBMC, Sepmate-50 density gradient centrifugation kit was used. Blood samples were diluted with equal volume of PBS containing 2% of fetal cow serum (FCS), then transferred to 50 ml Sepmate-50 tubes containing density gradient medium. After 10 minutes of centrifugation at 1200g at room temperature, the top layer of cells was collected into new 50 ml tubes. The collected cells were washed with PBS containing 2% FCS three times. Finally, the number of cells were counted, and then resuspended in RPMI1640 medium at a concentration of 1×10^8 cells/ml. For the transfer of the cells, 2×10^7 cells were injected intraperitoneally into each $Rag2^{-/-}/IL2rg^{-/-}$ mouse.

Serum preparation

To collect murine peripheral blood, mice were fixed in a holder. 100 µl of blood was collected from a small incision at the tip of the tail. The collected blood samples were incubated at room temperature for 30 min, centrifuged at 6000g for 10 min, then the supernatant (sera) was collected. Serum samples were transferred to sterilized tubes and stored at -80°C.

Cell isolation from murine blood

To isolate cells from murine blood, 100 µl of blood was collected from each mouse into a 1.5 ml tube containing 20 µl heparin solution. After collection, the collection tubes were gently mixed by inverting 8-10 times. Subsequently, the mixed blood samples were centrifuged for 10 min, at 500g, at 8°C to separate the plasma. The blood cell pellets were suspended with 1 ml red blood cell (RBC) lysis buffer and transferred to a 15 ml tube containing another 4 ml RBC lysis buffer to disrupt the erythrocytes. After 3 minutes of incubation, 10-15 ml of stop solution was added into the tube to stop the RBC lysis, then samples were centrifuged at 300g, at 4°C, for 10 min. Cell pellets were suspended and washed twice with cold PBS. Finally, numbers of cells were counted, 1 x 10^6 cells were used for flow cytometric analysis.

Cell isolation from mouse spleen

After mice were sacrificed using CO_2, the spleen was collected into a 15 ml tube with 5 ml cold RPMI1640 medium. The spleen was dissociated by gently meshing in cold RPMI1640 medium, and the dissociated spleen solution was filtered by passing a 70 µm cell strainer. Single cell suspension passed through the cell strainer was centrifuged at 300g, for 5 min, 4°C, then the cell pellets were incubated with RBC lysis buffer to remove the erythrocytes. After being washed with cold PBS twice, cells were resuspended in PBS and counted, 1 x 10^6 cells were used for flow cytometric analysis.

Flow Cytometry

One million cells from each sample were used for flow cytometric analysis. Prior to staining with fluorescent antibodies, cells were washed once with FACS buffer (PBS with 0.1% BSA). Then cells were incubated with corresponding fluorescent antibody mixture including Fc blocking antibody in 100 µl FACS buffer in a dark place at 4°C for 20 min. The antibody mixture used for the detection of human PBMC was composed of the following fluorescent chromes conjugated antibodies: BV421-mouse-anti-human CD3 (UCHT1, biolegend, USA), BV650-mouse-anti-human CD4 (2RPA-T4, biolegend, USA), APC-mouse-anti human CD8 (SK1, biolegend, USA), Percp/cy5.5-mouse-anti-human CD20 (2H7, biolegend, USA) and FITC-mouse-anti-human CD45 (2D1, biolegend, USA). After the incubation, cells were washed twice with 200 µl FACS buffer and then resuspended in 200 µl FACS buffer, and finally fixed by adding 50 µl of 4% paraformaldehyde solution. The fixed samples were measured by using LSR II flow cytometer (BD, USA) within three days, and the data was analyzed using FACS Express software (De Novo Software, USA, version 5).

Detection of human IgG in murine sera

Levels of human total IgG in immunodeficient mice received PBMC from SSc patients or healthy controls were determined using ELISA. First, a 96-well ELISA plate was coated with goat anti-human IgG, and subsequently incubated with serum samples prepared in log dilutions starting from $1:10^2$ to $1:10^7$. After washing steps, incubation with HRP-conjugated goat anti-human IgG antibody at room temperature for 1 hour, TMB was used for visualization. OD value was measured at 450 nm on a microreader (Tecan life science, Switzerland), then plotted against $\log_{10}$ scaled-dilution. The levels of human IgG were defined as the dilution at which the OD value reached the half of maximal OD values of the curve. Human IgG against AT1R or ETAR in the recipient mice were detected using commercial ELISA Kit (Celltrend, Germany) according to the manual. In brief, plates coated with membrane extract from CHO cells overexpressing human AT1R or human ETAR (Celltrend, Germany) were incubated with serum samples diluted at 1:100. After incubation with HRP-conjugated goat anti-human IgG antibody at room temperature for 1 hour, the signal was visualized by TMB. OD value was measured at 450 nm on a microreader (Tecan life science, Switzerland).

Immunization with human AT1R

Eight to nine week old female C57BL/6J mice were immunized with 0.2 mg of membrane extracts prepared from CHO cells overexpressing human AT1R in 50 µl PBS emulsified with an equal volume of complete Freund adjuvant (CFA, Sigma-Aldrich, USA) by subcutaneous injection into the footpad. Three weeks after the primary immunization, mice were boosted with the same amount of human AT1R emulsified with complete Freund adjuvant (IFA, Sigma-Aldrich, USA). In the control group, mice were treated with the same amount of membrane extract from untransfected CHO cells (ME). Six weeks after booster immunization, all mice were sacrificed for sample collection and evaluation of disease characteristics.

Differential leukocyte counting of Bronchoalveolar lavage fluids (BALF)

Immediately after scarifying the mice by CO_2, mice were fixed at supine position, skin and muscle on neck were removed to expose trachea. Afterwards, cannulas were inserted into the respiratory tract, and 1 ml PBS was injected slowly into the lung. Subsequently, BALF were collected and the total number of cells was counted by a hemocytometer. After centrifugation at 500 g for 5 min, cell pellets of the BALF were resuspended in PBS containing 30% of fetal bovine serum (FBS, PAN biotech, Germany), and cell suspensions were spun down onto slides and stained with Giemsa May-Grunwald reagent (Sigma-Aldrich, USA). Differential leukocytes were counted and 300 total cells were used for each sample.

Histological assessment

The skin and lung samples were fixed in 4% formalin for 24 hours. After dehydration and paraffinization, tissue samples are embedded in paraffin and sectioned at thickness of 3 µm. To evaluate the histopathology and fibrosis, paraffin sections were first deparaffinized in xylene and rehydrated in gradient ethanol solutions, then stained with hematoxylin and eosin solutions (H&E) (Roth, Germany) or Thrichome Masson staining kit (Sigma-Aldrich, USA), respectively. After dehydration and clearing, the stained sections were mounted. As shown in the below tables, A detailed procedure is summarized in the below tables. Scoring of the inflammation was

performed in blinded manner by two investigators. The inflammatory score was calculated based on the number and area of focal infiltrates or number of affected vessels. Skin thickness was measured as the thickness of the collagen layer.

Dehydration and paraffinization

Step	Reagent	Incubation
1	4% formalin	1 hour
2	70% ethanol	1 hour
3	80% ethanol	1 hour
4	90% ethanol	1 hour
5	96% ethanol	1 hour
6	absolute ethanol	1 hour
7	absolute ethanol	1 hour
8	absolute ethanol	1 hour
9	xylene	1 hour
10	xylene	1 hour
11	paraffin	1 hour and 30 min
12	paraffin	1 hour and 30 min

HE staining

Step	Reagent	Incubation
Deparaffinization	Xylene I	5 min
	Xylene II	5 min
	Xylene III	5 min
Re-hydration	Absolute ethanol I	5 min
	Absolute ethanol II	5 min
	Ethanol 96%	5 min
	Ethanol 70%	5 min
	Tap water	5 min
Staining	Gill's hematoxylin solution (No.2)	20 min
Bluing	running tap water	10 min
Staining	Eosin (1%, acidic) counterstain	3 min
	Tap water	10 seconds
De-hydration	Ethanol 70%	10 seconds
	Ethanol 96% I	10 seconds
	Ethanol 96% II	10 seconds
	Absolute ethanol I	10 seconds
	Absolute ethanol II	3 min
Clearing	Xylene I	5 min
	Xylene II	5 min
	Xylene III	5 min
Mounting	Entellan (Merck)	

Masson staining

Step	reagent	Incubation
Deparaffinization	Xylene I	5 min
	Xylene II	5 min
	Xylene III	5 min
Re-hydration	Absolute ethanol I	5 min
	Absolute ethanol II	5 min
	Ethanol 96%	5 min
	Ethanol 70%	5 min
	Ethanol 40%	5 min
	Deionized water	5 min
Fixation	Bouin`s solution	Overnight, room
	Running tap water	5 min
Staining	Gill's hematoxylin solution (No.2)	5 min
	Running tap water	5 min
	Deionized water	10 seconds
	Biebrich scarlet-Acid Fucshin	5 min
	Deionized water	10 seconds, twice
	Phosphotungstic/Phosphomolybdic Acid solution	5 min
	Aniline Blue solution	5 min
	1% Acetic Acid	1 min and 30 seconds
	Deionized water	10 seconds, twice
De-hydration	Absolute ethanol I	5 min
	Absolute ethanol II	5 min
Clearing	Xylene I	5 min
	Xylene II	5 min
	Xylene III	5 min
Mounting	Entellan (Merck)	

Immunohistochemistry

Immunohistochemistry staining was performed on skin and lung sections after fixation with formalin followed by paraffin embedding. Tissue sections were deparaffinized in xylol and rehydrated in gradient ethanol. Antigen retrieval was performed by heating slides at 121 ℃ in 10 mM citrate buffer (PH 6.0) for 1 hour, endogenous peroxidase, endogenous biotin and unspecific binding was blocked with 3% H_2O_2, biotin blocking solution (Vector, USA) and 5% BSA solution, respectively. Then, sections were incubated overnight at 4°C with primary antibodies against murine CD3 (Polycone, Abcam, HongKong), murine CD45R (RA3-6B2, eBioscience, USA), murine neutrophil marker (07-APR, Cedarlane, Canada), or human CD20 (L26, Dako, USA). Incubation of biotinylated secondary antibody (Polyclone, Jackson immunoreaearch, USA) was conducted for 45 minutes at room temperature, followed by incubation with avidin biotinylated-HRP solution (Vector, USA) for 20 minutes. Diaminobenzidine (Vector Laboratories, USA) was applied to visualize immunoreactivity. Afterwards, the sections were counter-stained with hematoxylin for 5 minutes. Images were taken by bright-field microscopy (Nikon, Japan). The below table summarizes the detailed procedure of the immunohistochemstry staining.

Immunohistochemistry

Step	Reagent	Incubation
Deparaffinization	Xylene I	5 min
	Xylene II	5 min
	Xylene III	5 min
Re-hydration	Absolute ethanol I	5 min
	Absolute ethanol II	5 min
	Ethanol 96%	5 min
	Ethanol 70%	5 min
	Ethanol 40%	5 min
	Deionized water	5 min

Antigen retrieval	10Mm citrate buffer (PH＝6.0)	121°C , 4 (50 min in
Cool down	10Mm citrate buffer (PH＝6.0)	20 min
Blocking endogenous peroxidase	3% H_2O_2 solution	15 min
	PBS	5 min, three times
Blocking endogenous biotin	Avidin solution	15 min
	PBS	5 min
	Biotin solution	15 min
	PBS	5 min, three times
Blocking unspecific binding	5% BSA	50 min
Incubation of primary antibodies	Primary antibodies diluted in PBS	4°C , overnight
	PBS	5 min, three times
Incubation of biotinylated secondary antibodies	Biotinylated secondary antibodies diluted in PBS	50 min, RT
	PBS	5 min, three times
Preparation of avidin and biotinylated HRP complex (ABC solution)	100 ul of avidin solution and 100 ul of biotinylated HRP solution in 5 ml of PBS	30 min, RT
Incubation of ABC solution	ABC solution	30 min, RT
	PBS	5 min, three times
Incubation of DAB solution	84 ul of buffer stock solution, 100 ul of DAB reagent and 80 ul of H_2O_2 in 5 ml of Deionized water	2 min, RT
	Tap water	5 min, three times
Counterstaining	Gill's hematoxylin solution (No.2)	1 min
Bluing	running tap water	5 min
Dehydration	Ethanol 70%	10 seconds
	Ethanol 96% I	10 seconds
	Ethanol 96% II	3 min

	Absolute ethanol I	3 min
	Absolute ethanol II	3 min
Clearing	Xylene I	5 min
	Xylene II	5 min
	Xylene III	5 min
Mounting	Entellan (Merck)	

Immunofluorescence staining

Immunofluorescence staining was used to detect the IgG and complement deposition on 6 µm cryosections prepared from murine lung. IgG deposition in the lung tissue of mice was detected with Dylight 649-labeled goat anti-mouse IgG antibody (Polyclone, Biolegend, USA), and deposition of complement component 3 was detected by indirect immunofluorescence staining with primary rat anti-mouse complement 3 antibody (RMC11H9, Cedarlane, Canada) and Alex-488-conjugated goat anti-rat IgG (Polyclone, Invitrogen, USA) was used as the detecting reagent. Coverslips were mounted with Gold mounting agent (Thermo Fisher, USA). Fluorescence was determined by confocal microscopy (Leica SP5, Germany).

Detection of apoptotic endothelial cells

After fixation in pre-chilled 4% paraformaldehyde solution and blocking with 5% BSA solution, 6 µm cryosections of lung samples were incubated with rat anti-mouse CD31 antibody (390, Biolegend, USA) and subsequently with Alex546 conjugated goat anti-rat IgG (Polyclonal, Thermo Fisher, USA). After labeling endothelial cells, the apoptotic cells were detected with TUNEL kit (Promega, USA) according to the product manual. Briefly, the sections were permeabilized with 0.5% Triton X-100 and equilibrated in 100 ul of equilibration buffer. Immediately before the reaction, the TUNEL mixture was freshly prepared and added to the sections. After incubation at 37°C for 60 min, the sections were immersed in 2x SSC buffer to stop the reaction. Coverslips were mounted with Gold mounting agent (Thermo Fisher, USA).

Fluorescent signals were determined by confocal microscopy (Leica SP5, Germany). To quantify the level of apoptotic endothelial cells, 10 random fields containing vessels were observed from each lung sample; the number of apoptotic endothelial cells and total endothelial cells were counted, then the level of apoptotic endothelial cells were presented as the ratios of apoptotic to total endothelial cells.

Determination of collagen content

To assess the collagen content in tissues, 0.25 mm^2 of skin tissues or post caval lobe of lungs were homogenized in 0.5 M acetic acid solution containing 0.1 mg/ml porcine pepsin, and incubated at 4°C overnight. The pepsin soluble collagen was collected after removal of the insoluble debris, then centrifuged at 12,000g, for 10 min, at 4°C. The extracted collagen was measured by using Sircol collagen detection kit (Biocolor, UK). 10-100 µl of extracted collagen sample was mixed with 1 ml of Sircol dye solution, and incubated on shaker for 30 minutes. Samples were centrifuged at 12000g for 10 minutes, and pellets were washed with 750 µl ice cold acid salt wash buffer. Finally, 250 µl of alkali buffer was added to each sample to release collagen from pellets. OD values of samples were measured on micro-plate reader (Tecan life science, Switzerland) at wavelength of 555 nm. Standard curve was plotted with gradient diluted collagen standard and used for calculating amount of collagen in samples.

Detection of mouse anti-human AT1R antibody (ELISA)

Levels of mouse anti-human AT1R antibodies in sera of immunized mice were determined by using ELISA Kit (Celltrend, Germany) with modification. Briefly, plates coated with membrane extract from CHO cells overexpressing human AT1R (Celltrend, Germany) were incubated with serum samples prepared in log dilutions starting from $1:10^2$ to $1:10^7$. After incubation with HRP-conjugated goat anti-mouse IgG antibody at room temperature for 1 hour, TMB was applied to visualize the signal. OD value was measured at 450 nm on a microreader (Tecan life science, Switzerland), then plotted against dilution (log_{10} scaled). To determine the levels of anti-AT1R antibodies, standard curves were generated using serum samples from an AT1R immunized

mouse. The levels of anti-AT1R antibodies were defined as the dilution at which the OD value reached the half of maximal OD values of the curve.

Purification of serum IgG

IgG from murine serum was purified by affinity chromatography on a HiTrap protein G Affinity column (GE Healthcare, USA). Before loading of sera, the protein G column was washed with 10 column volumes of binding buffer (sterile PBS, pH 7.2-7.6) at a flowrate of 1 ml/min. Sera were added to the column by a Luer syringe after mixing with equal volume of binding buffer (sterile PBS, pH 7.2-7.6). To remove unbound materials, column was washed with 10 column volumes of binding buffer (sterile PBS, pH 7.2-7.6) until no protein could be detected in the flowthrough. Subsequently, 2-5 column volume of elution buffer (0.1M glycine HCl buffer, pH 2.7) was used to elute IgG fractions, and neutralization buffer (1M Tris-HCl buffer, pH 9.0) was added to neutralize the eluted IgG. Finally, the concentration of IgG was determined photometrically at a wavelenght of 280 nm (Nanodrop 1000 spectrophotometer, Thermo Fisher, USA), and IgG was sterilized by filtering with 0.22 μm filter and stored at -80 ℃.

IL-8 release assay

Cells of the human monocyte cell line (THP1) were grown in 48 well plates at the concentration of $8.3x10^6$/ml and treated with 50 μg/ml of IgG purified from ME- or AT1R-immunized mice. In inhibitory studies, Losartan potassium (Sigma-Aldrich, USA) was added 5 hours before IgG treatment. The supernatants were collected 24 hours after IgG stimulation. IL8 concentrations in the supernatants were detected by ELISA according to manufacturer's instructions (Biolegend, USA).

Determination of cytokines in sera and BALF

A 12-plex cytokines kit (AYOXXA biosystem, Germany) was used to determine serum and BALF levels of murine cytokines including IL-1β, IL-2, IL-4, IL-5, IL-6, IL-10, IL-12, IL-13, IL-

17A, IFN-γ, and GM-CSF. Both detection and quantification were performed according to the protocol provided by the manufacturer. Serum and BALF samples were diluted with equal volumes of assay diluent, standard was prepared in serial dilutions at 1:5. Biochips were incubated with the diluted samples at room temperature for 3 hours, the detection antibody mix and SA-PE solution were applied to visualize the signal. Prior to data acquisition, the biochip was washed with wash buffer and dried in bench at dark for at least 1.5 hours. The image of the biochip was acquired using AYOXXA reader (LRS-001, AYOXXA biosystem, Germany).

Transfer of serum IgG

Murine IgG purified from AT1R-immunized mice or control mice was transferred into C57BL/6 mice. Therefore, 50 μg of the respective IgG fraction (1 mg/ml in PBS) was injected intradermally into each mouse ear. Twenty-four hours after the transfer, ear samples were collected for histological assessment.

Statistical analysis

All data are expressed as the mean ± SD. For quantitative data with normal distribution, statistical analysis was performed with two-tailed unpaired Student's t test or one-way ANOVA test. For values that did not follow Gaussian distribution, a two-tailed Mann-Whitney U test was applied. Fisher`s test was used to assess the significance of qualitative data. $P < 0.05$ was considered as statistically significant.

4. Result

4.1 Establishment of a novel humanized mouse model for SSc by transfer of PBMC from patients

Transfer of PBMC from patients into immunodeficient mice is a strategy for establishing humanized mouse models for autoimmune diseases. This strategy has been used for generation of mouse models for many autoimmune disorders [156], but not SSc. Given the important role of autoimmunity in the development of SSc, transferring PBMC from patients with SSc into mice should induce some pathological manifestations. To verify this hypothesis, the experiment was performed following the procedure summarized in figure 4.

The PBMC was isolated from SSc patients and transferred into $Rag2^{-/-}/IL2rg^{-/-}$ mice. These mice lack T cells, B cells, and NK cells which facilitates the survival of the transferred human PBMC. In total, PBMC isolated from 5 SSc patients were transferred into 7 $Rag2^{-/-}/IL2rg^{-/-}$ mice, where each mouse received $2x10^7$ cells from one patient. In the control group, PBMC isolated from 4 healthy donors (HD) were transferred into 8 $Rag2^{-/-}/IL2rg^{-/-}$ mice. When considering the important role of B cells in SSc, I decided to include a further experimental group, in which PBMC isolated from 2 patients treated with rituximab, a B cell-depleting monoclonal antibody, were transferred to 5 $Rag2^{-/-}/IL2rg^{-/-}$ mice. Twelve weeks after the transfer of human PBMC, mice were sacrificed and blood and tissue samples were collected for further evaluation. Detailed information of the patients is summarized in table 5.

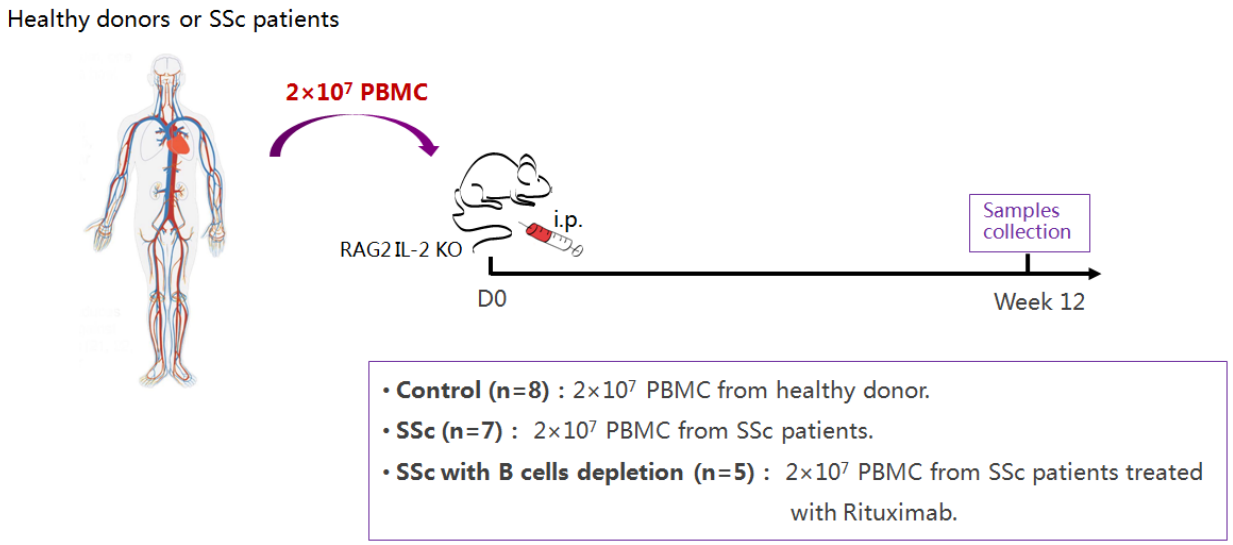

Figure 4. Schematic representation of the adoptive transfer of human PBMC induced mouse model for SSc. PBMCs were isolated from healthy donor and SSc patients, and transferred into RAG2 IL-2 double knock-out mice. 12 weeks after transfer, the organs were collected for disease evaluation.

Table 5. Characteristics of healthy donors and SSc patients.

ID of donor	Gender	Age (years)	SSc subtype	Autoantibodies	Clinical phenotypes							Rituxmab treatment
					Raynaud`s syndrome	Digital ulcer	ILD	PAH	Myalgia	Esophagus involvement	Arthralgia	
G1	F	49	NA	NA	NA	NA	NA	NA	NA	NA	NA	NA
G2	M	55	NA	NA	NA	NA	NA	NA	NA	NA	NA	NA
G3	F	29	NA	NA	NA	NA	NA	NA	NA	NA	NA	NA
G4	F	24	NA	NA	NA	NA	NA	NA	NA	NA	NA	NA
P1	F	76	dcSSc	ANA, ATA, anti-ETAR aab	+	+	+	+	-	-	-	-
P2	F	56	lcSSc	ANA, ACA	+	+	-	+	+	-	+	-
P3	M	69	dcSSc	Anti-PM-Scl aab	+	+	+	-	+	-	+	-
P5	F	48	lcSSc	ANA, ACA	+	+	-	-	-	+	-	-
P6	F	51	lcSSc	ANA, ACA, anti-AT1R aab, anti-ETAR aab	+	+	-	-	-	-	-	-
P8	M	69	dcSSc	NA	+	-	-	+	-	-	-	+
P9	F	34	dcSSc	ANA	+	+	-	-	-	+	+	+

G1-G4: healthy donors, P1-P9: patients with SSc. M: male; F: female; NA: not available; aab: autoantibodies.

4.1.1 Survival and proliferation of human PBMCs in mice

I first determined whether the transferred human PBMC survived in the recipient mice. To do this, I collected blood samples from the recipient mice and detected the presence of human $CD45^+$

leukocytes by flow cytometry. As shown in Figure 5, at week 4 after the transfer via the i.p. injection, human leukocytes were detectable in peripheral blood of recipient mice. At this time points, levels of human leukocytes indicated as percentages of all leukocytes in murine blood were comparable among all three experimental groups. At week 12 after PBMC transfer, when the mice were sacrificed, the mice which received PBMC from SSc patients showed significantly higher levels of human leukocytes than mice which received PBMC from healthy controls (2.6% ± 0.96 vs 0.7% ± 0.85, p= 0.033). Noteworthy, levels of human cells in mice which received PBMC from patients treated with rituximab were significantly lower than those observed in mice transferred with cells from untreated patients (0.31% ± 0.55 vs 2.6% ± 0.96, p=0.036) (Figure 5). As compared with week 4, levels of human leukocytes were significantly elevated 12 weeks after transfer (0.03% ± 0.048 vs 2.6% ± 0.96, p=0.042) in mice received PBMC from SSc patients, but not in the other two groups (Figure 5).

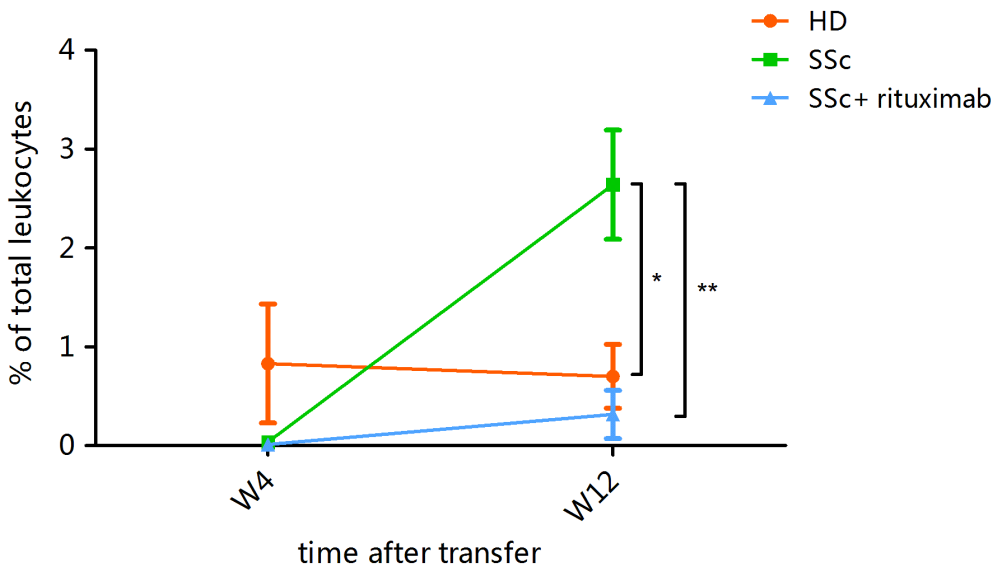

Figure 5. Survival and proliferation of human PBMC in recipient mice.
The presence of human leukocytes in murine blood was detected by flow cytometry at week 4 (W4) and week 12 (W12) after transfer of human PBMC. Human leukocyte levels of cells derived from healthy donors (HD, orange), SSc patients (SSc, green), and SSc patients treated with rituximab (SSc + rituximab, blue) were compared. Levels of human leukocytes were defined as the percentage of human leukocytes of total leukocytes in murine blood. Human leukocytes were identified by their expression of human CD45 using flow cytometry. Total leukocytes were identified according to their morphology. All data are presented as mean ± SD, and statistical analysis was performed using ANOVA (*= $p<0.05$, **=$p<0.01$).

4.1.2 Production of human autoantibodies in recipient mice

Given that the transferred human PBMC survived in the recipient mice, in the next step I investigated their functional activity by determining their production of human IgG. Human IgG was detected in the sera of both groups of mice received PBMC from and HD and PBMC from SSc produced human IgG, and levels of human IgG in the two groups were comparable (Figure 6A). The mice which received PBMC from SSc patients treated with rituximab did not produce any human IgG.

Since autoantibodies are one major hallmark of SSc, I investigated whether the three experimental groups differed from each other in the production of autoantibodies. Specifically, levels of human IgG autoantibodies against AT1R and ETAR which had been suggested to be present in SSc patients and associated disease clinical features were analyzed [157]. As shown in Figure 6B, serum levels of human IgG autoantibodies against AT1R were significantly higher in mice which received PBMC from SSc patients than mice which received PBMC from HD ($p<0.05$). Additionally, mice which received PBMC from SSc patients also produced significantly higher levels of human IgG autoantibodies against ETAR than HD (Figure 6C, $p<0.01$). Furthermore, as expected, mice which received PBMC from SSc patients treated with rituximab did not produce human IgG autoantibodies against AT1R or ETAR.

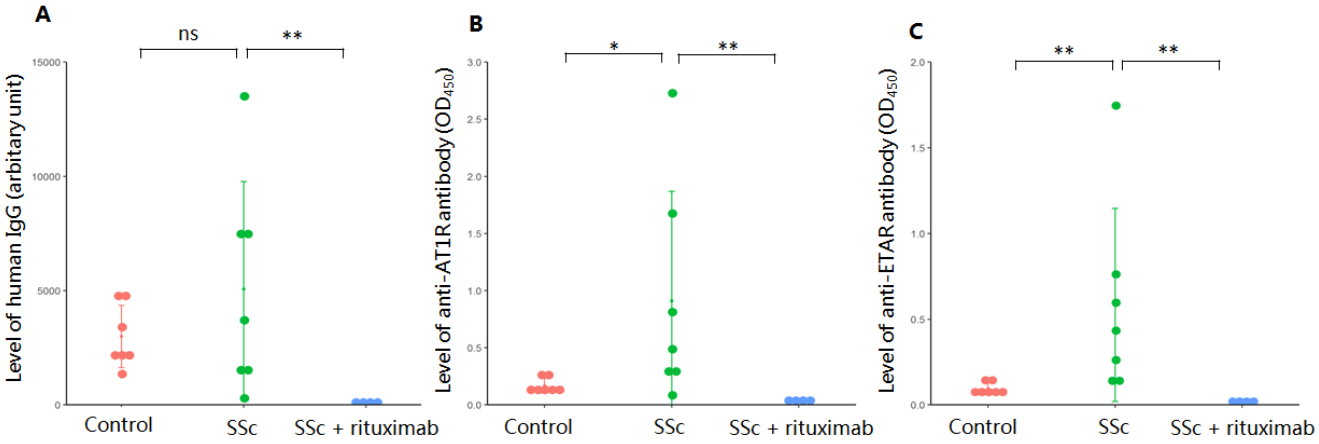

Figure 6. Production of human IgG and autoantibodies in the PBMC transferred mice.
Mice were inoculated with human PBMC, and after 12 weeks sera were collected for the detection of human IgG, anti-AT1R and ETAR autoantibodies. (A) Total human IgG was measured using sandwich ELISA, the IgG levels were presented as arbitrary unit defined as the dilution at which the OD value reached half of the maximal OD values of the curve. Human IgG autoantibodies against AT1R (B) and ETAR (C) were detected by ELISA coated with membrane extracts from CHO cells overexpressing

hAT1R or hETAR, the level of the autoantibodies was measured by OD value at 450 nm. All data are presented as mean ± SD, and statistical analysis was performed using ANOVA (*= $p<0.05$, **=$p<0.01$).

4.1.3 Systemic inflammation in mice received PBMC from SSc patients

To further characterize disease features in the recipient mice, histological analysis was performed to evaluate inflammation and fibrosis in multiple organs including skin, lung, kidney, heart, and muscle. As compared to the mice which received PBMC from HD, the SSc PBMC-transferred mice developed a more severe pulmonary inflammation (6.36 ±7.79 vs 38.21 ±30.37, $p<0.05$) (Figure 7A and 7B), which was characterized by perivascular, peribronchial, as well as intra-alveolar infiltrates (Figure 7A). Prominent inflammatory infiltrates were also observed in the kidneys of the mice which received PBMC from SSc patients, while renal inflammation was significantly lower in mice which received PBMC from HD (0.54 ±0.69 vs 38.58 ±32.85, $p< 0.01$) (Figure 7C and 7D). The muscle tissue was also affected where five out of seven mice which received PBMC from SSc patients showed severe infiltrates around muscle bundles, whereas none of the eight mice which received PBMC from HD showed such inflammation (Figure 7E and F. $p<0.05$). Unexpectedly, no obvious histological change was observed in the skin in any experimental groups (Figure 7G and 7H). In addition, all mice were free of inflammation in the heart (data not shown).

Notably, in contrast to mice received PBMC from SSc patients, no inflammatory symptoms were detected in mice which received PBMC from SSc patients treated with rituximab (Figure 7).

Analysis of fibrosis in the SSc target organs by Masson staining revealed that, in spite of the severe inflammation seen, fibrosis was not observed in any tissue of the experimental mice (data not shown).

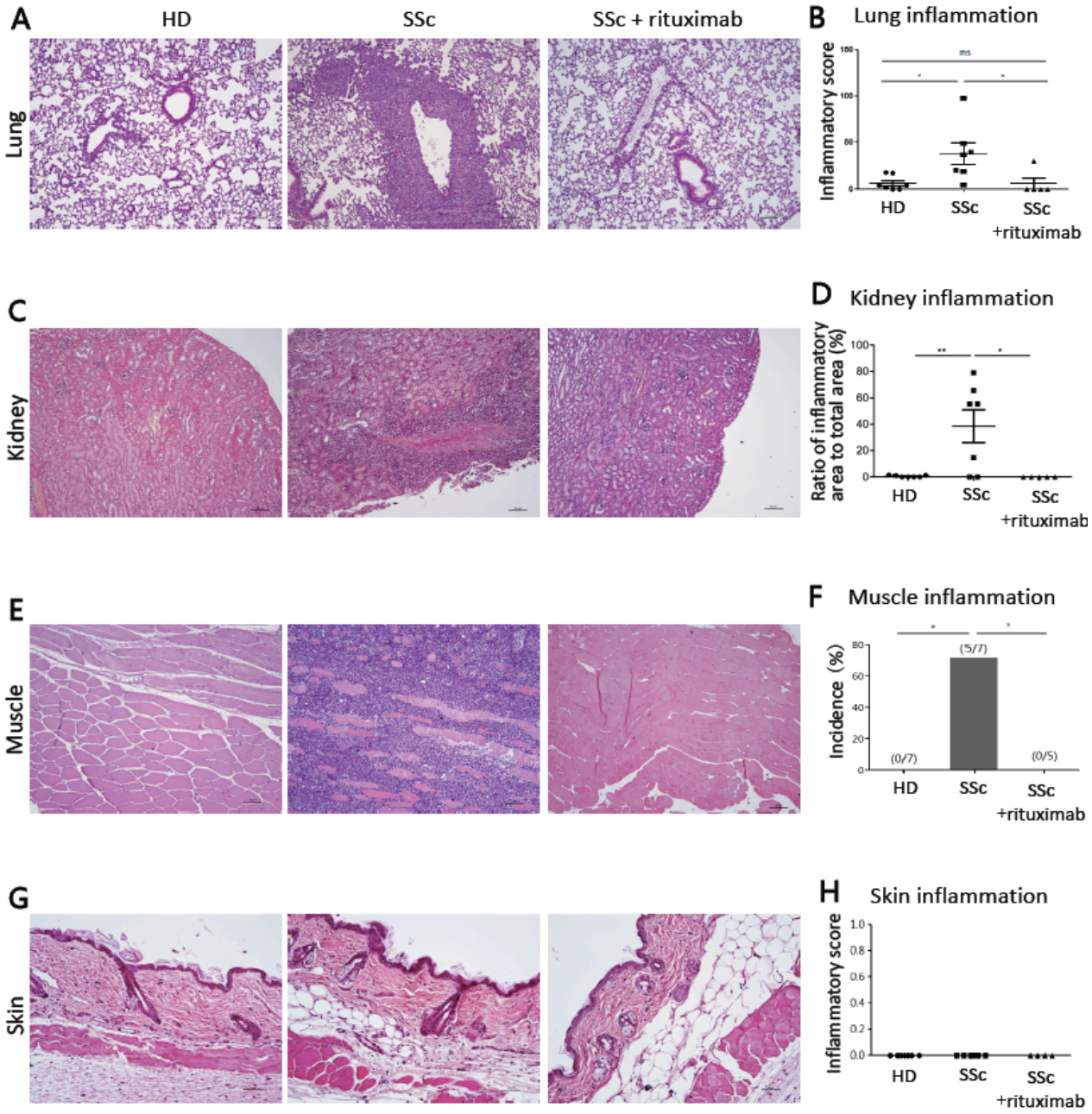

Figure 7. Development of systemic inflammation in PBMC transferred mice.
Histology of (A) lung, (C) kidney, (E) muscle and (G) skin were evaluated by H&E staining in mice transplanted with PBMC from healthy donors (HD), SSc patients (SSc) or SSc patients treated with rituximab (SSc + rituximab). Representative histologic images (A, C, E, G) and results of quantitative analysis (B, D, F, H) are shown (100x). The severity or incidence of inflammation in each organ was evaluated in a blinded manner. Statistical analysis was performed using ANOVA and Fisher`s test (* = $p<0.05$)

6.1.4. B cells are dominant in the inflammatory infiltrates

Given the lack of inflammation in mice received PBMC from SSc patients treated with rituximab, we hypothesized that B cells are the major cell type in the infiltrates. To verify this hypothesis, we performed immunohistochemistry to determine human B cells in the infiltrates. As shown in Figure 8, human $CD20^+$ B cells were the main infiltrative cells in the lung, kidney, and muscle of mice which received PBMC from SSc patients.

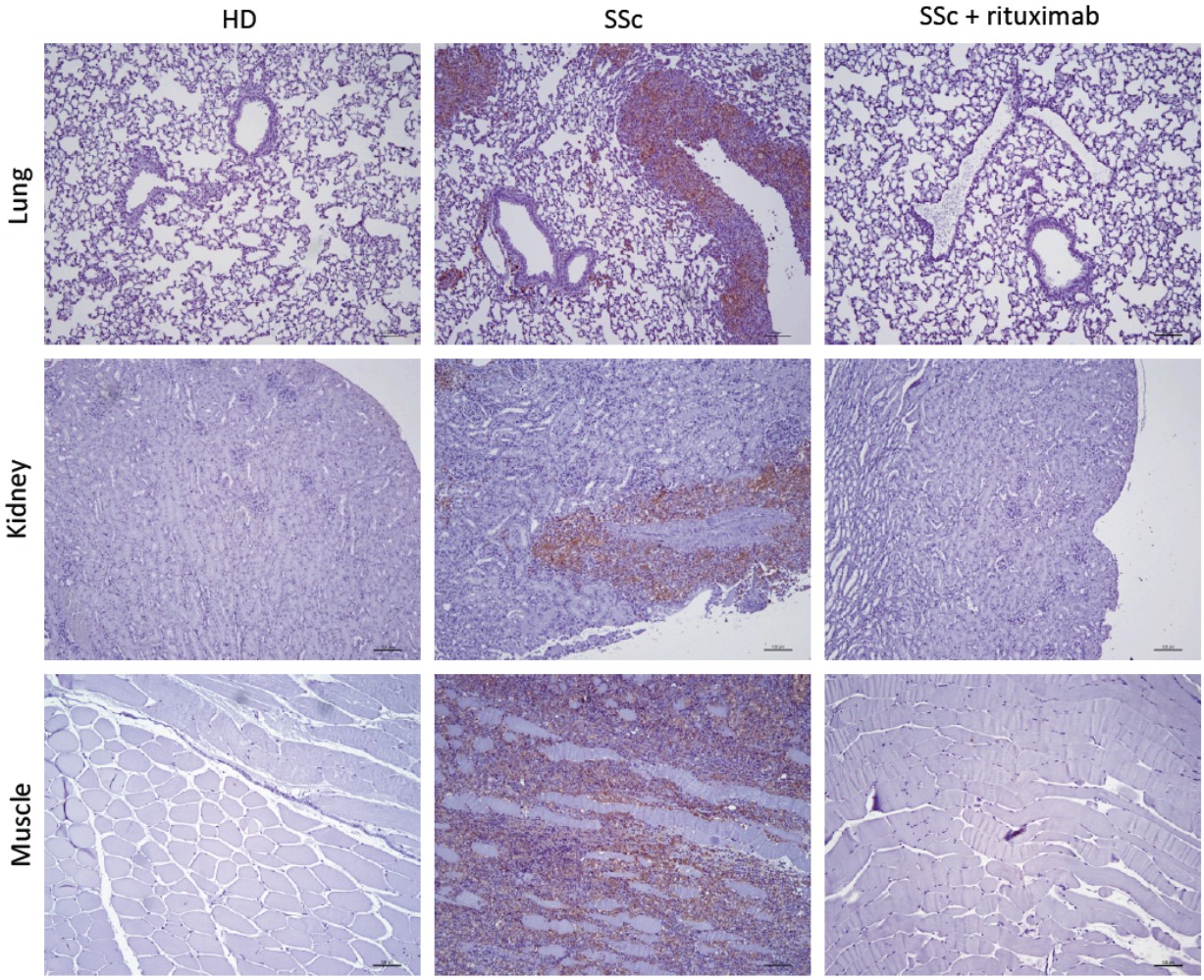

Figure 8. Presence of human B cells in infiltrations of mice transferred with human PBMC.
Representative micrographs of the cellular composition of infiltrates in the lung, kidney, and muscle are shown (100x). Infiltrated human B cells were detected by immunohistochemistry staining with anti-human $CD20^+$ antibodies (stained as brown color).

In summary, in order to establish a novel humanized SSc model, PBMC was transferred from SSc patients to $Rag2^{-/-}/IL2rg^{-/-}$ mice. As compared with mice receiving PBMC from healthy donor, the mice transferred with PBMC from SSc patients generated human autoantibodies against AT1R and ETAR, and showed severe B cells dominated inflammatory infiltrates in multiple organs. By contrast, mice that received PBMC from healthy donors produced significantly lower levels of anti-AT1R and anti-ETAR autoantibodies, and did not show obvious inflammation in any organs. Furthermore, neither autoantibodies nor tissue inflammation was detected in mice, which received PBMC from SSc patients treated with rituximab, a clinically-used anti-B cells monoclonal antibody.

4.2 Establishment of a SSc mouse model by immunization with hAT1R

Previous studies have shown that autoantibodies against AT1R in SSc patients are functional and associated with severity, progression and mortality of the disease [105], [106], implying that autoimmunity against AT1R is pathogenic for SSc. However, this hypothesis is still not validated *in vivo*. To determine the pathogenicity of autoimmunity against AT1R, we immunized female C57BL/6J mice with membrane extracts prepared from CHO cells overexpressing human AT1R (hAT1R), which maintain conformational epitopes of receptors and thus help to induce the production of functional autoantibodies to AT1R [158], [159]. The control mice were immunized with membrane extracts (ME) prepared from CHO cells. Nine weeks after immunization, mice were sacrificed, blood and tissue samples were collected for evaluation.

4.2.1 Induction of functional autoantibodies directed against human AT1R in mice

I first analyzed whether immunization with ME of CHO cells overexpressing hAT1R could induce the production of antibodies against hAT1R in mice. Levels of murine IgG against hAT1R were determined by using ELISA with immunized extracts of CHO cells overexpressing hAT1R as antigen. As shown in Figure 9A, hAT1R-immunized mice started to generated high levels of anti-hAT1R IgG after immunization. Levels of the anti-hAT1R IgG increased over time, and reached a peak of about $4.0x10^5$ arbitrary units at week 8 after first immunization followed by a subsequent decrease. By contrast, control mice immunized with ME from CHO cells did not produce anti-hAT1R antibodies (Figure 9A). Analysis of the subclasses of anti-hAT1R IgG at day 63 after immunization revealed that hAT1R-reactive antibodies belong to the IgG1, IgG2a and IgG2b subclasses, while IgG3 subclass could not be detected (Figure 9B).

Next, binding of these antibodies to mouse tissues or cells was determined. IgG deposition in the lung tissue of immunized mice was detected using direct immunofluorescence staining. As depicted in Figure 10, IgG deposition was observed in mice immunized with hAT1R but not in control mice. Given that IgG against hAT1R were of IgG1, IgG2a and IgG2b subclasses, an activation of complement induced by their corresponding immune complexes could be expected.

Surprisingly, no deposition of complement component 3 was observed, indicating that binding of these antibodies to the autoantigen in the lung did not result in complement activation (Figure 10).

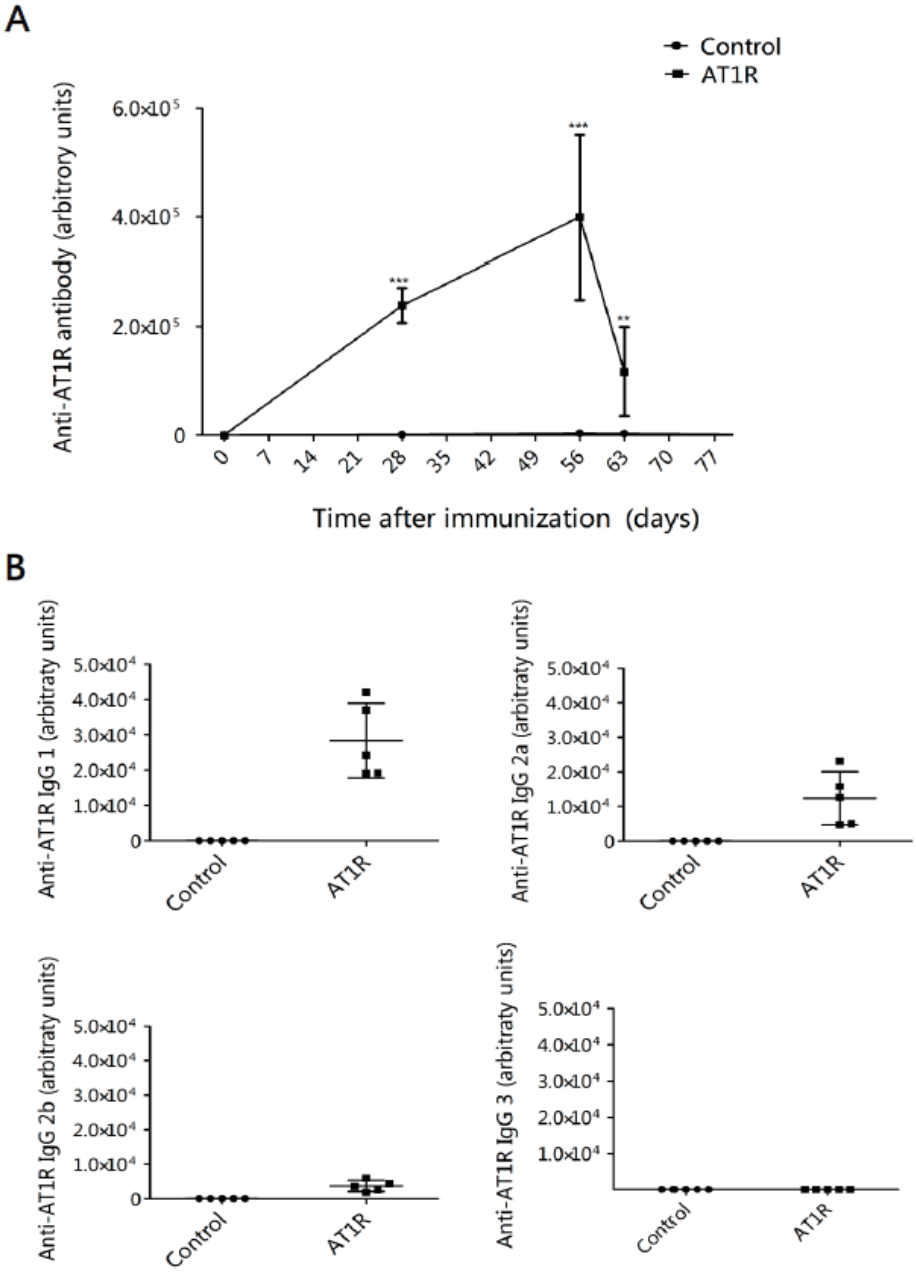

Figure 9. **Generation of antibodies to hAT1R in mice.** C57BL/6J mice were immunized with ME from CHO cells overexpressing hAT1R or untransfected cells. Anti-hAT1R autoantibodies were detected with ELISA coated with membrane extracts from CHO cells overexpressing hAT1R. (A) Time course of anti-hAT1R antibody generation. Serum samples were collected at day 0, 28, 56, and 63 after first immunization and AT1R antibody was measured in arbitrary unit. (B) Subclasses of anti-hAT1R IgG (IgG 1 and IgG2a) in hAT1R-immunized and control mice were measured in arbitrary for units. Arbitrary units are defined as the dilution at which the OD value reached the half of maximal OD values of the curve.

Results were presented as mean ± SD, and statistical analysis was performed using Mann-Whitney test and t- test (** = $p<0.01$, *** = $p<0.001$).

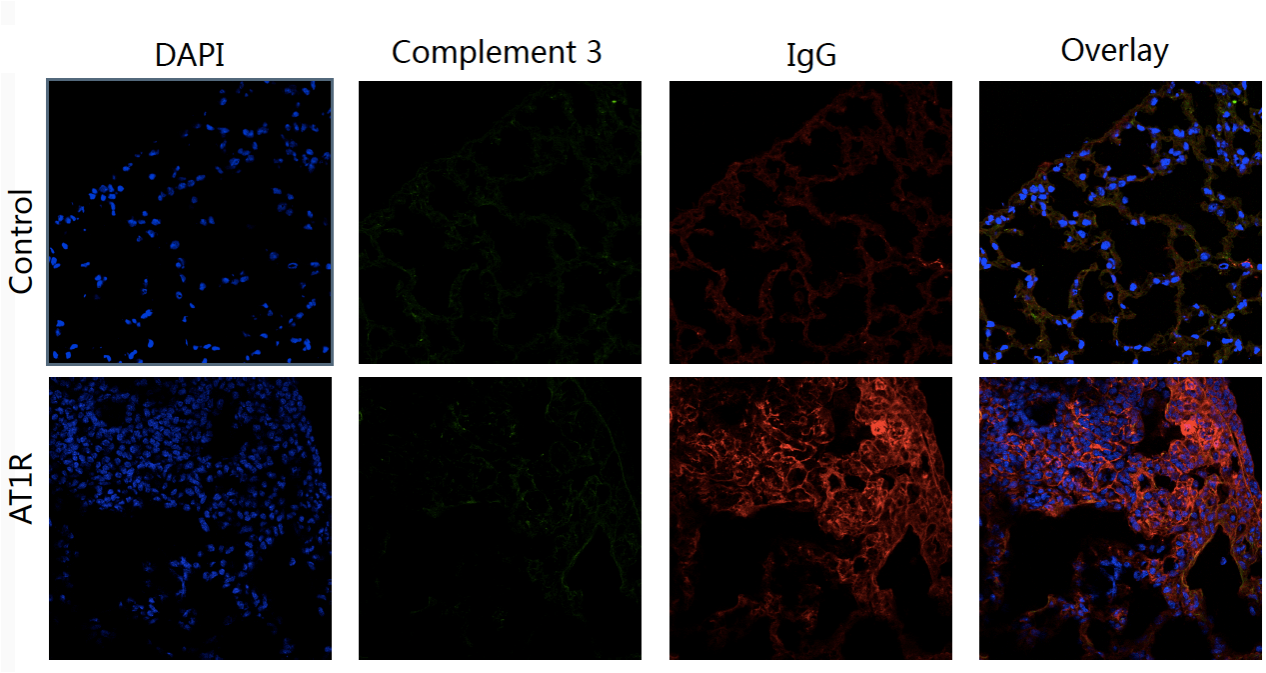

Figure 10. IgG and complement 3 deposition in the lung of hAT1R-immunized mice.
Representative micrographs of the immunofluorescence are shown (630x). Cryosection of the lung tissue of hAT1R-immunized mice and control mice were incubated with rat anti-mouse complement 3 antibody, and further stained with Dylight 649 labeled goat anti-mouse IgG and Alex-488 conjugated goat anti rat IgG to detect the IgG (red) and C3 deposition (green), respectively.

To investigate whether these antibodies were able to functionally activate AT1R, I stimulated human THP-1 monocytes with IgG derived from the sera of mice immunized with hAT1R and control mice. Treatment of cells with IgG elevated IL-8 production in general, irrespective of the specificity of the sera (Figure 11). However, concentrations of IL-8 observed in cells stimulated with IgG from hAT1R-immunized mice significantly surmounted those obtained by stimulation with IgG from controls. Furthermore, AT1R-IgG-induced effects could be blocked by Losartan, suggesting a functional effect of IgG on AT1R.

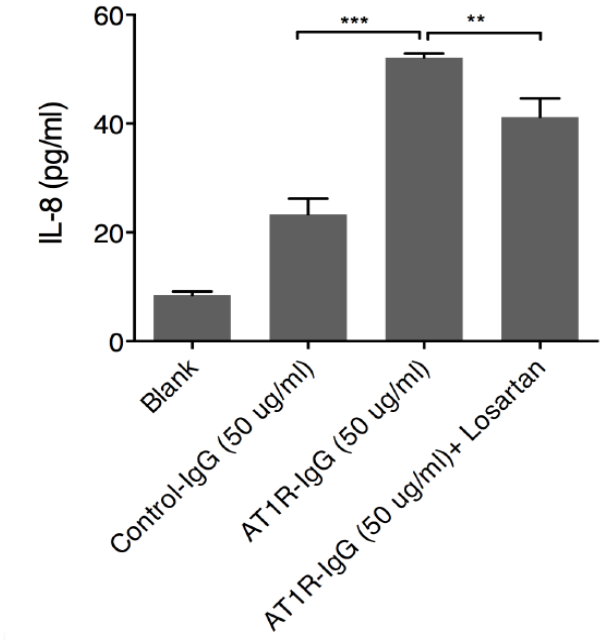

Figure 11. Effect of IgG from hAT1R-immunized mice on human monocytes.
Human monocytes (THP-1 cell line) were co-cultured with IgG from hAT1R-immunized mice or control mice in presence or absence of 1 μM Losartan for 24 hours. The concentration of IL-8 in the supernatant was determined using ELISA. Results were presented as mean± SD, and statistical analysis was performed using one way ANOVA test (** = $p<0.01$, *** = $p<0.001$). Data represent three independent experiments.

4.2.2 Autoimmunity against AT1R is associated with disease manifestations in the lung

Given the evidence for functional anti-hAT1R antibodies in immunized mice, we next examined whether the hAT1R-immunized mice developed disease symptoms resembling SSc in humans. Since AT1R is extensively expressed in vascular system [69], I first analyzed the vascular changes in the lung. As compared to control mice, mice immunized with hAT1R developed inflammatory infiltrates around vessels (Figure 12). Immunohistochemical staining showed that the infiltrates predominantly consisted of T and B cells (Figure 12). Subsequently, I performed a TUNEL assay to examine apoptosis of endothelial cells, which is often accompanied by perivascular inflammation [160,161]. As shown in the representative micrograph (Figure 13A), apoptotic endothelial cells were visible in pulmonary vessels in hAT1R-immunized mice but not

in control ME-immunized mice. Consistently, the quantification data revealed a significant increase in the percentage of apoptotic endothelial cells in hAT1R-immunized mice compared to control mice (Figure 13B, $p<0.01$). However, vascular remodeling, key feature of vasculopathy in human SSc, was not observed in hAT1R-immunized mice.

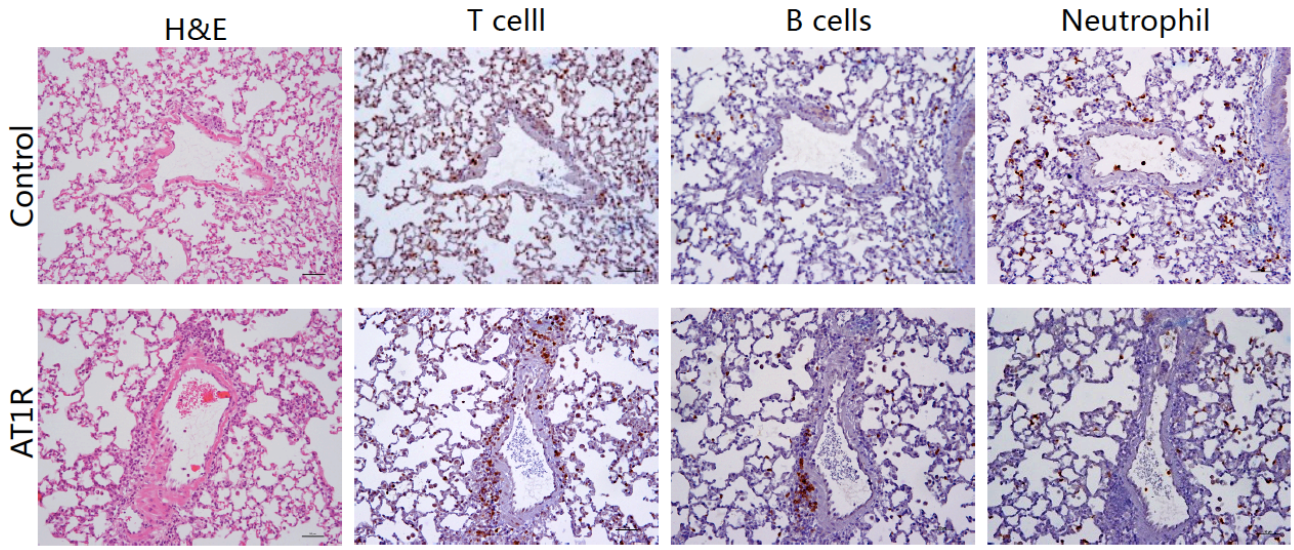

Figure 12. Perivascular inflammatory infiltrates in lung of hAT1R- immunized mice.
Representative micrographs of the histology and cellular composition of the infiltrates in the lung are shown (200x). Histology of lung sections was evaluated using H&E staining. Infiltrated T cells, B cells, and neutrophils (brown) were detected by immunohistochemistry staining with anti-CD3, anti-CD45R and anti-neutrophil antibodies, respectively.

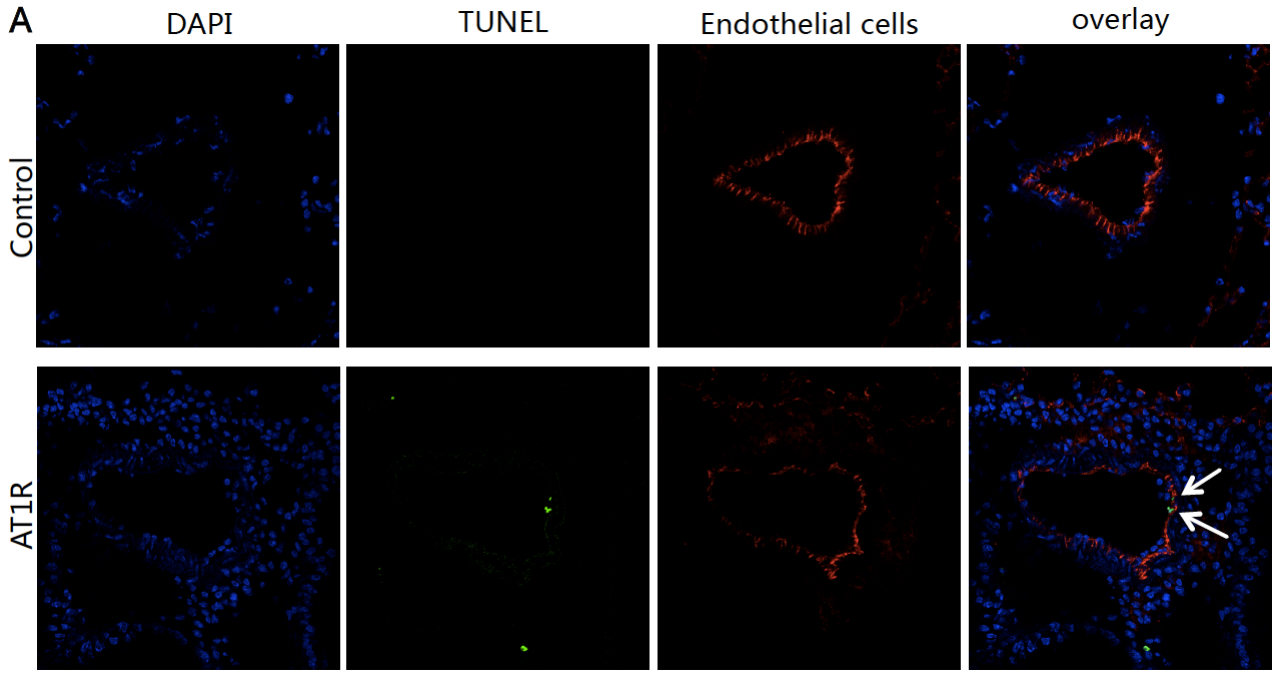

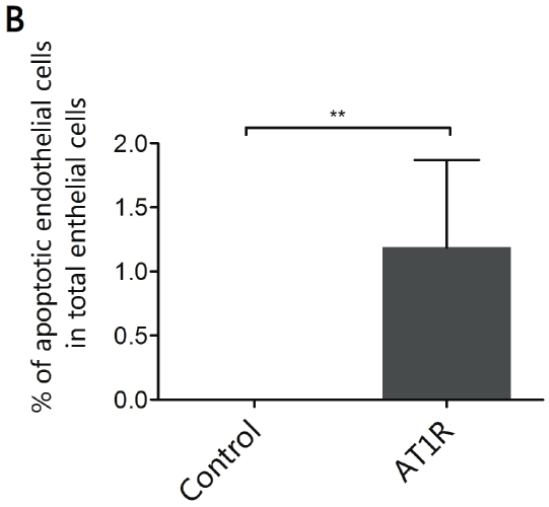

Figure 13. Immunization with hAT1R induces apoptosis of endothelial cells in the lung.
(A) Apoptotic endothelial cells in the lung of hAT1R-immunized mice (630x). Cryosections of the lung tissue of hAT1R-immunized mice and control mice were incubated with rat anti-mouse CD31 antibody and Alex 594 conjugated goat anti-rat antibody to detect the endothelial cells (red), and TUNEL assay was applied to detected apoptotic cells (green). Representative micrographs of immunofluorescent staining are shown. The white arrows indicate apoptotic endothelial cells. (B) Quantitative analysis of apoptotic endothelial cells. The percentages of apoptotic endothelial cells of total endothelial cells were calculated. Results were presented as mean ±SD, and statistical analysis were performed using t-test (** $p<0.01$).

Beside pulmonary vascular changes, interstitial lung disease (ILD) represents a further typical SSc-related lung complication, which is characterized by interstitial inflammation and fibrosis [22]. Therefore, we wanted to evaluate inflammation in the lung, especially the intra-alveolar areas. Leukocytes differential analysis of BALF revealed a significant increase in number of lymphocytes in BALF of hAT1R-immunized mice as compared to control mice (Figure 14A, $p<0.001$). However, no significant change in numbers of macrophages and neutrophils were observed between the two groups (Figure 14A). Moreover, subsequent histopathological analysis showed that hAT1R-immunized mice developed a profound inflammation in intra-alveolar areas of the lung, which was not observed in the control mice (Figure 14B). The inflammatory score was calculated based on numbers of infiltrates and sizes of the infiltrated areas. The inflammatory score was significantly higher in hAT1R-immunized mice as compared to mice treated with control ME (Figure 14C, $p<0.01$). Immunohistochemical staining showed that the infiltrates predominantly consisted of T and B cells (Figure 14D), which is in line with the increased number of lymphocytes found in the BALF.

Considering the severe interstitial inflammation, I subsequently assessed the pulmonary fibrosis by using Masson Trichrome staining and by quantification of the collagen content in the lung. However, neither histological analysis (Figure 15A) nor biochemical determination of collagen (Figure 15B) revealed any sign of pulmonary fibrosis in hAT1R-immunized mice or in the corresponding controls, indicating that in the lung the effect of an immunization with hAT1R is restricted to lung inflammation and mild vasculopathy.

Collectively, hAT1R immunization induced two types of histopathological changes in the lung, vascular change which is characterized by perivascular infiltration and endothelial apoptosis, and interstitial lung inflammation.

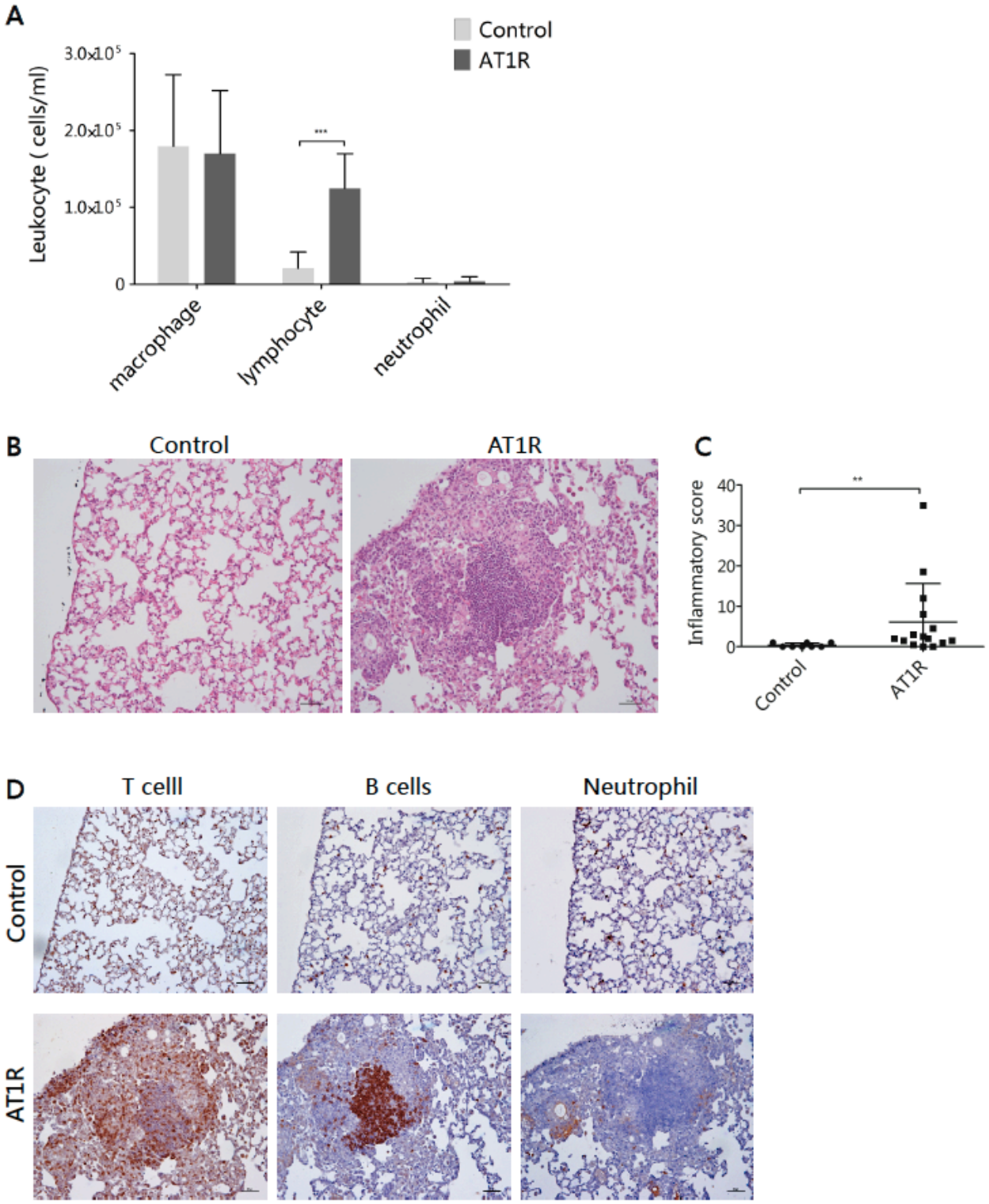

Figure 14. Intra-alveolar inflammation in hAT1R-immunized mice.

(A) Quantitative analysis of leukocyte populations in the BALF of control and hAT1R-immunized mice. (B) Histology of the lungs of control (left) and hAT1R-immunized mice (right) (200x). Representative micrographs of H&E staining are shown. (C) Quantitative analysis of lung inflammation. Lung inflammation was quantified as the size and number of infiltrates in intra-alveolar areas and scored in a

double-blinded fashion. (D) Cellular composition of the infiltrates in the lung of mice (200x). Infiltrated T cells, B cells, and neutrophils were detected by immunohistochemistry staining with anti-CD3, anti-CD45R and anti-neutrophil antibodies, respectively. Results were presented as mean±SD, and statistical analysis was performed using Mann-Whitney test (* = $p<0.05$, *** = $p<0.001$).

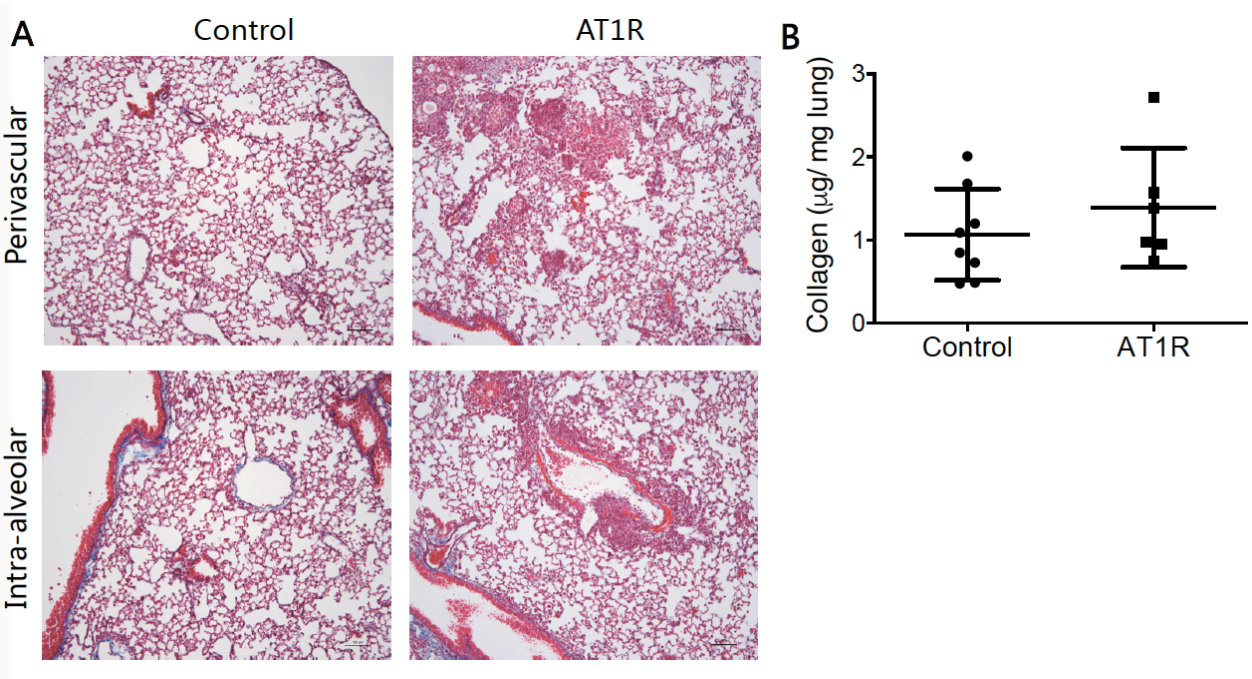

Figure 15. Immunization with AT1R does not induce lung fibrosis in mice.
(A) Representative lung sections after Masson Trichrome staining of control and hAT1R immunized mice (100x). (B) Collagen content of the lung in control and hAT1R-immunized mice. Collagen content was determined using Sircol collagen detection kit and expressed as µg per mg of the lung tissue. Data is presented as mean ±SD and statistical analysis was performed using t-test.

4.2.3 Immunization with hAT1R induces skin manifestations resembling SSc

Beside lung, skin represents the main target tissue in SSc patients [6], [10]. Therefore, the histopathology of this organ was analyzed in detail. Nine weeks after immunization, perivascular infiltrates were observed in the dermis in 60% of the hAT1R-immunized mice, while none of the mice treated with control ME developed comparable symptoms ($p<0.01$) (Figure 16A and 16B). As shown by immunohistochemical staining, these perivascular infiltrates were dominated by T cells while B cells and neutrophils were far less prominent or absent (Figure 16C). However,

thickening of vessel walls, which is a common clinical feature in patients with SSc [8], was not observed in hAT1R-immunized mice.

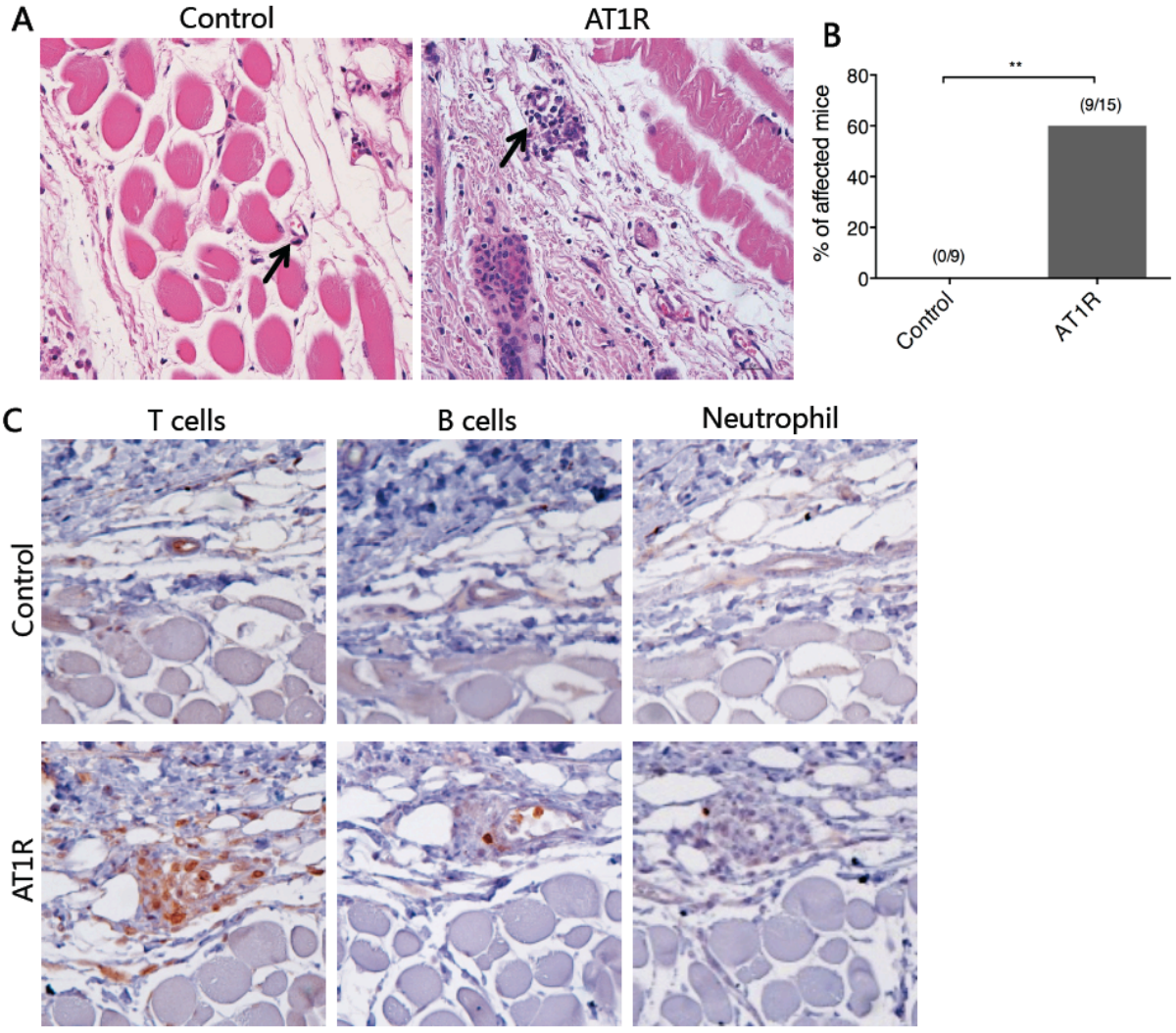

Figure 16. hAT1R immunization leads to vasculitis in the skin.
(A) Representative HE staining of skin sections from control (left) and hAT1R-immunized mice (right) (400x). Black arrows indicate blood vessels in the dermis. (B) Incidence of vasculitis in control and hAT1R-immunized mice. Numbers on top of the bars indicate the ratio between the number of mice with vasculitis and the total number of mice evaluated. (C) Cellular composition of the perivascular infiltrates in the skin of mice (400x). The infiltrative T cells, B cells, and neutrophils were detected using immunohistochemistry staining with anti-CD3, anti-CD45R and anti-neutrophil antibodies, respectively. Statistical analysis was performed using Fisher exact test (** = $p<0.01$.)

Beside perivascular inflammation of skin, skin fibrosis is another hallmark of SSc. I next determined the amount of skin fibrosis by evaluation of skin thickness after Masson's Trichrome

staining and quantification of the collagen content. As compared to control ME-immunized mice, skin thickness increased significantly in mice immunized with hAT1R (Figure 17A and B, $p<0.05$). Furthermore, quantitative assessment of the collagen content in the skin revealed that the amount of collagen in the skin of hAT1R-immunized mice was significantly higher than that of control mice (Figure 17C, $p<0.001$), confirming the development of skin fibrosis in the hAT1R immunized mice. Taken together, these findings show that immunization with hAT1R results in inflammation and fibrosis in the skin reflecting cardinal symptoms in SSc patients.

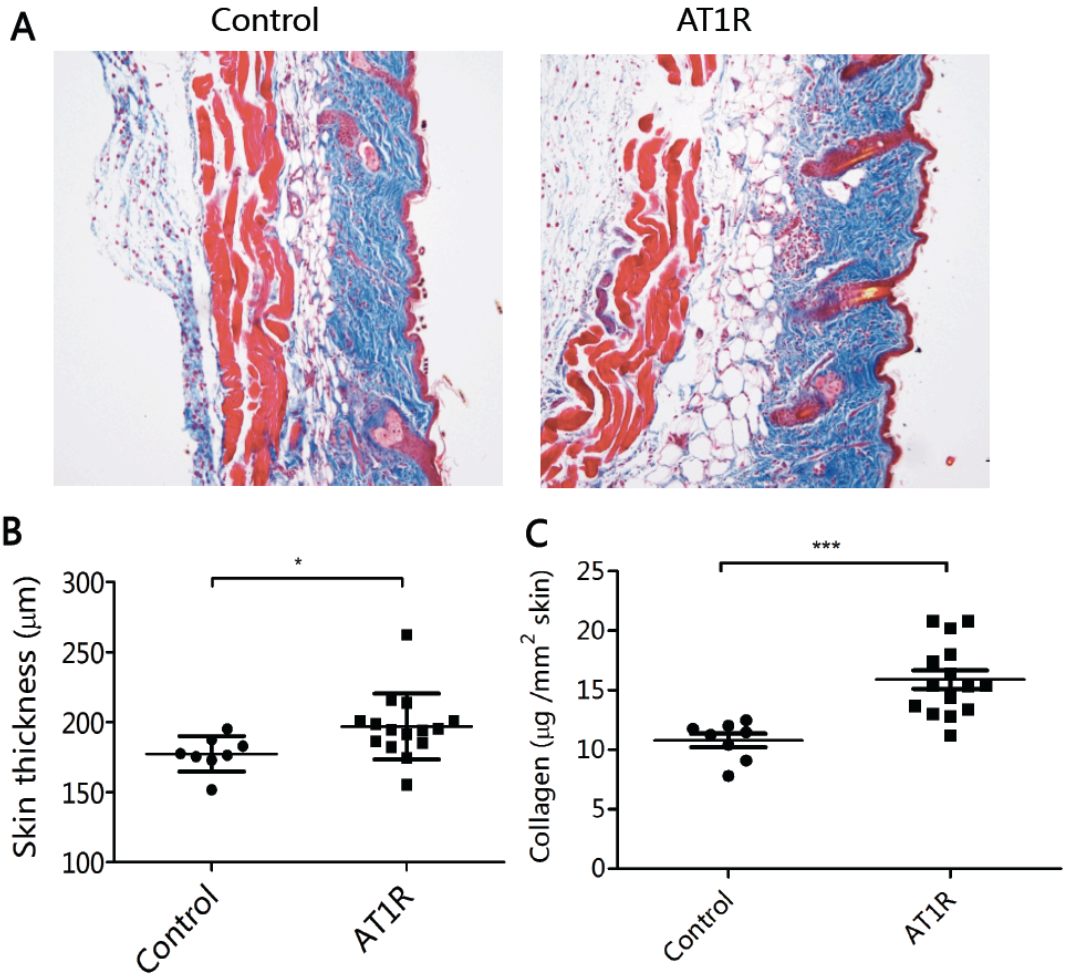

Figure 17. Skin Fibrosis in hAT1R-immunized mice.
(A) Representative dorsal skin sections after Masson Trichrome staining of control (left) and hAT1R-immunized mice (right) (100x). (B) Quantitative analysis of skin thickness. Thickness of the skin was defined as the thickness of the collagen layer stained in blue from the Masson Trichrome staining. (C) Collagen content in the skin in control and hAT1R-immunized mice. Collagen content was determined using Sircol collagen detection kit and expressed as µg per mm^2 of the skin. Data are presented as mean ±SD, and statistical analysis was performed using Mann-Whitney test and t-test. (* = $p<0.05$, *** = $p<0.001$).

4.2.4 hAT1R immunization induces localized inflammation

Since SSc is a systemic autoimmune disease which often affects several organs, the histopathology of kidney, hearts, and esophagus was evaluated. As shown in Figure 18, there was no evidence for histopathological changes in any of these organs in hAT1R immunized mice. These results suggest a dominance of hAT1R-induced autoimmunity in lung and skin.

Severe systemic autoimmune diseases are frequently characterized by an elevation of proinflammatory cytokines in the blood [162]. To examine this issue in my model of SSc induced by AT1R immunization, we compared the levels of 12 inflammatory cytokines between serum and BALF samples. The concentrations of 10 from 12 cytokines detected in BALF were significantly increased in hAT1R-immunized mice as compared to the corresponding control-ME treated mice, including IL-1β, IL-2, IL-4, IL-5, IL-6, IL-10, IL-12, IFN-γ and GM-CSF (Figure 19). By contrast, no differences in cytokine expression between these groups were observed in serum samples analyzed, supporting the notion that immunization with hAT1R preferentially provokes a local disease manifestation rather than a systemic phenotype.

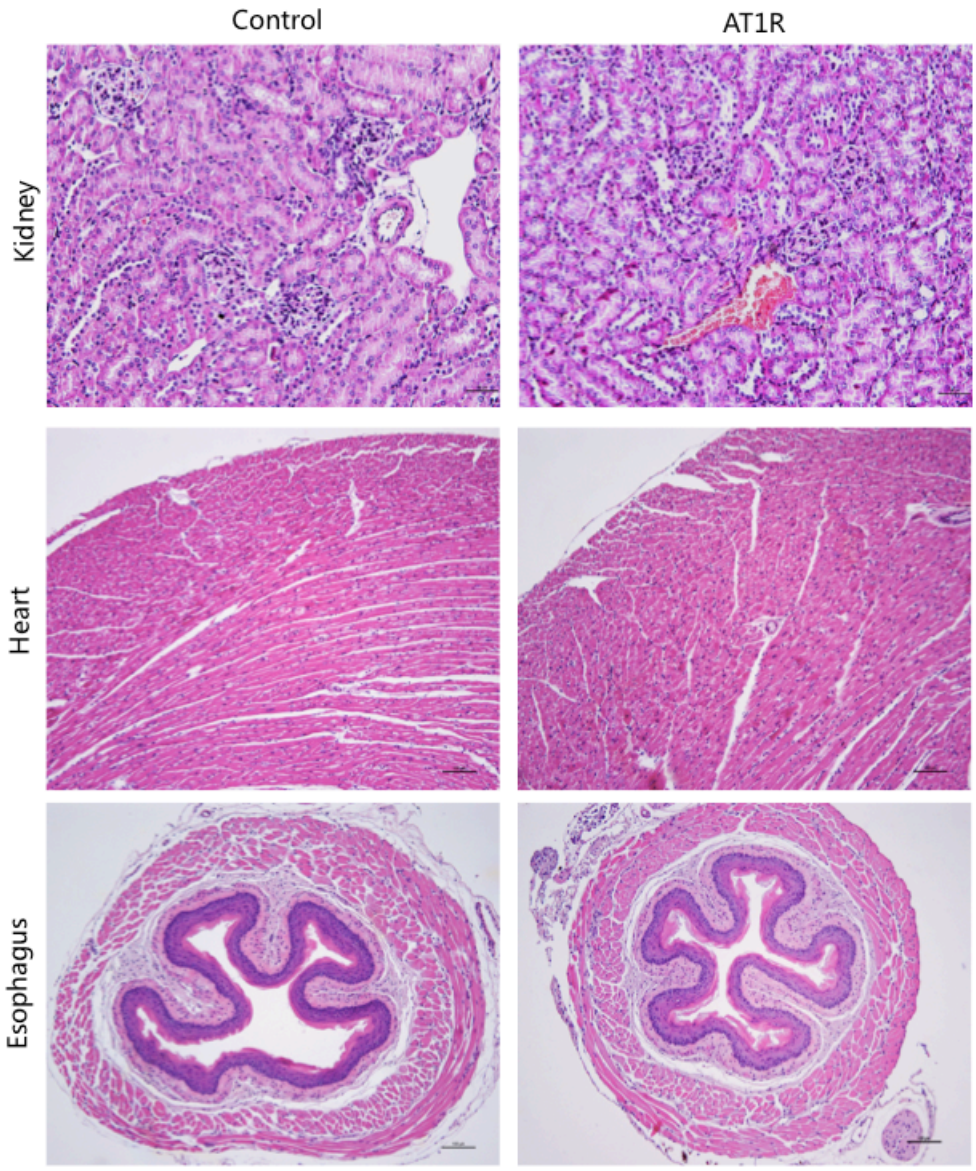

Figure 18. Immunization with hAT1R does not cause inflammation in kidney, heart and esophagus. Inner organs including kidney, heart and esophagus were collected and histological sections were evaluated by H&E staining. Representative micrographs are shown (100x).

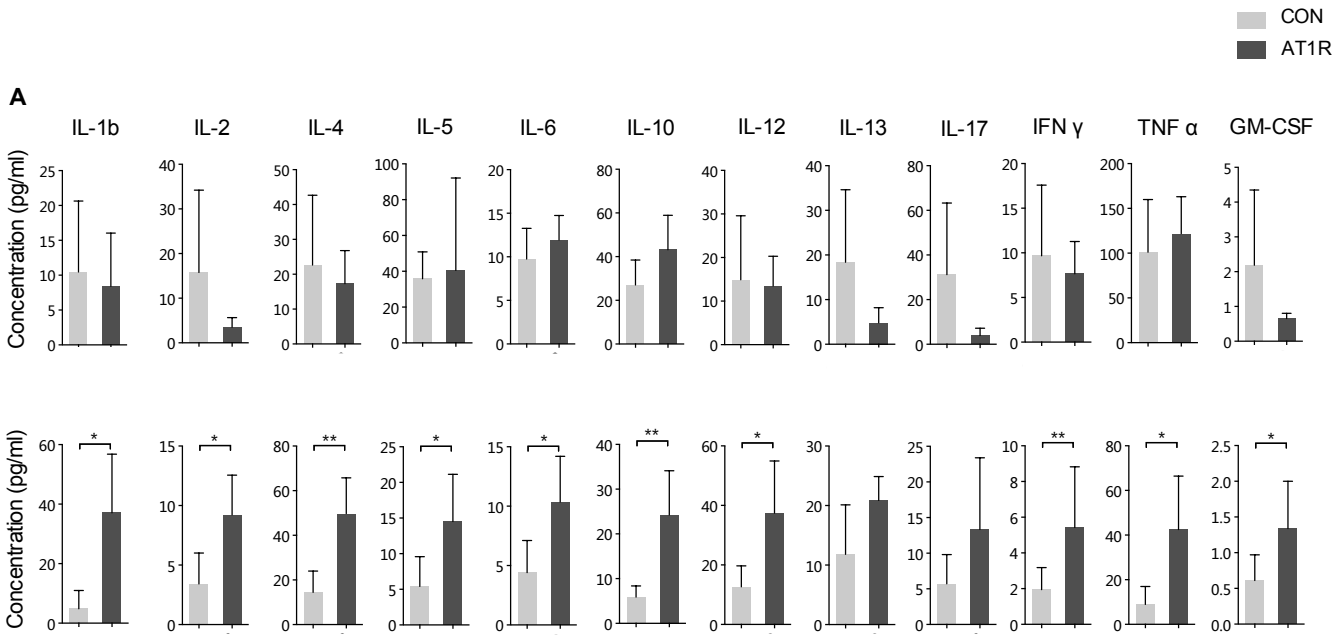

Figure 19. **Inflammatory cytokines in BALF and sera of mice.**
Serum (A) and BALF (B) samples derived from control (grey bars) and hAT1R-immunized mice (black bars) were collected at the end of the experiment (12 weeks post immunization) and cytokine levels were measured using 12-plex cytokine kit. Results are presented as mean ±SD, and statistical analysis was performed using Mann-Whitney test and t-test (n=6, * = $p<0.05$, ** = $p<0.01$).

4.2.5 Transfer of IgG from hAT1R-immunized mice induces local inflammation

To evaluate the role of antibodies in the pathogenesis of experimental SSc, I investigated whether a transfer of IgG isolated from hAT1R-immunized mice into healthy C57BL/6 animals would induce histopathological changes. In the recipients, purified IgG from mice immunized with hAT1R or control ME was injected i.d. into ears of healthy C57BL/6 mice. Twenty-four hours after injection, mice were sacrificed and ears were collected for histological evaluation. As shown in Figure 20A and B, inflammatory infiltrates were observed in mouse ears. The incidence of the induced inflammation in the ear was significantly higher in mice which received IgG from hAT1R-immunized mice (60%) than that in mice treated with IgG from control ME-immunized mice (22.7%) ($p<0.05$).

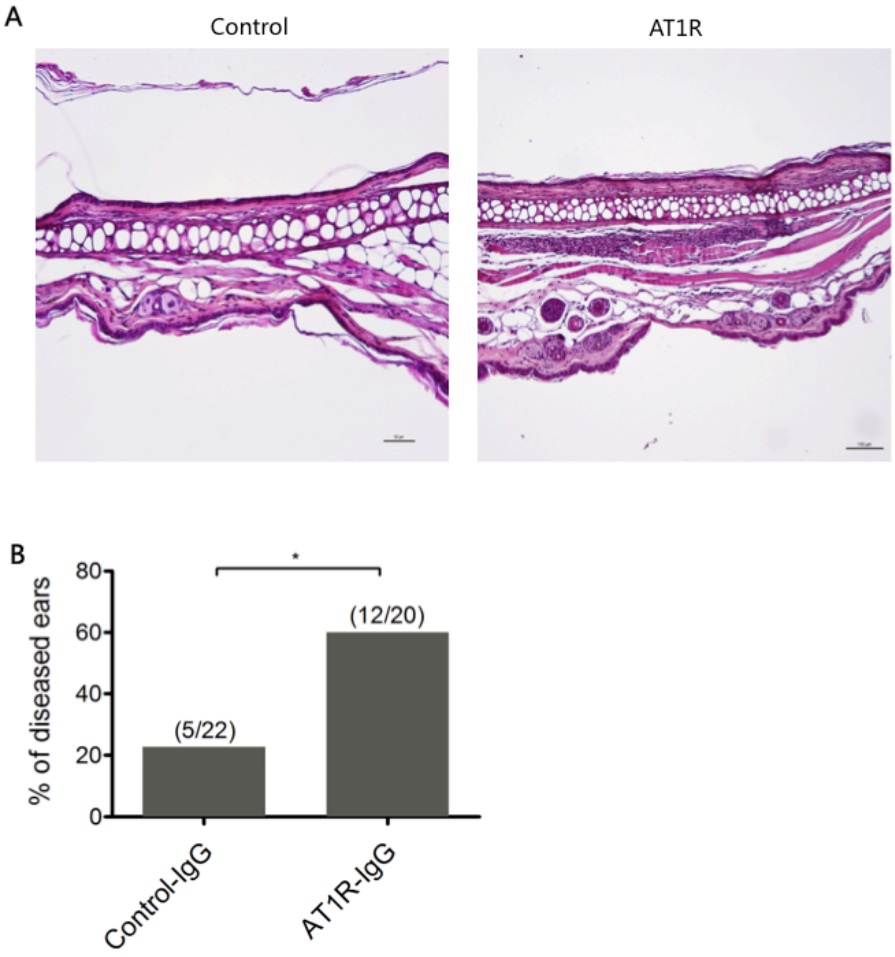

Figure 20. Transfer of IgG isolated from hAT1R-immunized mice induces inflammation.
(A) Representative micrograph of the histology of ears injected with IgG isolated from control ME-immunized mice (left) or hAT1R-immunized mice (right) (200x). (B) Incidence of the induced inflammation in ears treated with control-IgG and AT1R-IgG. Numbers on top of the bars indicate the ratio between the number of diseased ears and the total number of treated ears. Statistical analysis was performed using Fisher exact test (*= $p<0.05$).

In summary, in order to determine the pathogenicity of autoimmunity against AT1R in SSc, mice were immunized with membrane extracts prepared from CHO cells overexpressing hAT1R. After immunization, the AT1R-immunized mice produced high levels of autoantibodies against AT1R. Notably, these autoantibodies could functionally bind to AT1R as indicated by stimulatory effects on human monocytes which could be blocked by AT1R antagonist. Moreover, the AT1R-immunized mice developed vasculopathy and interstitial inflammation in lung, as well as perivascular infiltrations and fibrosis in the skin. However, these immunological and clinical features were not observed in mice immunized with control membrane extract (ME). In addition, transfer of IgG from AT1R-immunized mice could induce local inflammation in healthy recipient mice, which was not observed in the control ME-immunized mice.

5. Discussion

According to Witebsky's postulates for autoimmune disease from 1957 which have been further modified during time, autoimmune diseases have to fulfill two important criteria: i) disease should be transferable by pathogenic antibodies or T cells, ii) autoimmune disease should be reproducible in experimental animals [163], [164]. With regard to SSc, both criteria are only partially fulfilled until now. In the current study, I provide experimental evidence that both postulates are also valid for SSc.

SSc is a complex autoimmune disease with a still largely unknown pathogenesis. In the current study, the *in vivo* pathogenicity of immune cells from SSc patients and autoimmunity against AT1R was evaluated for a deeper understanding of the disease mechanisms. In the first part of this study, peripheral blood mononuclear cells (PBMC) were transferred from patients with SSc into immunodeficient $Rag2^{-/-}/IL2rg^{-/-}$ mice. Twelve weeks after the transfer of patient-derived PBMC, the recipient mice generated human autoantibodies against AT1R and ETAR and showed severe inflammatory infiltrates in multiple organs with B cells as the predominant cell type. By contrast, mice that received PBMC from healthy donors produced no or very low amounts of anti-AT1R and anti-ETAR autoantibodies and did not show obvious inflammation in any organs. Furthermore, neither autoantibodies nor tissue inflammation was detected in mice which received PBMC from SSc patients treated with rituximab, a clinically-used anti-B cells monoclonal antibody.

In order to investigate the pathogenicity of autoimmunity against AT1R, in the second part of this study we immunized mice with membrane extracts prepared from CHO cells overexpressing hAT1R. The hAT1R-immunized mice produced autoantibodies against hAT1R, which were able to bind the naive form of receptor on the cell membrane. Notably, these autoantibodies showed agonistic effects on AT1R as indicated by stimulatory effects on human monocytes, which could be ameliorated by AT1R blockade. Moreover, the hAT1R-immunized mice developed vasculopathy and interstitial inflammation in the lung, as well as perivascular infiltrations and fibrosis in the skin, partially resembling clinical manifestations of SSc. These immunological and clinical features were not observed in mice immunized with control membrane extract (ME). In

addition, transfer of IgG from hAT1R-immunized mice could induce local inflammation in healthy recipient mice, which was not observed in the control ME-immunized mice.

5.1 Animal models for SSc

Mouse models are powerful tools for studying human disease and have provided numerous insights into their pathomechanisms and pathogenesis. However, there are some general limitations in the translation of findings from mouse models to human diseases. A major problem is the prominent difference between both species in many aspects, especially the immune system [154]. Humanized mouse models are supposed to be a powerful tool to overcome this issue. Up to now, humanized models have been generated for several autoimmune diseases, including primary biliary cirrhosis, systemic lupus erythematosus, myasthenia gravis and pemphigus vulgaris, but not yet for SSc [165], [166], [167]. In the present study, for the first time a humanized model for SSc was generated, which is characterized by autoimmunity and systemic inflammation that partially resembles disease features of human SSc. This model offers a series of advantages as compared to previous models. First, as mentioned above, this novel model reflects more closely the nature of human disease. Therefore, results derived from it can be better transferred into patients and will reduce the gaps between animal studies and clinical applications. Second, since PBMC are composed of various types of cells, including T cells, B cells and monocytes, the individual role of each type of cells in SSc disease manifestation is not clear. By depleting defined cell populations prior to transfer, my model allows the analysis of the role of specific cell types in disease. Finally, the current study demonstrates that transfer of PBMC from different patients induces different patterns of systemic inflammation, indicating that this humanized mouse model might be further developed to a personalized model. Such model could be used in the future for the predicting of disease progressionand the evaluation of personalized therapies.

Beside insights of SSc disease itself, the humanized model established here provides some important information for the selection of strains suitable for cell transfer in general. As early as 1989, transfer of PBMC into immune-deficient mice was used to generate humanized mouse

model for human autoimmune disease. Since then, such humanized mouse models have been successfully generated for several autoimmune diseases [165], [166], [167], [168]. However, due to two major reasons this simple and effective strategy was limited to a small number of human autoimmune diseases. First, the difference between humans and mice in autoantigens or target tissues is critical. After being transferred into recipient mice, autoimmune cells from human patients are functionally active only when they are able to properly recognize the corresponding murine autoantigens. If human autoantigens differ significantly from their murine equivalent activation of the transferred human autoimmune cells will fail and no disease features are developed. Nonetheless, induction of SSc-like features was indeed seen in mice which had received PBMC from patients, suggesting that at least some relevant autoantigens in human SSc reached a sufficient level of crossreactivity to those in the recipient mice. A second reason limiting the success of this transfer approach in autoimmune diseases relates to the transplantation reaction and tolerance in the recipient mice. Ideal recipient mice should have two major characteristics. On one hand, the mice need to be immunodeficient, which largely reduces the transplantation reactions and thus allows the transferred human cells to survive in mice. On the other hand, the mice need to be tolerant to graft-versus-host-disease (GVHD), which enables the recipient mice to survive long enough for autoimmune disease manifestation. Previously, all PBMC-transfer induced humanized mouse models for autoimmune diseases used C.B-17 (SCID) mice as recipient mice [165], [166], [167], [169]. C.B-17 (SCID) mice have a Balb/c background and are homozygous for the *Prkdc*^{scid} mutation resulting in a lack of both T and B cells due to a defect in V(D)J recombination [165]. Since C.B-17 (SCID) mice still have NK cells which affect the survival of transferred human PBMC, these recipient mice may not be ideal for PBMC transfer. In the current study, we used Rag2$^{-/-}$/IL2rg$^{-/-}$ mice which lack T cells, B cells, and NK cells [170]. Furthermore, the Rag2$^{-/-}$/IL2rg$^{-/-}$ mice used in this study are on a C57BL/6 background which has been reported to be relatively tolerant to GVHD [171]. The lack of T cells, B cells, and NK cells, as well as the tolerance to GVHD make Rag2$^{-/-}$/IL2rg$^{-/-}$ mice ideal recipient for transfer of human PBMC. Thus, this mouse strain may be recommendable for other autoimmune disease models based on PBMC transfer-induced too which could not be established so far.

It is important to mention that the model established in this study does not reflect all features of SSc. Different to SSc patients, the recipient mice did not develop fibrosis and vasculopathy, two

hallmarks of the disease. A possible reason for the incomplete pathology may be the lack of proper interaction between immune cells and tissue non-hematopoietic cells. In SSc patients, disease manifestation is a consequence of such interaction in target tissues. Although transferred patient immune cells are activated in the mouse model, species-specific differences may disable or decrease the proper interaction between human and murine cells [172]. A further discrepancy to the disease in humans is the lack of any abnormality in the skin of recipient mice. Why this major target tissue in humans is not impaired in the mouse model remains unclear. One explanation could be that autoantigens involved in human skin fibrosis and inflammation are absent in mice or not recognized by human immune cells or autoantibodies [172].

A major disadvantage of the humanized model is the fact that it does not provide any information about the potential autoantigens involved in the pathogenesis. To solve this problem, an active SSc model based on immunization with a defined antigen was established in addition to the previously described approach. SSc is widely regarded as a complex autoimmune disease and its pathogenic autoantigens are still largely unclear. Although more than ten mouse models have been established to help to understand SSc pathogenesis [109], [173], the majority of them lack autoimmunity and/or vasculopathy [109] and are, therefore, not suitable for analyzing pathogenic autoantigens in the disease. So far, the only SSc-like model established by true immunization with an antigen was reported in 2011, where Yoshizaki and colleagues induced disease in mice by immunization with human Topisomerase I [151]. Although these results suggest that Topisomerase I could be a pathogenic autoantigen, it should be noted that this model has not been reproduced by other groups and subsequent reports elucidating its underlying pathomechanisms are missing.

In previous studies, functional autoantibodies against AT1R showed strong association with the development and manifestations of SSc [105], [106], which implies that autoimmunity against AT1R may be pathogenic for SSc. To validate this hypothesis, a novel active SSc model has been established in the current study. Immunization with membrane extract from AT1R over-expressing CHO cells induced the production of high levels of anti-AT1R antibodies. Importantly, these antibodies were not only able to bind to AT1R but also to activate the receptor, which resemble functional feature of IgG from SSc patients [104], [105]. Moreover, the hAT1R-immunized mice developed many disease features resembling SSc. First, these mice developed

several clinical manifestations reported for the human disease [173], [174], including skin fibrosis, interstitial lung disease, and vascular changes. Second, hAT1R-immunized mice share many immunological features with human SSc. Beside producing autoantibodies against AT1R, hAT1R-immunized mice were characterized by a T cell-dominated skin inflammation, which is consistent to clinical observation that T cells are increased dramatically in the perivascular area of skin lesions in SSc patients [54]. Also, an increased number of lymphocytes was detected in BALF, which is consistent to corresponding findings in the BALF of SSc patients [175]. In addition, real-time PCR data showed an elevated level of IL-4 in lung tissue and BALF of immunized mice, which has been shown also in the human disease [176]. Taken together, this model mimics several key features of SSc disease and represents a useful tool to explore the disease pathogenesis and to search for novel therapeutic targets in SSc. In addition, this approach provides a new possibility to validate potential pathogenic autoantigens, especially membrane receptor, in SSc. Finally, by this novel model, the pathogenicity of autoimmunity to AT1R is demonstrated, the results identify AT1R as an important autoantigen in SSc, and extend previous epidemiological findings and *in vitro* experimental data that demonstrate the capacity of anti-AT1R antibodies to induce effector functions in different cells linked to SSc pathogenesis and disease severity, progression, and mortality [105], [106].

Of note, some limitations of this novel mouse model for SSc need to be mentioned. Firstly, in contrast to SSc where autoantibodies against several autoantigens are observed [10], autoimmunity in our model is limited to AT1R. Secondly, fibrosis, a hallmark of SSc, was only detected in the skin of diseased mice but not in other organs. Moreover, vasculopathy in hAT1R-immunized mice was limited to perivascular infiltration and apoptosis of endothelial cells while an obliterative vasculopathy usually found in SSc was missing. There might be at least two possible reasons for the limited spectrum of symptoms observed in this mouse model. While pathogenesis in SSc may involve autoimmunity to multiple autoantigens, the disease in this model is driven by autoimmunity to a single autoantigen. For example, beside autoantibodies to ETAR, which is functionally related to AT1R [159], autoantibodies against CXCR4 have been shown to be present in SSc [177] and CXCR4 signaling has been demonstrated to play an important role in animal models of pulmonary fibrosis [178]. A further reason may be the limited stability of the model. Although levels of autoantibodies to AT1R in mice increased during the first 8 weeks after immunization, they declined rapidly over time. This lack of a sustained

autoimmune responses due to the immunization with heterologous antigens might affect the expression of full pathology in mice [179], [180].

5.2 Role of B cells in SSc

In patients with SSc, inflammatory infiltrates of lymphocytes and macrophages are frequently observed in multiple organs. These cells produce high levels of cytokines, chemokines and autoantibodies which exert pro-inflammatory and/or pro-fibrotic effects [52] and, therefore may play an important role in the development of SSc. This notion is further supported by numerous animal models for SSc, in which the importance of murine immune cells for the pathogenesis of the disease could be demonstrated. However, there is currently no direct evidence *in vivo* for the pathogenicity of specific immune cells from SSc patients. Since the murine immune system differs from the human in many aspects [181], direct evidence for the *in vivo* pathogenicity of human immune cells requires a humanized model. The current study has shown that transfer of PBMC from SSc patients could induce the production of autoantibodies and systemic inflammation, for the first time demonstrating the pathogenic effect of immune cells from SSc patients using an *in vivo* system.

Beside showing the *in vivo* pathogenic effect of PBMC, my study provides further evidence that B cells are indeed indispensable for disease manifestation. Notably, immunohistochemical staining showed that the inflammatory infiltrates in mice treated with PBMC from SSc patients were predominantly composed of human B cells. Together with the observed production of autoantibodies both findings highlight the important role of B cells in this humanized model. This view was further supported by the observation that autoimmunity and extensive inflammation was not developed in mice transferred with PBMC from SSc patients were treated with rituximab, a B cell depleting monoclonal antibody. Taken together, the current study provides first direct evidence for a pathogenic role of B cells in SSc. In future studies, the mechanism behind the role of B cells will be explored by depleting B cells in SSc PBMC prior to transfer to the mice.

Beside the humanized mouse model, the hAT1R-induced model also provides some evidence for a role of B cells in the pathogenesis of SSc. This became evident from histological analysis

which demonstrated a prominent infiltration of B cells into the lung. Moreover, functional autoantibodies against hAT1R as a B cell product, most likely play an essential in the pathogenesis of the hAT1R-induced model. However, the role of B cells in this mouse model need to be verified in the future by investigating B cell deficient mice.

The critical role of B cells in the pathogenesis of SSc enables some future treatment options. Since the current study shows that B cells are involved in autoantibody production and systemic inflammation, B cell-targeted treatments might help for subset of SSc with multiple organ involvement, e.g. dcSSc. This notion is in line with recent clinical findings. Rituximab (RTX), a monoclonal IgG antibody directed against the CD20 molecule on B cells that result in a rapid and sustained depletion of most B cells, has been used for the treatment of many autoimmune diseases [182]. A systemic review on rituximab treatment in SSc suggested that rituximab is effective in the subset of diffuse SSc in particular in skin and interstitial disease involvements [183].

5.3 Functional autoantibodies

Beside activating the complement system or Fc receptors [184], autoantibodies can contribute to the progression of disease via dysregulating the function of receptors. In this case, the antibody mimics the natural ligand of the receptor and antibody binding results either in an activation or a blocking of the corresponding receptor [185]. However, investigations on the physiological and pathogenic role of such “functional autoantibodies” [186] has been hindered for a long time by the lack of appropriate analytical methods enabling the detection of these type of immunoglobulins. Binding of functional antibodies is mediated largely by their interaction with conformational epitopes on the receptors [186] which are not established in classical peptide ELISAs or denaturing Western Blots. Furthermore, since conformational epitopes of receptors maintain their physiological structure only in the context of the membranes, immunizations with recombinant or denatured receptor proteins will not succeed in the induction of functional autoantibodies [158], [159]. In some studies, genetic immunizations with plasmids expressing human receptors were used to circumvent this problem [179], [180], [187]. Although genetic immunizations help to break immune tolerance and to induce autoimmune symptoms in mice,

autoantibody levels, disease incidences, and severities are low and vary among the animals, probably due to the lack of adjuvans in these methods [179], [180], [187]. Thus, alternative strategies enabling a higher efficiency in the induction of functional autoantibodies against GPCR are required.

My current study provides a novel strategy for induction of functional autoantibodies, in which the physiological structure of the receptor is well maintained in context of ME. Notably, all mice immunized with hAT1R developed high levels of antibodies against hAT1R. Purified sera derived from hAT1R-immunized mice exerted a stimulatory function to AT1R. Therefore, this novel immunization strategy may represent a robust and efficient method for the induction of functional autoantibodies against hAT1R and most likely other receptors, too. Although low amounts of proteins beside AT1R also present in the ME could theoretically also generate an immune reaction, mice immunized with control extracts lacking hAT1R overexpression did neither develop disease symptoms nor antibodies to the receptor. This identifies hAT1R as the predominant immunogenic and pathogenic antigen in the ME overexpressing hAT1R. To our knowledge, these data show for the first time that immunization with ME from cells overexpressing a G protein-coupled receptor (GPCR) can raise receptor-specific functional autoantibodies. Since such autoantibodies have been suggested to be relevant for many autoimmune diseases [159], [188], [189], these results could be of general interest for the induction of functional autoantibodies against other membrane-bound receptors, too.

This study substantiate by experimental data the previous hypothesis on the important role of functional anti-AT1R autoantibodies in SSc [105], [106], which was mainly based on epidemiological and clinical surveys. Moreover, elevated levels of these antibodies were not only shown in SSc patients but were also detectable in the humanized mouse model which had received PBMC from SSc patients. This identifies anti-AT1R autoantibodies as a functional biomarker of SSc.

Furthermore, the hAT1R-induced mouse model provides direct and convincing evidence for a role of functional autoantibodies against AT1R in the pathogenesis of SSc. As shown, hAT1R-immunized mice produced high amounts of functional autoantibodies against hAT1R with an agonistic function on the receptor similar to that described for human anti-hAT1R autoantibodies [105]. In addition, the presence of these antibodies is associated with a SSc-pathology in both

mice and humans [106]. Of importance, the diseases of hAT1R-immunized mice could be partially transferred to normal mice by serum IgG, which supported that the autoantibodies against hAT1R can induce pathologic changes possibly by over-activation of hAT1R. The pathogenecity of over-activation of AT1R in SSc is further supported by *in vivo* observations in which mice developed skin inflammation and fibrosis upon sustained hAT1R activation by its nature ligand, angiotensin II [98]. Our results suggest that specific receptor blockers targeting the hAT1R-mediated induction of inflammation and fibrosis could be a future treatment concept to reduce SSc symptoms in the skin and lung. Our SSc mouse model offers the possibility to evaluate such specific therapies for a future treatment strategy in humans.

5.4 Conclusions

In this study, immune cells from SSc patients and autoimmunity against AT1R in the pathogenesis of experimental SSc were identified as essential drivers of experimental SSc *in vivo*. This became evident from a novel humanized SSc model established here in which the pathogenicity of human immune cells from SSc patient could be demonstrated by their transfer to immune-deficient mice. Moreover, the pathogenic role of antibodies to AT1R could be shown by a mouse model based on a new strategy for the induction of functional autoantibodies by immunization with receptor proteins in their native conformation. By using this strategy a novel active model for SSc was established by induction of an immune response against AT1R. Results of this study identify AT1R as a pathogenic autoantigen for some typical SSc features and suggest a pathogenic role of anti-AT1R autoantibodies in SSc, which shed some new light on our understanding of the disease pathogenesis and enable the development of novel therapeutics.

5.5 Outlook

In the current study, it has been shown that PBMC from SSc patients can partially induce SSc-like disease. However, since PBMC contain various types of cells, including monocytes, T cells

and B cells, the exact role of each type of cells in SSc disease manifestation is still not clear. Therefore, it is highly interesting to investigate the pathogenic role of different type of immune cells in SSc. Furthermore, although several features of SSc can be modeled by immunization with AT1R, some characteristic symptoms like lung fibrosis and pulmonary hypertension are missing. A comprehensive comparison between diseased mice and humans revealed that the pro-fibrotic cytokine IL-13 is present in SSc but is not elevated in the mouse model. Therefore, IL-13 may be a key regulator of the fibrotic arm of the disease. In future study, it is of significance to include IL-13 in present AT1R immunized SS model, which could optimize the lung fibrosis feature of our active model and determine the pro-fibrotic role of IL-13 in SSc. Besides AT1R, other GRCRs are also associated with the development of SSc. It has been reported that autoantibodies against ETAR and CXCR4 increase significantly in SSc patents and the level of them are correlated with disease complications, which suggests the pathogenic role of autoimmunity against them in SSc. Therefore, immunizing mice with ETAR or CXCR4 appears to be a promising strategy to clarify the role of this GPCR in SSc and to establish novel extended models of the disease.

6. References

[1] LeRoy EC, Black C, Fleischmajer R, Jablonska S, Krieg T, Medsger TA, et al. Scleroderma (systemic sclerosis): classification, subsets and pathogenesis. J Rheumatol 1988;15:202–5.

[2] Barnes J, Mayes MD. Epidemiology of systemic sclerosis. Curr Opin Rheumatol 2012;24:165–70.

[3] Barnes J, Mayes MD. Epidemiology of systemic sclerosis: incidence, prevalence, survival, risk factors, malignancy, and environmental triggers. Curr Opin Rheumatol 2012;24:165–70.

[4] Tyndall AJ, Bannert B, Vonk M, Airò P, Cozzi F, Carreira PE, et al. Causes and risk factors for death in systemic sclerosis: A study from the EULAR Scleroderma Trials and Research (EUSTAR) database. Ann Rheum Dis 2010;69:1809–15.

[5] Lawrence RC, Helmick CG, Arnett FC, Deyo RA, Felson DT, Giannini EH, et al. Estimates of the prevalence of arthritis and selected musculoskeletal disorders in the United States. Arthritis Rheum 1998;41:778–99.

[6] Hinchcliff M, Varga J. Systemic sclerosis/scleroderma: a treatable multisystem disease. Am Fam Physician 2008;78:961–8.

[7] Hunzelmann N, Genth E, Krieg T, Lehmacher W, Melchers I, Meurer M, et al. The registry of the german network for systemic scleroderma: Frequency of disease subsets and patterns of organ involvement. Rheumatology 2008;47:1185–92.

[8] Eisenberg M, Nguyen B, Karnath B. Clinical Features of Systemic Sclerosis. Hosp Physician 2008;22:333–6.

[9] Walker UA, Tyndall A, Czirják L, Denton C, Farge-Bancel D, Kowal-Bielecka O, et al. Clinical risk assessment of organ manifestations in systemic sclerosis: A report from the EULAR Scleroderma Trials and Research group database. Ann Rheum Dis 2007;66:754–63.

[10] Allanore Y, Simms R, Distler O, Trojanowska M, Pope J, Denton CP, et al. Systemic sclerosis. Nat Rev Dis Prim 2015;1:15002.

[11] Domsic RT, Medsger TA. Autoantibodies and Their Role in Scleroderma Clinical Care. Curr Treat Options Rheumatol 2016;2:239–51.

[12] Prescott RJ, Freemont AJ, Jones CJ, Hoyland J, Fielding P. Sequential dermal microvascular and perivascular changes in the development of scleroderma. J Pathol 1992;166:255–63.

[13] Asano Y, Sato S. Vasculopathy in scleroderma. Semin Immunopathol 2015;37:489–500.

[14] Wei J, Bhattacharyya S, Tourtellotte WG, Varga J. Fibrosis in systemic sclerosis: Emerging concepts and implications for targeted therapy. Autoimmun Rev 2011;10:267–75.

[15] Hachulla E, Launay D, De Groote P, Moranne O, Tillie-Leblond I, Seguy D, et al. Severe organ involvement in systemic sclerosis. Reanimation 2005;14:576–86.

[16] al-Sabbagh MR, Steen VD, Zee BC, Nalesnik M, Trostle DC, Bedetti CD, et al. Pulmonary arterial histology and morphometry in systemic sclerosis: a case-control autopsy study. J Rheumatol 1989;16:1038–42.

[17] Cool CD, Kennedy D, Voelkel NF, Tuder RM. Pathogenesis and evolution of plexiform lesions in pulmonary hypertension associated with scleroderma and human immunodeficiency virus infection. Hum Pathol 1997;28:434–42.

[18] McNearney TA, Reveille JD, Fischbach M, Friedman AW, Lisse JR, Goel N, et al. Pulmonary involvement in systemic sclerosis: Associations with genetic, serologic, sociodemographic, and behavioral factors. Arthritis Care Res 2007;57:318–26.

[19] Bouros D, Wells AU, Nicholson AG, Colby T V., Polychronopoulos V, Pantelidis P, et al. Histopathologic subsets of fibrosing alveolitis in patients with systemic sclerosis and their relationship to outcome. Am J Respir Crit Care Med 2002;165:1581–6.

[20] Harrison NK, Myers AR, Corrin B, Soosay G, Dewar A, Black CM, et al. Structural features of interstitial lung disease in systemic sclerosis. Am Rev Respir Dis 1991;144:706–13.

[21] Tamby MC, Chanseaud Y, Guillevin L, Mouthon L. New insights into the pathogenesis of systemic sclerosis. Autoimmun Rev 2003;2:152–7.

[22] Herzog EL, Mathur A, Tager AM, Feghali-Bostwick C, Schneider F, Varga J. Interstitial Lung Disease Associated With Systemic Sclerosis and Idiopathic Pulmonary Fibrosis: How Similar and Distinct? Arthritis Rheumatol 2014;66:1967–78.

[23] Roberts CGP, Hummers LK, Ravich WJ, Wigley FM, Hutchins GM. A case-control study of the pathology of oesophageal disease in systemic sclerosis (scleroderma). Gut 2006;55:1697–703.

[24] Marie I, Lévesque H, Dominique S, Hatron PY, Michon-Pasturel U, Remy-Jardin M, et al. Pulmonary involvement in systemic scleroderma. Part I. Chronic fibrosing interstitial lung disease. La Rev Med interne 1999;20:1004–16.

[25] Denis P, Ducrotte P, Pasquis P, Lefrançois R. Esophageal motility and pulmonary function in progressive systemic sclerosis. Respiration 1981;42:21–4.

[26] Lock G, Holstege A, Lang B, Schölmerich J. Gastrointestinal manifestations of progressive systemic sclerosis. Am J Gastroenterol 1997;92:763–71.

[27] Batal I, Domsic RT, Medsger TA, Bastacky S. Scleroderma Renal Crisis: A Pathology Perspective. Int J Rheumatol 2010;2010:1–7.

[28] Sugimoto T, Soumura M, Danno K, Kaji K, Kondo M, Hirata K, et al. Scleroderma renal crisis in a patient with anticentromere antibody-positive limited cutaneous systemic sclerosis. Mod Rheumatol 2006;16:309–11.

[29] Denton CP, Lapadula G, Mouthon L, Müller-Ladner U. Renal complications and scleroderma renal crisis. Rheumatology (Oxford) 2009;48 Suppl 3:iii32-5.

[30] Steen VD, Medsger TA. Changes in causes of death in systemic sclerosis, 1972-2002. Ann Rheum Dis 2007;66:940–4.

[31] Ho KT, Reveille JD. The clinical relevance of autoantibodies in scleroderma. Arthritis Res Ther 2003;5:80–93.

[32] Hohenstein B, Bornstein SR, Aringer M. Immunoadsorption for connective tissue disease. Atheroscler Suppl 2013;14:185–9.

[33] Douvas AS, Achten M, Tan EM. Identification of a nuclear protein (Scl-70) as a unique target of human antinuclear antibodies in scleroderma. J Biol Chem 1979;254:10514–22.

[34] Spencer-Green G, Alter D, Welch HG. Test performance in systemic sclerosis: Anti-centromere and anti-Scl-70 antibodies. Am J Med 1997;103:242–8.

[35] Kallenberg CGM, Wouda AA, Hoet MH, Van Venrooij WJ. Development of connective tissue disease in patients presenting with Raynaud's phenomenon: A six year follow up with emphasis on the predictive value of antinuclear antibodies as detected by immunoblotting. Ann Rheum Dis 1988;47:634–41.

[36] Perera A, Fertig N, Lucas M, Rodriguez-Reyna TS, Hu P, Steen VD, et al. Clinical subsets, skin thickness progression rate, and serum antibody levels in systemic sclerosis patients with anti-topoisomerase I antibody. Arthritis Rheum 2007;56:2740–6.

[37] Levesque H, Baudot N, Delpech B, Vayssairat M, Gancel A, Lauret P, et al. Clinical correlations and prognosis based on hyaluronic acid serum levels in patients with progressive systemic sclerosis. Br J Dermatol 1991;124:423–8.

[38] Jacobsen S, Ullman S, Shen GQ, Wiik A, Halberg P. Influence of clinical features, serum antinuclear antibodies, and lung function on survival of patients with systemic sclerosis. J Rheumatol 2001;28:2454–9.

[39] Reveille JD, Solomon DH. Evidence-based guidelines for the use of immunologic tests: Anticentromere, Scl-70, and nucleolar antibodies. Arthritis Rheum 2003;49:399–412.

[40] Murata I, Takenaka K, Shinohara S, Suzuki T, Sasaki T, Yamamoto K. Diversity of myocardial involvement in systemic sclerosis: an 8-year study of 95 Japanese patients. Am Heart J 1998;135:960–9.

[41] Tan EM, Rodnan GP, Garcia I, Moroi Y, Fritzler MJ, Peebles C. Diversity of antinuclear antibodies in progressive systemic sclerosis. Anti-centromere antibody and its relationship to CREST syndrome. Arthritis Rheum 1980;23:617–25.

[42] Sato S, Fujimoto M, Ihn H, Takehara K. Antibodies to centromere and centriole in scleroderma spectrum disorders. Dermatology 1994;189:23–6.

[43] CHAN H -L, LEE Y -S, HONG H -S, KUO T -T. Anticentromere antibodies (ACA): clinical distribution and disease specificity. Clin Exp Dermatol 1994;19:298–302.

[44] Kampolis C, Plastiras SC, Vlachoyiannopoulos PG, Moyssakis I, Tzelepis GE. The presence of anti-centromere antibodies may predict progression of estimated pulmonary arterial systolic pressure in systemic sclerosis. Scand J Rheumatol 2008;37:278–83.

[45] Wigley FM, Wise RA, Miller R, Needleman BW, Spence RJ. Anticentromere antibody as a predictor of digital ischemic loss in patients with systemic sclerosis. Arthritis Rheum 1992;35:688–93.

[46] Ferri C, Valentini G, Cozzi F, Sebastiani M, Michelassi C, La Montagna G, et al. Systemic sclerosis: demographic, clinical, and serologic features and survival in 1,012 Italian patients. Medicine (Baltimore) 2002;81:139–53.

[47] Scussel-Lonzetti L, Joyal F, Raynauld J-P, Roussin A, Rich E, Goulet J-R, et al. Predicting mortality in systemic sclerosis: analysis of a cohort of 309 French Canadian patients with emphasis on features at diagnosis as predictive factors for survival. Medicine (Baltimore) 2002;81:154–67.

[48] Hudson M, Mahler M, Pope J, You D, Tatibouet S, Steele R, et al. Clinical correlates of CENP-A and CENP-B antibodies in a large cohort of patients with systemic sclerosis. J Rheumatol 2012;39:787–94.

[49] Mitri GM, Lucas M, Fertig N, Steen VD, Medsger TAJ. A comparison between anti-Th/To- and anticentromere antibody-positive systemic sclerosis patients with limited cutaneous involvement. Arthritis Rheum 2003;48:203–9.

[50] Wirz EG, Jaeger VK, Allanore Y, Riemekasten G, Hachulla E, Distler O, et al. Incidence and predictors of cutaneous manifestations during the early course of systemic sclerosis: a 10-year longitudinal study from the EUSTAR database. Ann Rheum Dis 2016;75:1285–92.

[51] Hamaguchi Y, Kodera M, Matsushita T, Hasegawa M, Inaba Y, Usuda T, et al. Clinical and immunologic predictors of scleroderma renal crisis in Japanese systemic sclerosis patients with anti-RNA polymerase III autoantibodies. Arthritis Rheumatol 2015;67:1045–52.

[52] Sakkas LI, Chikanza IC, Platsoucas CD. Mechanisms of disease: The role of immune cells in the pathogenesis of systemic sclerosis. Nat Clin Pract Rheumatol 2006;2:679–85.

[53] Fuschiotti P. Current perspectives on the immunopathogenesis of systemic sclerosis. ImmunoTargets Ther 2016;5:21–35.

[54] Kalogerou A, Gelou E, Mountantonakis S, Settas L, Zafiriou E, Sakkas L. Early T cell activation in the skin from patients with systemic sclerosis. Ann Rheum Dis 2005;64:1233–5.

[55] Whitfield ML, Finlay DR, Murray JI, Troyanskaya OG, Chi J-T, Pergamenschikov A, et al. Systemic and cell type-specific gene expression patterns in scleroderma skin. Proc Natl Acad Sci U S A 2003;100:12319–24.

[56] Sakkas LI, Platsoucas CD. Is systemic sclerosis an antigen-driven T cell disease? Arthritis Rheum 2004;50:1721–33.

[57] Abraham DJ, Varga J. Scleroderma: from cell and molecular mechanisms to disease models. Trends Immunol 2005;26:587–95.

[58] Mavalia C, Scaletti C, Romagnani P, Carossino AM, Pignone A, Emmi L, et al. Type 2 helper T-cell predominance and high CD30 expression in systemic sclerosis. Am J Pathol 1997;151:1751–8.

[59] Chizzolini C, Parel Y, De Luca C, Tyndall A, Akesson A, Scheja A, et al. Systemic sclerosis Th2 cells inhibit collagen production by dermal fibroblasts via membrane-associated tumor necrosis factor alpha. Arthritis Rheum 2003;48:2593–604.

[60] Kurasawa K, Hirose K, Sano H, Endo H, Shinkai H, Nawata Y, et al. Increased interleukin-17 production in patients with systemic sclerosis. Arthritis Rheum 2000;43:2455–63.

[61] Fossiez F, Djossou O, Chomarat P, Flores-Romo L, Ait-Yahia S, Maat C, et al. T cell interleukin-17 induces stromal cells to produce proinflammatory and hematopoietic cytokines. J Exp Med 1996;183:2593–603.

[62] Fukasawa C, Kawaguchi Y, Harigai M, Sugiura T, Takagi K, Kawamoto M, et al. Increased CD40 expression in skin fibroblasts from patients with systemic sclerosis (SSc): role of CD40-CD154 in the phenotype of SSc fibroblasts. Eur J Immunol 2003;33:2792–800.

[63] Baroni SS, Santillo M, Bevilacqua F, Luchetti M, Spadoni T, Mancini M, et al. Stimulatory autoantibodies to the PDGF receptor in systemic sclerosis. N Engl J Med 2006;354:2667–76.

[64] Kraaij MD, van Laar JM. The role of B cells in systemic sclerosis. Biologics 2008;2:389–95.

[65] Worda M, Sgonc R, Dietrich H, Niederegger H, Sundick RS, Gershwin ME, et al. *In vivo* analysis of the apoptosis-inducing effect of anti-endothelial cell antibodies in systemic sclerosis by the chorionallantoic membrane assay. Arthritis Rheum 2003;48:2605–14.

[66] Stifano G, Christmann RB. Macrophage Involvement in Systemic Sclerosis: Do We Need More Evidence? Curr Rheumatol Rep 2015;18:1–6.

[67] Matsushita T, Hasegawa M, Hamaguchi Y, Takehara K, Sato S. Longitudinal analysis of serum cytokine concentrations in systemic sclerosis: association of interleukin 12 elevation with spontaneous regression of skin sclerosis. J Rheumatol 2006;33:275–84.

[68] Nabel EG, Shum L, Pompili VJ, Yang ZY, San H, Shu HB, et al. Direct transfer of transforming growth factor beta 1 gene into arteries stimulates fibrocellular hyperplasia. Proc Natl Acad Sci U S A 1993;90:10759–63.

[69] Allen AM, Zhuo J, Mendelsohn FA. Localization and function of angiotensin AT1 receptors. Am J Hypertens 2000;13:31S–38S.

[70] Timmermans PB, Wong PC, Chiu AT, Herblin WF, Benfield P, Carini DJ, et al. Angiotensin II receptors and angiotensin II receptor antagonists. Pharmacol Rev 1993;45:205–51.

[71] Steckelings UM, Kaschina E, Unger T. The AT2 receptor--a matter of love and hate. Peptides 2005;26:1401–9.

[72] Atlas SA. The Renin-Angiotensin Aldosterone System: Pathophysiological Role and Pharmacologic Inhibition. J Manag Care Pharm 2007;13:9–20.

[73] Suzuki Y, Ruiz-Ortega M, Lorenzo O, Ruperez M, Esteban V, Egido J. Inflammation and angiotensin II. Int J Biochem Cell Biol 2003;35:881–900.

[74] Egido J. Vasoactive hormones and renal sclerosis. Kidney Int 1996;49:578–97.

[75] Touyz RM, Chen X, Tabet F, Yao G, He G, Quinn MT, et al. Expression of a functionally active gp91phox-containing neutrophil-type NAD(P)H oxidase in smooth muscle cells from human resistance arteries: regulation by angiotensin II. Circ Res 2002;90:1205–13.

[76] Chua CC, Hamdy RC, Chua BH. Upregulation of vascular endothelial growth factor by angiotensin II in rat heart endothelial cells. Biochim Biophys Acta 1998;1401:187–94.

[77] Laura Piqueras B, Kubes P, Alvarez A, O'Connor E, Issekutz AC, Esplugues J V, et al. Angiotensin II induces leukocyte-endothelial cell interactions *in vivo* via AT1 and AT2 receptor-mediated P-selection upregulation. Circ 2000:2118–23.

[78] Pueyo ME, Gonzalez W, Nicoletti A, Savoie F, Arnal J-F, Michel J-B. Angiotensin II Stimulates Endothelial Vascular Cell Adhesion Molecule-1 via Nuclear Factor- B Activation Induced by Intracellular Oxidative Stress. Arterioscler Thromb Vasc Biol 2000;20:645–51.

[79] Álvarez Á, Cerdá-Nicolás M, Abu Nabah YN, Mata M, Issekutz AC, Panés J, et al. Direct evidence of leukocyte adhesion in arterioles by angiotensin II. Blood 2004;104:402–8.

[80] Banchereau J, Steinman RM. Dendritic cells and the control of immunity. Nature 1998;392:245–52.

[81] Lapteva N, Ide K, Nieda M, Ando Y, Hatta-Ohashi Y, Minami M, et al. Activation and suppression of renin-angiotensin system in human dendritic cells. Biochem Biophys Res Commun 2002;296:194–200.

[82] Nahmod KA, Vermeulen ME, Raiden S, Salamone G, Gamberale R, Fernández-Calotti P, et al. Control of dendritic cell differentiation by angiotensin II. FASEB J 2003;17:491–3.

[83] Chang Y, Wei W. Angiotensin II in inflammation, immunity and rheumatoid arthritis. Clin Exp Immunol 2015;179:137–45.

[84] Ruiz-Ortega M, Lorenzo O, Egido J. Angiotensin III increases MCP-1 and activates NF-kappaB and AP-1 in cultured mesangial and mononuclear cells. Kidney Int 2000;57:2285–98.

[85] Lijnen PJ, Petrov V V, Fagard RH. Induction of cardiac fibrosis by angiotensin II. Methods Find Exp Clin Pharmacol 2000;22:709–23.

[86] Aki K, Shimizu A, Masuda Y, Kuwahara N, Arai T, Ishikawa A, et al. ANG II receptor blockade enhances anti-inflammatory macrophages in anti-glomerular basement membrane glomerulonephritis. Am J Physiol Renal Physiol 2010;298:F870-82.

[87] Hisada Y, Sugaya T, Yamanouchi M, Uchida H, Fujimura H, Sakurai H, et al. Angiotensin II plays a pathogenic role in immune-mediated renal injury in mice. J Clin Invest 1999;103:627–35.

[88] Mateo T, Abu Nabah YN, Abu Taha M, Mata M, Cerda-Nicolas M, Proudfoot AEI, et al. Angiotensin II-induced mononuclear leukocyte interactions with arteriolar and venular endothelium are mediated by the release of different CC chemokines. J Immunol 2006;176:5577–86.

[89] Nabah YNA, Mateo T, Estelles R, Mata M, Zagorski J, Sarau H, et al. Angiotensin II induces neutrophil accumulation *in vivo* through generation and release of CXC chemokines. Circulation 2004;110:3581–6.

[90] Kvakan H, Kleinewietfeld M, Qadri F, Park J-K, Fischer R, Schwarz I, et al. Regulatory T cells ameliorate angiotensin II-induced cardiac damage. Circulation 2009;119:2904–12.

[91] Guzik TJ, Hoch NE, Brown KA, McCann LA, Rahman A, Dikalov S, et al. Role of the T cell in the genesis of angiotensin II induced hypertension and vascular dysfunction. J Exp Med 2007;204:2449–60.

[92] Shao J, Nangaku M, Miyata T, Inagi R, Yamada K, Kurokawa K, et al. Imbalance of T-cell subsets in angiotensin II-infused hypertensive rats with kidney injury. Hypertension 2003;42:31–8.

[93] Wolf G, Neilson EG. Angiotensin II as a renal growth factor. J Am Soc Nephrol 1993;3:1531–40.

[94] Johnson RJ, Alpers CE, Yoshimura A, Lombardi D, Pritzl P, Floege J, et al. Renal injury from angiotensin II-mediated hypertension. Hypertens (Dallas, Tex 1979) 1992;19:464–74.

[95] Ruiz-Ortega M, Lorenzo O, Suzuki Y, Ruperez M, Egido J. Proinflammatory actions of angiotensins. Curr Opin Nephrol Hypertens 2001;10:321–9.

[96] Border WA, Noble NA. Interactions of transforming growth factor-beta and angiotensin II in renal fibrosis. Hypertens (Dallas, Tex 1979) 1998;31:181–8.

[97] Crawford DC, Chobanian a V, Brecher P. Angiotensin II induces fibronectin expression associated with cardiac fibrosis in the rat. Circ Res 1994;74:727–39.

[98] Stawski L, Han R, Bujor AM, Trojanowska M. Angiotensin II induces skin fibrosis: a novel mouse model of dermal fibrosis. Arthritis Res Ther 2012;14:R194.

[99] Hitomi H, Kiyomoto H, Nishiyama A. Angiotensin II and oxidative stress. Curr Opin Cardiol 2007;22:311–5.

[100] Gragasin FS, Xu Y, Arenas IA, Kainth N, Davidge ST. Estrogen reduces angiotensin II-induced nitric oxide synthase and NAD(P)H oxidase expression in endothelial cells. Arterioscler Thromb Vasc Biol 2003;23:38–44.

[101] Landmesser U, Spiekermann S, Preuss C, Sorrentino S, Fischer D, Manes C, et al. Angiotensin II induces endothelial xanthine oxidase activation: role for endothelial dysfunction in patients with coronary disease. Arterioscler Thromb Vasc Biol 2007;27:943–8.

[102] Kimura S, Zhang G-X, Nishiyama A, Shokoji T, Yao L, Fan Y-Y, et al. Role of NAD(P)H oxidase- and mitochondria-derived reactive oxygen species in cardioprotection of ischemic reperfusion injury by angiotensin II. Hypertens (Dallas, Tex 1979) 2005;45:860–6.

[103] Benigni A, Cassis P, Remuzzi G. Angiotensin II revisited: New roles in inflammation, immunology and aging. EMBO Mol Med 2010;2:247–57.

[104] Becker MO, Kill A, Kutsche M, Guenther J, Rose A, Tabeling C, et al. Vascular receptor autoantibodies in pulmonary arterial hypertension associated with systemic sclerosis. Am J Respir Crit Care Med 2014;190:808–17.

[105] Kill A, Tabeling C, Undeutsch R, Kühl AA, Günther J, Radic M, et al. Autoantibodies to angiotensin and endothelin receptors in systemic sclerosis induce cellular and systemic events associated with disease pathogenesis. Arthritis Res Ther 2014;16:R29.

[106] Riemekasten G, Philippe A, Nather M, Slowinski T, Muller DN, Heidecke H, et al. Involvement of functional autoantibodies against vascular receptors in systemic sclerosis. Ann Rheum Dis 2011;70:530–6.

[107] Sgonc R, Gruschwitz MS, Boeck G, Sepp N, Gruber J, Wick G. Endothelial cell apoptosis in systemic sclerosis is induced by antibody-dependent cell-mediated cytotoxicity via CD95. Arthritis Rheum 2000;43:2550–62.

[108] Katsumoto TR, Whitfield ML, Connolly MK. The Pathogenesis of Systemic Sclerosis. Annu Rev Pathol Mech Dis 2011;6:509–37.

[109] Morin F, Kavian N, Batteux F. Animal models of systemic sclerosis. Curr Pharm Des 2015;21:2365–79.

[110] Siracusa LD, McGrath R, Ma Q, Moskow JJ, Manne J, Christner PJ, et al. A tandem duplication within the fibrillin 1 gene is associated with the mouse tight skin mutation. Genome Res 1996;6:300–13.

[111] Green MC, Sweet HO, Bunker LE. Tight-skin, a new mutation of the mouse causing excessive growth of connective tissue and skeleton. Am J Pathol 1976;82:493–512.

[112] Sgonc R, Dietrich H, Sieberer C, Wick G, Christner PJ, Jimenez SA. Lack of endothelial cell apoptosis in the dermis of tight skin 1 and tight skin 2 mice. Arthritis Rheum 1999;42:581–4.

[113] Muryoi T, Kasturi KN, Kafina MJ, Cram DS, Harrison LC, Sasaki T, et al. Antitopoisomerase I monoclonal autoantibodies from scleroderma patients and tight skin mouse interact with similar epitopes. J Exp Med 1992;175:1103–9.

[114] Bocchieri MH, Henriksen PD, Kasturi KN, Muryoi T, Bona CA, Jimenez SA. Evidence for autoimmunity in the tight skin mouse model of systemic sclerosis. Arthritis Rheum 1991;34:599–605.

[115] Hatakeyama a, Kasturi KN, Wolf I, Phelps RG, Bona C a. Correlation between the concentration of serum anti-topoisomerase I autoantibodies and histological and biochemical alterations in the skin of tight skin mice. Cell Immunol 1996;167:135–40.

[116] Winstone TA, Assayag D, Wilcox PG, Dunne J V, Hague CJ, Leipsic J, et al. Predictors of mortality and progression in scleroderma-associated interstitial lung disease: a systematic review. Chest 2014;146:422–36.

[117] Christner PJ, Peters J, Hawkins D, Siracusa LD, Jim??nez SA. The tight skin 2 mouse: An animal model of scleroderma displaying cutaneous fibrosis and mononuclear cell infiltration. Arthritis Rheum 1995;38:1791–8.

[118] Christner PJ, Siracusa LD, Hawkins DF, McGrath R, Betz JK, Ball ST, et al. A high-resolution linkage map of the tight skin 2 (Tsk2) locus: a mouse model for scleroderma (SSc) and other cutaneous fibrotic diseases. Mamm Genome 1996;7:610–2.

[119] Long KB, Artlett CM, Blankenhorn EP. Tight skin 2 mice exhibit a novel time line of events leading to increased extracellular matrix deposition and dermal fibrosis. Matrix Biol 2014;38:91–100.

[120] Gentiletti J, McCloskey LJ, Artlett CM, Peters J, Jimenez S a, Christner PJ. Demonstration of autoimmunity in the tight skin-2 mouse: a model for scleroderma. J Immunol 2005;175:2418–26.

[121] Christner PJ, Peters J, Hawkins D, Siracusa LD, Jimenez SA. The tight skin 2 mouse. An animal model of scleroderma displaying cutaneous fibrosis and mononuclear cell infiltration. Arthritis Rheum 1995;38:1791–8.

[122] Morin F, Kavian N, Batteux F. Animal models of systemic sclerosis. Curr Pharm Des 2015;21:2365–79.

[123] Walton KL, Johnson KE, Harrison CA. Targeting TGF-β Mediated SMAD Signaling for the Prevention of Fibrosis. Front Pharmacol 2017;8:461.

[124] Feghali CA, Wright TM. Identification of multiple, differentially expressed messenger RNAs in dermal fibroblasts from patients with systemic sclerosis. Arthritis Rheum 1999;42:1451–7.

[125] Sonnylal S, Denton CP, Zheng B, Keene DR, He R, Adams HP, et al. Postnatal induction of transforming growth factor β signaling in fibroblasts of mice recapitulates clinical, histologic, and biochemical features of scleroderma. Arthritis Rheum 2007;56:334–44.

[126] Denton CP, Zheng B, Evans L a., Shi-Wen X, Ong VH, Fisher I, et al. Fibroblast-specific Expression of a Kinase-deficient Type II Transforming Growth Factor β (TGFβ) Receptor Leads to Paradoxical Activation of TGFβ Signaling Pathways with Fibrosis in Transgenic Mice. J Biol Chem 2003;278:25109–19.

[127] Maurer B, Reich N, Juengel A, Kriegsmann J, Gay RE, Schett G, et al. Fra-2 transgenic mice as a novel model of pulmonary hypertension associated with systemic sclerosis. Ann Rheum Dis 2012;71:1382–7.

[128] Reich N, Maurer B, Akhmetshina A, Venalis P, Dees C, Zerr P, et al. The transcription factor Fra-2 regulates the production of extracellular matrix in systemic sclerosis. Arthritis Rheum 2010;62:280–90.

[129] Bozec A, Bakiri L, Jimenez M, Schinke T, Amling M, Wagner EF. Fra-2/AP-1 controls bone formation by regulating osteoblast differentiation and collagen production. J Cell Biol 2010;190:1093–106.

[130] Foletta VC. Transcription factor AP-1, and the role of Fra-2. Immunol Cell Biol 1996;74:121–33.

[131] Maurer B, Busch N, Jüngel A, Pileckyte M, Gay RE, Michel B a., et al. Transcription factor fos-related antigen-2 induces progressive peripheral vasculopathy in mice closely resembling human systemic sclerosis. Circulation 2009;120:2367–76.

[132] Venalis P, Kumánovics G, Schulze-Koops H, Distler A, Dees C, Zerr P, et al. Cardiomyopathy in Murine Models of Systemic Sclerosis. Arthritis Rheumatol 2015;67:508–16.

[133] Maurer B, Distler JHW, Distler O. The Fra-2 transgenic mouse model of systemic sclerosis. Vascul Pharmacol 2013;58:194–201.

[134] Noda S, Asano Y, Nishimura S, Taniguchi T, Fujiu K, Manabe I, et al. Simultaneous downregulation of KLF5 and Fli1 is a key feature underlying systemic sclerosis. Nat Commun 2014;5:5797.

[135] Spyropoulos DD, Pharr PN, Lavenburg KR, Jackers P, Papas TS, Ogawa M, et al. Hemorrhage, impaired hematopoiesis, and lethality in mouse embryos carrying a targeted disruption of the Fli1 transcription factor. Mol Cell Biol 2000;20:5643–52.

[136] Asano Y, Bujor AM, Trojanowska M. The impact of Fli1 deficiency on the pathogenesis of systemic sclerosis. J Dermatol Sci 2010;59:153–62.

[137] Samuel CS, Zhao C, Yang Q, Wang H, Tian H, Tregear GW, et al. The relaxin gene knockout mouse: A model of progressive scleroderma. J Invest Dermatol 2005;125:692–9.

[138] Hocher B, Schwarz A, Fagan KA, Thöne-Reineke C, El-Hag K, Kusserow H, et al. Pulmonary fibrosis and chronic lung inflammation in ET-1 transgenic mice. Am J Respir Cell Mol Biol 2000;23:19–26.

[139] Wei J, Melichian D, Komura K, Hinchcliff M, Lam AP, Lafyatis R, et al. Canonical Wnt signaling induces skin fibrosis and subcutaneous lipoatrophy: A novel mouse model for scleroderma? Arthritis Rheum 2011;63:1707–17.

[140] Castello-Cros R, Whitaker-Menezes D, Molchansky A, Purkins G, Soslowsky LJ, Beason DP, et al. Scleroderma-like properties of skin from caveolin-1-deficient mice: Implications for new treatment strategies in patients with fibrosis and systemic sclerosis. Cell Cycle 2011;10:2140–50.

[141] Jaffee BD, Claman HN. Chronic graft-versus-host disease (GVHD) as a model for scleroderma. I. Description of model systems. Cell Immunol 1983;77:1–12.

[142] Claman HN, Jaffee BD, Huff JC, Clark RA. Chronic graft-versus-host disease as a model for scleroderma. II. Mast cell depletion with deposition of immunoglobulins in the skin and fibrosis. Cell Immunol 1985;94:73–84.

[143] McCormick LL, Zhang Y, Tootell E, Gilliam a C. Anti-TGF-beta treatment prevents skin and lung fibrosis in murine sclerodermatous graft-versus-host disease: a model for human scleroderma. J Immunol 1999;163:5693–9.

[144] Gabrielli A, Svegliati S, Moroncini G, Pomponio G, Santillo M, Avvedimento E V. Oxidative stress and the pathogenesis of scleroderma: the Murrell's hypothesis revisited. Semin Immunopathol 2008;30:329–37.

[145] Simonini G, Cerinic MM, Generini S, Zoppi M, Anichini M, Cesaretti C, et al. Oxidative stress in Systemic Sclerosis. Mol Cell Biochem 1999;196:85–91.

[146] Herrick AL, Matucci Cerinic M. The emerging problem of oxidative stress and the role of antioxidants in systemic sclerosis. Clin Exp Rheumatol 2001;19:4–8.

[147] Servettaz a, Guilpain P, Goulvestre C, Chéreau C, Hercend C, Nicco C, et al. Radical oxygen species production induced by advanced oxidation protein products predicts clinical evolution and response to treatment in systemic sclerosis. Ann Rheum Dis 2007;66:1202–9.

[148] Servettaz A, Goulvestre C, Kavian N, Nicco C, Guilpain P, Chereau C, et al. Selective Oxidation of DNA Topoisomerase 1 Induces Systemic Sclerosis in the Mouse. J Immunol 2009;182:5855–64.

[149] Yamamoto T, Takagawa S, Katayama I, Yamazaki K, Shinkai H, Nishioka K. Animal Model of Sclerotic Skin . I : Local Injections of 1999:456–62.

[150] Yoshizaki A, Iwata Y, Komura K, Ogawa F, Hara T, Muroi E, et al. CD19 regulates skin and lung fibrosis via Toll-like receptor signaling in a model of bleomycin-induced scleroderma. Am J Pathol 2008;172:1650–63.

[151] Yoshizaki A, Yanaba K, Ogawa A, Asano Y, Kadono T, Sato S. Immunization with DNA topoisomerase I and Freund's complete adjuvant induces skin and lung fibrosis and autoimmunity via interleukin-6 signaling. Arthritis Rheum 2011;63:3575–85.

[152] Luchetti MM, Moroncini G, Jose Escamez M, Svegliati Baroni S, Spadoni T, Grieco A, et al. Induction of Scleroderma Fibrosis in Skin-Humanized Mice by Administration of Anti−Platelet-Derived Growth Factor Receptor Agonistic Autoantibodies. Arthritis Rheumatol 2016;68:2263–73.

[153] Christner PJ, Artlett CM, Conway RF, Jiménez SA. Increased numbers of microchimeric cells of fetal origin are associated with dermal fibrosis in mice following injection of vinyl chloride. Arthritis Rheum 2000;43:2598–605.

[154] Koboziev I, Jones-Hall Y, Valentine JF, Webb CR, Furr KL, Grisham MB. Use of Humanized Mice to Study the Pathogenesis of Autoimmune and Inflammatory Diseases. Inflamm Bowel Dis 2015;21:1652–73.

[155] van den Hoogen F, Khanna D, Fransen J, Johnson SR, Baron M, Tyndall A, et al. 2013 classification criteria for systemic sclerosis: an American College of Rheumatology/European League against Rheumatism collaborative initiative. Arthritis Rheum 2013;65:2737–47.

[156] Yu X, Petersen F. A methodological review of induced animal models of autoimmune diseases. Autoimmun Rev 2018;17:473–9.

[157] Riemekasten G, Philippe A, Nather M, Slowinski T, Muller DN, Heidecke H, et al. Involvement of functional autoantibodies against vascular receptors in systemic sclerosis. Ann Rheum Dis 2011;70:530–6.

[158] Carayanniotis G, Huang GC, Nicholson LB, Scott T, Allain P, McGregor a M, et al. Unaltered thyroid function in mice responding to a highly immunogenic thyrotropin receptor: implications for the establishment of a mouse model for Graves' disease. Clin Exp Immunol 1995;99:294–302.

[159] Riemekasten G, Philippe A, Näther M, Slowinski T, Müller DN, Heidecke H, et al. Involvement of functional autoantibodies against vascular receptors in systemic sclerosis. Ann Rheum Dis 2011;70:530–6.

[160] Frech TM, Revelo MP, Drakos SG, Murtaugh MA, Markewitz BA, Sawitzke AD, et al. Vascular Leak Is a Central Feature in the Pathogenesis of Systemic Sclerosis. J Rheumatol 2012;39:1385–91.

[161] Mahoney WM, Fleming JN, Schwartz SM. A Unifying Hypothesis for Scleroderma: Identifying a Target Cell for Scleroderma. Curr Rheumatol Rep 2011;13:28–36.

[162] Raja J, Denton CP. Cytokines in the immunopathology of systemic sclerosis. Semin Immunopathol 2015;37:543–57.

[163] Witebsky E, Rose NR, Terplan K, Paine JR, Egan RW. Chronic thyroiditis and autoimmunization. J Am Med Assoc 1957;164:1439–47.

[164] Rose NR, Bona C. Defining criteria for autoimmune diseases (Witebsky's postulates revisited). Immunol Today 1993;14:426–30.

[165] Krams SM, Dorshkind K, Gershwin ME. Generation of biliary lesions after transfer of human lymphocytes into severe combined immunodeficient (SCID) mice. J Exp Med 1989;170:1919–30.

[166] Duchosal MA, McConahey PJ, Robinson CA, Dixon FJ. Transfer of human systemic lupus erythematosus in severe combined immunodeficient (SCID) mice. J Exp Med 1990;172:985–8.

[167] Martino G, Grimaldi LM, Wollmann RL, Bongioanni P, Quintans J, Arnason BG. The hu-SCID myasthenic mouse. A new tool for the investigation of seronegative myasthenia gravis. Ann N Y Acad Sci 1993;681:303–5.

[168] Martino G, Grimaldi LM, Wollmann RL, Bongioanni P, Quintans J, Arnason BG. The hu-SCID myasthenic mouse. A new tool for the investigation of seronegative myasthenia gravis. Ann N Y Acad Sci 1993;681:303–5.

[169] Juhasz I, Lazarus GS, Murphy GF, Shih IM, Herlyn M. Development of pemphigus vulgaris-like lesions in severe combined immunodeficiency disease mice reconstituted with lymphocytes from patients. J Clin Invest 1993;92:2401–7.

[170] Kwant-Mitchell A, Pek EA, Rosenthal KL, Ashkar AA. Development of functional human NK cells in an immunodeficient mouse model with the ability to provide protection against tumor challenge. PLoS One 2009;4:e8379.

[171] Lavender KJ, Pang WW, Messer RJ, Duley AK, Race B, Phillips K, et al. BLT-humanized C57BL/6 Rag2-/-gammac-/-CD47-/- mice are resistant to GVHD and develop B- and T-cell immunity to HIV infection. Blood 2013;122:4013–20.

[172] Rongvaux A, Takizawa H, Strowig T, Willinger T, Eynon EE, Flavell RA, et al. Human hemato-lymphoid system mice: current use and future potential for medicine. Annu Rev Immunol 2013;31:635–74.

[173] Sapadin AN, Esser AC, Fleischmajer R. Immunopathogenesis of scleroderma--evolving concepts. Mt Sinai J Med 2001;68:233–42.

[174] Rossi GA, Bitterman PB, Rennard SI, Ferrans VJ, Crystal RG. Evidence for Chronic Inflammation as a Component of the Interstitial Lung Disease Associated with Progressive Systemic Sclerosis 1 . 2. Am Rev Respir Dis 1985;131:612–7.

[175] Yurovsky V V, Wigley FM, Wise RA, White B. Skewing of the CD8+ T-cell repertoire in the lungs of patients with systemic sclerosis. Hum Immunol 1996;48:84–97.

[176] Atamas SP, Yurovsky V V, Wise R, Wigley FM, Goter Robinson CJ, Henry P, et al. Production of type 2 cytokines by CD8+ lung cells is associated with greater decline in pulmonary function in patients with systemic sclerosis. Arthritis Rheum 1999;42:1168–78.

[177] Weigold F, Gunther J, Pfeiffenberger M, Cabral-Marques O, Siegert E, Dragun D, et al. Antibodies against chemokine receptors CXCR3 and CXCR4 predict progressive deterioration of lung function in patients with systemic sclerosis. Arthritis Res Ther 2018;20:52.

[178] Chen Y, Yu X, He Y, Zhang L, Huang X, Xu X, et al. Activation of A2aR attenuates bleomycin-induced pulmonary fibrosis via the SDF-1/CXCR4 axis-related pathway. Am J Transl Res 2017;9:4125–36.

[179] Lapierre P, Djilali-Saiah I, Vitozzi S, Alvarez F. A murine model of type 2 autoimmune hepatitis: Xenoimmunization with human antigens. Hepatology 2004;39:1066–74.

[180] Yang H, Wu B, Tüzün E, Saini SS, Li J, Allman W, et al. A new mouse model of autoimmune ocular myasthenia gravis. Invest Ophthalmol Vis Sci 2007;48:5101–11.

[181] Mestas J, Hughes CCW. Of Mice and Not Men: Differences between Mouse and Human Immunology. J Immunol 2004;172:2731–8.

[182] Kazkaz H, Isenberg D. Anti B cell therapy (rituximab) in the treatment of autoimmune diseases. Curr Opin Pharmacol 2004;4:398–402.

[183] Thiebaut M, Launay D, Riviere S, Mahevas T, Bellakhal S, Hachulla E, et al. Efficacy and safety of rituximab in systemic sclerosis: French retrospective study and literature review. Autoimmun Rev 2018;17:582–7.

[184] Cochrane CG, Koffler D. Immune complex disease in experimental animals and man. Adv Immunol 1973;16:185–264.

[185] McGregor AM. Autoantibodies to the TSH receptor in patients with autoimmune thyroid disease. Clin Endocrinol (Oxf) 1990;33:683–5.

[186] Gleicher N, Barad D, Weghofer A. Functional autoantibodies, a new paradigm in autoimmunity? Autoimmun Rev 2007;7:42–5.

[187] Costagliola S, Many MC, Denef JF, Pohlenz J, Refetoff S, Vassart G. Genetic immunization of outbred mice with thyrotropin receptor cDNA provides a model of Graves' disease. J Clin Invest 2000;105:803–11.

[188] Cabral-Marques O, Riemekasten G. Functional autoantibodies targeting G protein-coupled receptors in rheumatic diseases. Nat Rev Rheumatol 2017;13:648–56.

[189] Wallukat G, Wollenberger A, Morwinski R, Pitschner HF. Anti-beta 1-adrenoceptor autoantibodies with chronotropic activity from the serum of patients with dilated cardiomyopathy: mapping of epitopes in the first and second extracellular loops. J Mol Cell Cardiol 1995;27:397–406.

7. Scientific achievement

7.1 Publications

1. **Yue X**, Yu X, Petersen F, Riemekasten G. Recent advances in mouse models for systemic sclerosis. Autoimmun Rev 2018; 17(12):1225-1234.

2. Yin J, Zheng J, Deng F, Zhao W, Chen Y, Huang Q, Huang R, Wen L, Geng G, Zhang Z, **Yue X**, Petersen F, Yu X. Gene expression profiling of lacrimal glands identifies the ectopic expression of MHC II on glandular cells as apresymptomatic feature in a mouse model of primary sjögren`s syndrome. Front Immunol 2018; 9: 2362.

3. Zheng J, Huang Q, Huang R, Deng F, **Yue X**, Yin J, Zhao W, Chen Y, Wen L, Zhou J, Huang R, Riemekasten G, Liu Z, Petersen F, Yu X. B Cells Are Indispensable for a Novel Mouse Model of Primary Sjögren's Syndrome. Front Immunol 2017;8:1384.

4. Petersen F, **Yue X**, Riemekasten G, Yu X. Dysregulated homeostasis of target tissues or autoantigens- A novel principle in autoimmunity. Autoimmun Rev 2017;16(6):602-611.

5. Zhao W, **Yue X**, Liu K, Zheng J, Huang R, Zou J, Riemekasten G, Petersen F, Yu X. The status of pulmonary fibrosis in systemic sclerosis is associated with IRF5, STAT4, IRAK1, and CTGF polymorphisms. Rheumatol Int 2017;37(8):1303-1310.

6. Zou J, **Yue XY**, Zheng SC, Zhang G, Chang H, Liao YC, Zhang Y, Xue MQ, Qi Z. Cholesterol modulates function of connexin 43 gap junction channel via PKC pathway in H9c2 cells. Biochim Biophys Acta 2014;1838(8):2019-25.

7.2 Workshops

Name	**Date**
Advanced Topics in Biostatistics	13.10.2017
Time and project management for early stage researchers	19.10.2017
Ethik in der Wissenschaft und gute wissenschaftliche Praxis	22.09.2017
Tierschutz- Tierversuche	12.12.2016
Scientific Writing	13.06.2016
Good scientific Practice	30.07.2017-31.07.2015
Basic statistic course	22.09.2016-23.09.2016

7.3 Attendance in scientific conferences

Name	Date	Contribution
GRK1727 Autumn retreat 2015	26.11.2015-27.11.2015	Presentation
GRK1727 Spring retreat 2016	10.05.2016	Presentation
GRK1727 Autumn retreat 2016	17.11.2016-18.11.2016	Presentation
GRK1727 Autumn retreat 2017	30.11.2017-01.12.2017	Presentation
BBRS retreat 2016	05.07.2016	Presentation
NDI meeting 2015	30.10.2015	attendance
NDI meeting 2016	07.10.2016	organization
NDI meeting 2017	10.11.2017	attendance
IPPF (International Pemphigus & Pemphigoid Foundation)	22.06.2017-23.06.2017	assistant
46th annual meeting of the german society for immunology	27.09.2016-30.09.2016	attendance
The 5th international annual symposium “inflammation at interface“	26.02.2015-28.02.2015	attendance
5th systemic sclerosis world congress	15.02.2018-17.02.2018	poster
5th European Congress of Immunology	02.09.2018-05.09.2018	poster
2nd symposium on regulatory autoantibodies targeting G-protein-coupled receptors	28.09.2018-30.09.2018	presentation and poster
1st symposium on functional autoantibodies targeting g-protein-coupled receptors	03.10.2016-07.10.2018	attendance

Acknowledgement

The present work was performed under the supervision of Prof. Xinhua Yu and Prof. Frank Petersen at the Research Center Borstel, Germany and with financial support provided by the GRK1727, DFG, between January 2005 and September 2005 while I was registered as a Ph.D. student at the University of Lübeck. During my study, I received so many warm help from people around me, and I could not have finished this work without their supports.

Firstly, I would like to express my great appreciation to Prof. Xinhua Yu and Prof. Frank Petersen. With their support, I obtained this important opportunity to study aboard, which greatly expand my view in scientific research. Every time when I faced confusions and troubles, they always gave me the helpful suggestions and advice. I learned so much from them, from methodologies to attitude on science, which have a huge impact on my understanding on research. In addition, I would like to thank them for their warm helps on my daily life, which has been imprinted on my memory.

I am sincerely thankful to Prof. Gabriela Riemekasten for her full support and great encouragement on my work. I am deeply impressed by her enthusiasm for research and learned a lot from her.

I also appreciate Dr. Zane Orinska for her patience and helpful suggestions on my project.

Special thanks also go to all members in my group, which is more like a big family, for giving me kind supports and helping me with all my questions. Many thanks to Dr. Brigitte Kasper for nice instructions and answers on my questions, Carola Schneider for help on my experiment and interesting talk on German culture, Christine Engellenner and Cindy Hass for detailed instruction on experimental procedure and helps on my daily life, Diana Heinrich for the kind support for experiment, Junie Tchudjin and Marjan Ahmadi for kind help on my daily life and work, Junping Yin, Xiaoqing Wang, Jacqueline Wax for kind helps on my projects, also my thanks go to Karin Böhm, Kai Yang and Yaqing Shu.

Last but not least, I would like to appreciate my parents and sister for their never-failing supports. Also, a special and great thank goes to my wife, Fengyuan Deng. She is the biggest treasure of my life. Her support behind me is my endless power to face the difficulties and uncertainties of the future.

Declaration

I declare that the dissertation in form and content and except for advices given by my supervisors constitutes my own work. I only used those sources and resources referred to in the thesis, and that I have identified citations as such. This work has been undertaken in compliance with the German Research Foundations (Deutsche Forschungsgemeinschaft, DFG) rules of good academic practice.

Furthermore, I confirm that this thesis has not yet been submitted as part of another examination process neither in identical nor in similar form.